INFORMATION TO USERS

This manuscript has been reproduced from the microfilm master. UMI films the text directly from the original or copy submitted. Thus, some thesis and dissertation copies are in typewriter face, while others may be from any type of computer printer.

The quality of this reproduction is dependent upon the quality of the copy submitted. Broken or indistinct print, colored or poor quality illustrations and photographs, print bleedthrough, substandard margins, and improper alignment can adversely affect reproduction.

In the unlikely event that the author did not send UMI a complete manuscript and there are missing pages, these will be noted. Also, if unauthorized copyright material had to be removed, a note will indicate the deletion.

Oversize materials (e.g., maps, drawings, charts) are reproduced by sectioning the original, beginning at the upper left-hand corner and continuing from left to right in equal sections with small overlaps. Each original is also photographed in one exposure and is included in reduced form at the back of the book.

Photographs included in the original manuscript have been reproduced xerographically in this copy. Higher quality 6" x 9" black and white photographic prints are available for any photographs or illustrations appearing in this copy for an additional charge. Contact UMI directly to order.

UMI

A Bell & Howell Information Company
300 North Zeeb Road, Ann Arbor MI 48106-1346 USA
313/761-4700 800/521-0600

Université d'Ottawa · University of Ottawa

MIXING AND TEMPORAL VARIATION IN THE GROUNDWATER FLOW SYSTEM AT THE CON MINE, YELLOWKNIFE, N.W.T., CANADA; AN ANALOGUE FOR A RADIOACTIVE WASTE REPOSITORY

by

Malcolm Charles Douglas

A thesis submitted to the School of Graduate Studies and Research

in partial fulfillment of the requirements

for the degree of M.Sc in Earth Sciences

OTTAWA-CARLETON GEOSCIENCE CENTRE

AND

UNIVERSITY OF OTTAWA

OTTAWA, CANADA

ABSTRACT

The spatial and temporal variations in geochemistry and isotopes of groundwaters at the Con Mine in Yellowknife, N.W.T., Canada, have provided insights to the impact of mining on the local hydrogeological environment. The study explores the use of mine hydrology in an analogous setting to assess the impact of a radioactive waste repository on groundwater flow, and surface to depth pathways in the Canadian Shield. The 50 years of mining activity at the Con mine fit the time frame envisaged for the construction and operation of a repository.

Inflow at eighteen boreholes and three faults was periodically monitored from 1994 to 1996. Groundwater discharge in the mine is a mixture of fresh water to brine, with maximum TDS of 290 g/L, at depths of 701 m to 1,615 m below surface. Three end-members are identified: (1) Shield brine typical of deep crystalline environments, (2) early Holocene precipitation and glacial melt water, and (3) recently recharged meteoric water. At salinities greater than 2,000-5,000 mg/L mixing between meteoric water and brine dominates over rock-water interaction as the mechanism controlling water composition. Irregular spatial distribution of water types has been observed in mixtures at sampling locations across the fault system, and is linked to fault conductivity and the disturbance to the groundwater flow system caused by mining activity.

Significant short term changes in composition are due to transient mixing and modification of pathways by drilling, drifting, and borehole shut-ins for transient pressure testing. Temporal trends in tritium measured in discharge at 1,372 m depth constrain fracture flow transit time for modern recharge from surface to discharge point to less than 20 years.

A body of glacial water emplaced at the time of deglaciation, has remained stable under the low hydraulic gradients in deep groundwater flow in the low-relief setting of the shield terrain, until disturbed by the steep surface to depth gradients imposed by mining activities. It suggests that a stable hydrogeological setting can exist under natural hydraulic gradients for time periods of thousands of years.

RÉSUMÉ

Les variations spatiales et temporales de géochimie et des isotopes des eaux souterraines dans la Con Mine à Yellowknife, T.N.O., Canada, ont donnés des perspectives aux conséquences à l'environnement hydrogéologique de faire des excavations minières. Cette étude examine l'utilisation de l'hydrologie minière dans une situation analogue pour évaluer l'impact d'un dépôt de déchets nucléaires sur l'écoulement des eaux souterraines, et des chemins d'écoulement, de la surface jusqu'en profondeur, dans le Bouclier Canadien. La période d'activité minière de 50 ans équivaut avec celle envisagée pour l'excavation et l'opération d'un dépôt souterrain.

L'écoulement à dix-huit trous de sondage et trois failles a été observé périodiquement de 1994 à 1996. Le déversement d'eau souterraine dans la mine est un mélange d'eau fraîche et d'eau saline avec un maximum MDT de 290 g/L, aux profondeurs de 701 m à 1,615 m sous la surface. Trois types d'origine d'eau sont identifiés: (1) l'eau salée du bouclier, caractéristique des environnements cristallins profonds, (2) précipitation de la première partie de l'époque Holocene combinée avec une eau de fonte glaciale, et (3)l'eau météorique récemment rechargée. À une salinité plus grande que 2,000-5,000 mg/L le mélange entre l'eau météorique et l'eau saline domine sur les réactions chimiques en tant que mécanisme controllant la composition de l'eau. L'irrégularité de la distribution spatiale de types d'eau a été observé dans les mélanges au point de prises d'échantillons au travers du système de failles, et est lié à la conductivité hydraulique et à la perturbation du mouvement du système d'écoulement causé par les activités minières.

Les changements importants à court terme dans la composition sont dû au mélange transitoire ainsi qu'à la modification des chemins d'écoulement par la forage, le percement de galeries souterraines, et la fermeture des trous de sondage pour évaluer la pression transitoire. Les tendances temporelles dans le tritium mesuré en débit à 1372 m de profondeur limitent la période de résidence de recharge moderne dans le système des failles avant de s'écouler, à moins de 20 ans.

Un corps d'eau glaciaire installé au temps de déglaciation est demeuré stable sous les gradients hydrauliques bas existant dans l'écoulement de l'eau souterraine profonde aux endroits de relief plats du terrain du bouclier, jusqu'à ce qu'il soit perturbé par les gradients élevés de surface jusqu'à la profondeur imposées par les activités minières. Ce qui suggère qu'un environnement hydrogéologique stable peut exister sous les gradients hydrauliques naturels pendant des périodes de milliers d'années.

ACKNOWLEDGEMENTS

Many thanks are due to Dr Ian Clark at the University of Ottawa for introducing me, not only to this project, but also to the world of isotope geochemistry. His teaching, supervision of my work, and most helpful comments and discussion were inspiring and are greatly appreciated.

The thesis work was part of a wider study carried out on behalf of the Atomic Energy Board of Canada. I am grateful to Joe Wallach and Dennis Bottomley of the Board for their advice and support.

Work was integrated with activity in other disciplines under the general management of Intera Consultants Limited in Ottawa who provided all the logistical support for sample collection visits to Yellowknife, including reconnaissance for suitable locations, site preparation, the teamwork required for sampling, and the financial assistance that kept me going. Thank you to all in the Intera office for their help, especially Ken Raven for accepting me for the project, and Austin Sweezey and Rob Timlin for their planning, help and guidance during field operations.

Without the agreement to allow access to the mine, and generous support of the Miramar Con Mine management and staff, this study could not have proceeded. I thank, amongst others, Harry McDougall, Bob Hauser, Dean McDonald, and Angel Dacanay for technical help and discussion, and for arranging the training and organisation necessary for visitors going underground. The cooperation of the mine extended to scheduling underground drilling of holes beneficial to the sampling programme.

Thanks go to the experienced and knowledgeable staff of the stable isotope and geochemistry laboratories in the Department of Geology at the University of Ottawa who taught me enough to complete all the analyses that I had to do, and a great deal more.

The readiness of fellow students to take the time to discuss ideas, to encourage, and to share helpful tips was a great help and very much appreciated.

Last, but not least, many thanks to my very patient wife, Myreille, and family for their moral support during the last couple of years, and advice and assistance with figure layout.

ORIGINAL CONTRIBUTION

The bulk of the data used in this study derive from water samples collected between 1994 and 1996. Some additional data have been incorporated from earlier published research done on water from three of the sample locations. Working with Intera personnel during three visits to the Con Mine in Yellowknife in July and November 1995, and June 1996, I collected comprehensive sets of samples following protocols appropriate for the range of different analyses required. I recorded field chemistry data and performed the field titrations on samples. My fieldwork included preparation and maintenance of borehole sampling instrumentation. Intera carried out early reconnaissance sampling in February 1994, February 1995, and May 1995, and some confirmatory sampling in September 1996.

I prepared and ran all water samples for anion chemistry in the University of Ottawa geochemistry laboratory, while samples for cation analysis were sent to be analysed at the Geological Survey of Canada laboratories. I performed the complete sequence of procedures from sample preparation through mass spectrometry to calculation of all final stable isotope results for ^{2}H, ^{18}O in water, ^{13}C in DIC, and ^{34}S in dissolved sulphate. Calcite ^{13}C results were produced by laboratory staff. ^{18}O in sulphate was analysed by the University of Waterloo. The barite used for this was prepared by me. Radiogenic isotopes, ^{14}C and ^{3}H, were analysed by the universities of Toronto and Waterloo, respectively. CO_2 used for ^{14}C determinations was prepared by me. All calculations using analytical data are my own.

TABLE OF CONTENTS:

LIST OF APPENDICES

LIST OF FIGURES

LIST OF PLATES

LIST OF TABLES

1 INTRODUCTION

1.1 Background

The Canadian concept for nuclear waste disposal is burial of material at depths in the range of 500 to 1000 m within the crystalline bedrock of the Canadian Shield. Waste would be contained in an environment which was able to isolate radionuclides against escape and transport in groundwater back to the biosphere. The host rock would be one of several barriers in a multiple barrier design to restrict release of radioactive material. Construction of an underground repository can be expected to disturb the regional groundwater flow system, to an extent controlled by discontinuities in the geosphere, by inducing flow through the surrounding rock towards excavated areas. Following emplacement and closure, the discontinuities could represent transport pathways for radionuclides as regional flow systems are re-established. The construction and operation period of a repository is envisaged to be 50 years after which excavated disposal areas would be backfilled and abandoned and a return towards natural groundwater gradients would occur.

1.2 Objectives

This study is part of a wider project to assess a location >500 m deep in the Canadian Shield as an analogue for the hydrogeological and hydrochemical perturbations that may be caused in the geosphere by the construction and operation of a repository for high level nuclear waste. Only geochemical and isotopic aspects of the project are addressed here,

with the objectives, 1) to characterise different water types contributing to groundwater mixtures, 2) to differentiate between individual groundwater flow systems using geochemical facies, 3) to establish groundwater provenance, 4) to constrain groundwater circulation times, 5) to observe redox conditions, and 6) to study change in groundwater composition with time.

1.3 Previous work

Earlier investigations at Yellowknife, amongst other locations across the Canadian Shield, directed at the geochemistry of groundwaters (Frape and Fritz, 1987) , rock-water interaction (Frape *et al.*, 1984; Macdonald, 1986), age of deep groundwaters (Fritz and Frape, 1982), and origins of shield brines (Bottomley *et al.*, 1994), have identified waters with distinct chemistries and stable isotope signatures. Data from the Con Mine were reported by Macdonald (1986), incorporating previous results from Frape and Fritz (1982). Some of the sampling points included were revisited during this study, extending the record of water composition data to 16 years.

Gascoyne and Kamineni (1994) have reviewed the isotope geochemistry of groundwaters from four plutons in the Canadian Shield down to a maximum depth of 1,100 m. Research into groundwater composition for nuclear waste disposal purposes has been conducted at two sites in crystalline settings in Sweden. Work at Stripa has been comprehensively described by a suite of papers published together in *Geochimica et Cosmochimica Acta*, 1989, v. 53. At the other location at Åspö; the chemical and isotopic

character of groundwater has been used as an indicator of flow direction and migration rate to assess the nature and level of disturbance caused by tunnel building (Smellie *et al.*, 1995).

Other researchers have demonstrated the presence of Ca-Na-Cl brine having salinity of up to 325 g/L TDS at depth at many locations across the shield, and have observed that major ion ratios are similar, but minor elements vary reflecting local differences in rock chemistry, and water origin, the latter a subject of considerable debate and outside the scope of this study.

The stable hydrogen and oxygen isotope character for shield brine was found to be very distinctive, being enriched in ^{2}H and ^{18}O compared with shallower groundwater. There are regional differences in ^{18}O enrichment in analysed waters but it has been suggested that data trends from areas so far observed can be extrapolated to a common shield brine end-member within the range of $\delta^{18}O = -10$ to $-12\ ^{0}/_{00}$ VSMOW and $\delta^{2}H = -20$ to $-50\ ^{0}/_{00}$ VSMOW (Frape *et al.*, 1984).

Closer to surface (<650 m), fresh to brackish meteoric waters have been identified at Yellowknife and other localities across the shield by their stable isotope signature (Frape and Fritz, 1987), in spite of highly variable chemical composition. These waters typically have high Na/Ca ratios compared with brines, and HCO_3 is the dominant anion (Frape *et al.*, 1984). High Na/Ca ratios have also been observed in groundwater from below 700 m in granite at Stripa in Sweden (Nordstrom *et al.*, 1989), and in water from depths of 300-

800 m at Åspö, Sweden (Smellie *et al.*, 1995). Variations in geochemistry of these waters reflect the level of evolution of meteoric water due to rock-water interaction. With increasing depth, and at salinities greater than 5,000 mg/L, the effect of the rock-water interaction becomes very minor compared with mixing along flow between brine and infiltrating fresh-brackish water.

The process of modification of deep brines by mixing with less saline waters infiltrating from above has been discussed by Frape *et al.* (1984) who note dilution trends between brine and shallow meteoric end-members.

2 SITE DESCRIPTION

2.1 The mine

2.1.1 Site selection

The Miramar Con Mine in Yellowknife, Northwest Territories was selected following a survey of 59 operating mines in the Canadian Shield (Raven and Clark, 1993) as a reasonable analogue for a Canadian concept radioactive waste repository at the end of its planned 50 year operating life. The advantages of this mine are first, that it has been operating for over 50 years and, secondly that it offers a 3-dimensional spread of subsurface sampling locations where there has been little or no overhead mining activity (Fig. 1.1) to cause changes in the water geochemistry and hydrogeological flow conditions more than has already been induced by the opening of the drifts.

The Con Mine workings cover an area of over 3.5 km north-south by over 1.5 km east-west. The mine is arranged with drifts mostly orientated north-south. Because of a westerly dip in the objective mineralised zone, drifts are progressively offset westwards with depth. The area covered by this study is at the south end of the mine and is approximately 1.5 km x 1.5 km, extending from surface to the 5300 level at 1.6 km depth.

2.1.2 Mine excavation chronology

1937 - Mine shaft excavation started

1946 - C1 (Con) shaft sunk to 745 m (2,443 ft)

1974 - Robertson shaft sunk to 1,890 m (6,200 ft)

Underground drifting and borehole drilling, influencing the groundwater flow system in the area covered by this project, were carried out from the late 1940's (2300 level), and after 1974, when the sinking of the Robertson Shaft was started, eventually reaching 1,890 m. The age of boreholes is given in Appendix 2.1.

2.1.3 Physical setting

The mine is located on the southern outskirts of the town of Yellowknife, on the west side of Yellowknife Bay, an arm of Great Slave Lake (Figs. 2.1, 2.2). There is relatively low surface relief in the district (Plate 2.1), which has an elevation approximately 200 m above sea level. There is considerable exposure of bedrock, and in lower-lying areas there is thin drift cover, with occasional lakes.

2.2 Geology

2.2.1 Bedrock

The mine location lies within the Yellowknife Greenstone Belt, in the southwestern part of the Slave province of the Canadian Shield (Fig. 2.1). The country rocks are 2.6-2.7 Ga volcanics, regionally metamorphosed by the emplacement of the nearby Western Plutonic Complex. These are mafic to intermediate tholeiites of the Kam Group (Helmstaedt and Padgham, 1986) across the mine site, becoming increasingly cherty and succeeded by intermediate to felsic volcanics (Cunningham and St.J.Lambert, 1988) of the Banting Group, found off-site to the south of the mine.

The earliest structural displacements within the volcanic sequence are mineralised shears, which are the targets for gold exploration, such as the Campbell (Plate 2.2) and Con shears (Fig. 2.3), formed during the emplacement of the granodiorite batholith of the Western Plutonic Complex (McDonald *et al.*, 1993).

Later Precambrian faulting produced three main fault orientations, mapped by Henderson and Brown (1966), and described in detail by Lindberg (1987). Many lesser faults have been mapped (Fig. 2.3) on the surface in the area of the mine, but the most obvious faults on-site are, in order of age:

- Negus Fault (NE-SW) having left-lateral horizontal displacement. It is the oldest fault.
- Pud Fault (NNW-SSE), on which the horizontal (left-lateral) movement is dominant. Some vertical displacement is seen, down to the west. It is younger than the NE-SW

Plate 2.1 View down the Yellowknife River to Yellowknife and the Con Mine's Robertson Shaft headframe, showing the typical low relief of the region.

Plate 2.2. Mineralisation on the Campbell Shear zone (view to NE).

faulting as shown by a 290 m offset of the Negus by the Pud at the mine. Probable splays from this fault are visible in the mine. Passing immediately to the east of the mine is the West Bay Fault, a major regional feature, having left-lateral displacement of 5 km (Campbell, 1948). Its orientation is closer to N-S than the "Pud" trend in the area of the mine. To the west of the Pud fault lies the Kam fault, and between the two, the Meg fault, which lies immediately to the south of the study area.

- Angel-type (E-W), e.g. Tibbit fault, showing right-lateral movement along vertical planes, and most probably the same age as the NNW oriented faults on the Pud trend. They are a geometrically required adjustment mechanism in response to left-lateral movement on the NNW-SSE faults (Lindberg, 1987), resulting in rotation of blocks between them.

Mine excavation and borehole drilling have shown Angel-type faults to vary from clean with no infilling at B8906 (Site 35-B), to having abundant gouge at B7126 (53-A) and a sand flow from this borehole during drilling. A mud seam was penetrated in B3457 (45-B) in an unidentified fault. Secondary mineralisation, carbonate and quartz, was described in the Angel fault in B5318 (45-E). Mineralisation was commonly found in faults, sometimes with rusty coloured staining as at B3362 (45-G), and B9362 (35-A).

2.2.2 Surficial geology

Surficial sediment of Quaternary age provides discontinuous cover for the Proterozoic bedrock which is normally well exposed throughout the district. This sediment may

derive from subaerial weathering, or from glacial environments producing till and lacustrine deposits. Areas of sediment are typically found in low-lying localities such as the depression at Rat Lake, marking the surface location of the Con Shear ore body (Plate 2.3).

2.3 Hydrological Setting

2.3.1 Surface water

The region contains numerous permanent lakes ranging in size from tens of metres across, to the very large Great Slave Lake, an inlet from which (Yellowknife Bay) lies immediately to the east of the mine. Water input to Great Slave Lake derives from Hay River and the Peace/Slave River systems draining an area extending for hundreds of km to the south. The lake is drained by the Mackenzie River. Of immediate geographical relevance to groundwater systems existing in the mine, the Pud Lakes lie on mine property directly above the sampled area (Fig. 2.3). They have been used for surface operations. Off-site, Yellowknife Bay, Kam Lake, and Frame Lake are large freshwater bodies potentially connected by faults to the mine groundwater system (Fig. 2.2).

The region around Great Slave Lake has experienced inundation during the relatively widespread late Ordovician to Devonian marine incursion, possibly during Cretaceous, also marine, and most recently by freshwater of the more localised glacial Lake McConnell (Craig, 1965) during glacial regression through the area. The district was covered by the retreating Laurentide ice sheet from approximately 45,000 to 11,000 years

Plate 2.3. Rat Lakes, located in the low-lying surface expression of the Con Shear.

BP, after which Lake McConnell developed and remained until the margin of the ice retreated from the Great Slave Lake area rapidly after 9,000 years BP (Dyke and Dredge, 1989).

Surface water is frozen from October to May/June.

2.3.2 Groundwater flow pathways

Infiltration will be possible in areas where permitted by the prevailing permafrost conditions, but only where the ground is not seasonally frozen, and under recharge lakes. The district is defined in the National Atlas of Canada (Natural Resources Canada, 1995) as currently having extensive discontinuous permafrost. Significantly, depending on its thermal history, ground could have been unfrozen under the glacial ice, and under associated glacial lakes.

Glacial ice can alter groundwater pressure, creating local flow, and has been linked to increased aquifer pressure causing a surface blow-out at Howe Lake in Saskatchewan (Christiansen *et al.*, 1982). A retreating ice sheet margin with high topography, and fracture and porosity development, could contain an elevated water table capable of generating the hydraulic gradients required for meteoric water and glacial meltwater to infiltrate the bedrock below (Fig. 4.7). Local high pressure at the base of the ice could potentially drive subsurface flow to discharge areas such as periglacial lakes. The depth to which these local flow systems extend would depend on factors such as hydraulic

pressure, fracture conductivity, and density of resident saline water and brine. The flow systems would only be active for a limited period of time after the retreat of the Laurentide ice sheet, while the ice margin remained in the district. In the Yellowknife area, the required conditions could only have existed from about 11,000 to 9,000 years ago, after which gradients would have diminished.

The crystalline country rock matrix is faulted. The main faults mapped in the mine are the Pud, Negus and Angel-type (e.g. Tibbit) faults (Fig. 2.3), the positions of which are fairly well constrained by intersection with boreholes and drifts. The West Bay Fault is the most important fault encountered in the mine, but is not intersected in the area covered by this study. The fault traces are also evident on the surface. Numerous similarly orientated faults are mapped on surface in the area of the mine.

Dilute water, with TDS less than 1,500 mg/L at the 2300 and 3500 levels, and the relatively high rates of influx (Appendix 2.1) associated with them, point to the Negus and Angel-type faults as important conduits for recent recharge. This is consistent with stress analysis results from the mine (Canmet, 1996) which indicate principal regional stress directions varying from E-W at the 3500 level, sub-parallel to the Angel fault orientation, to WSW-ENE by the 5700 level, sub-parallel to the Negus Fault, implying a tendency for these to be open. Pud-orientated faults are normal to the principal stress.

The main faults are recognised and traced to depth in the mine, Angel and Pud-orientated planes being identified down to the 5300 level, and are associated with virtually all of the seepages and stronger inflow in the area investigated.

Pre-mining regional hydraulic gradients are not known. Modern meteoric water is currently discharging in mine openings down to 1,615 m (5300 level) below surface indicating a strong surface-to-depth groundwater flow.

2.3.3 Meteorology

Meteorological data were collected at Yellowknife under a monitoring programme by F. Michel of Carleton University in association with the International Atomic Energy Agency (IAEA) for the years 1989 to 1993 inclusive. During this period precipitation averaged 295 mm / year, mostly as rain in summer. Mean monthly precipitation from these data is shown in Fig. 2.4. Mean monthly temperature and $\delta^{18}O$ data are presented in Fig. 2.5, showing the relationship of oxygen isotopic content and temperature. A rain sample collected in June 1996 gave a $\delta^{18}O$ of -15.88 ‰, consistent with the mean for June from the monitoring data.

3 RESULTS AND OBSERVATIONS

3.1 Introduction

3.1.1 Objectives of data collection programme

The data collection and analytical programmes were designed to address the following objectives:

- Geochemical characterisation of water based on major cation and anion content, and isotopic composition.

- Examining fracture minerals to assess their controls over the aqueous phase composition.

- Evaluating the sources and origin of groundwater using the stable isotopes of water (^{18}O, ^{2}H), sulphate (^{34}S, ^{18}O), and ^{13}C.

- Differentiation of flow paths by comparison of major ions and stable isotopes.

- Assessment of mixing in the flow system between different water types using major ions and stable isotopes.

- Estimation of residence times of groundwater components, and assessment of flow rates using radiogenic isotopes, ^{14}C and ^{3}H.

- Evaluate temporal change in water composition.

- Assessment of redox conditions from field readings of Eh and dissolved oxygen, and sulphide determination.

3.1.2 Water sampling

A preliminary survey of the mine assessed all points of water influx to identify those that were most remote from active overhead mining activity, and with sufficient flow to be sampled, with the outcome that the sampling programme was focussed on the southern part of the mine. Sampling locations (Fig. 1.1) were selected on levels 2300 (701 m depth below surface), 3500 (1,067 m), 4500 (1,372 m), 4900 (1,494 m), and 5300 (1,615 m), originally named according to depth in feet below surface. Additional *ad hoc* samples

were collected on levels 3900 (1,189 m) and 4300 (1,311 m). Sampled locations have been named for clarity such that the two digits represent the drift level, and the letter indicates position in sequence from south to north. For example, 23-A is the most southerly sample on the 2300 level (Fig. 3.1). Coordinates of locations, and borehole data are listed in Appendix 2.1.

Fourteen groundwater inflow points were fitted with "Margo" plugs and valves (Plate 3.1) enabling collection of geochemical field data representative of true groundwater conditions from water piped into a flow cell directly from the borehole installation, thereby avoiding exposure to the atmosphere (Plate 3.2).

The sample set for this project was collected between February 1994 and June 1996. The earliest groundwater samples (41-1 to 41-12), taken in February 1994 and February 1995, were used to make a preliminary assessment of the viability of the project, those collected in May 1995 represented the first complete set from all sites to be included in the study, that were available at that time. Samples collected in May 1995 are recognised by the suffix 1, eg. 23-A-1. Later samples obtained in July 1995, November 1995, June 1996, and September 1996 are identified by the suffixes 2, 3, 4, and 5, respectively. Groundwater samples dedicated to specific analyses were collected from selected locations in July 1995. At this time, fifteen surface waters from locations on and around the mine and other water bodies in the Yellowknife region were collected (Plates 2.1, 2.3, 3.3). Further groundwater sampling was carried out in November 1995 and June 1996 at

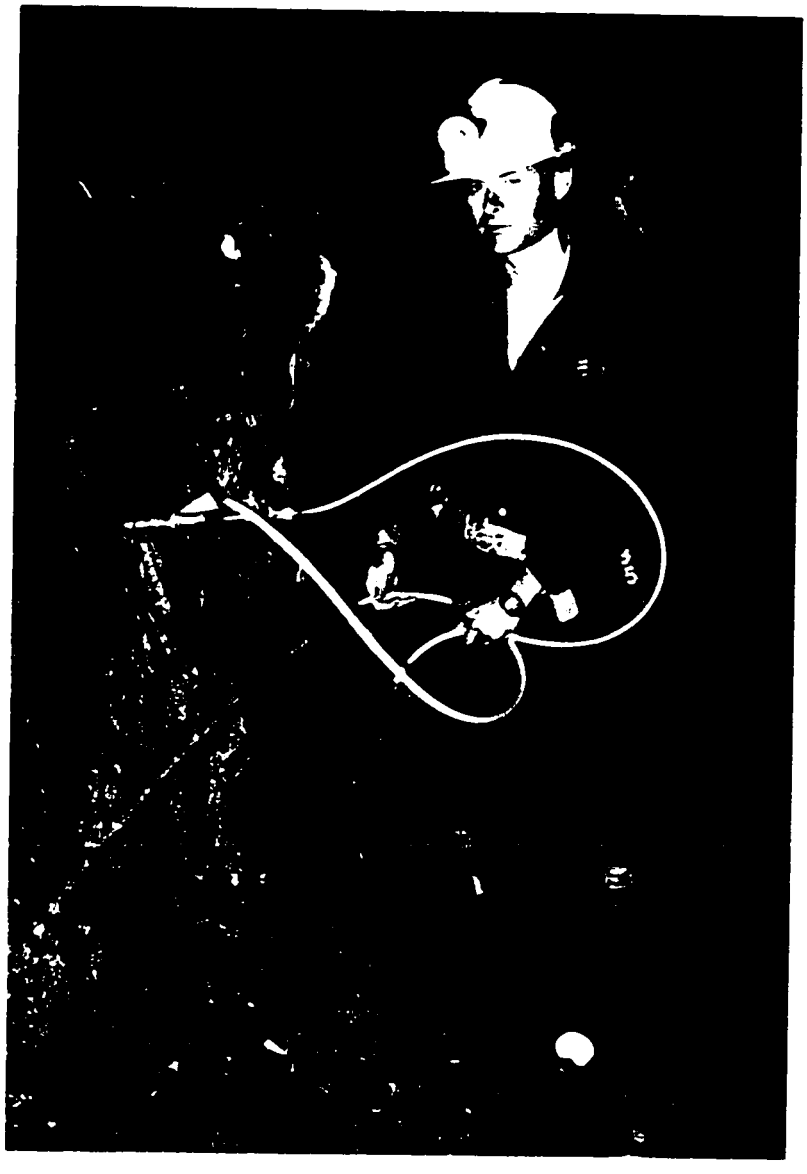

Plate 3.1. Borehole 5318 (Site 45-E), fitted with a "Margo" plug and valve. The two tubes were arranged to tap flow separately from the Negus and Angel faults intersected by the borehole, and between which a plug had been installed.

Plate 3.2. Preparing borehole 3457 (site 45-B), for monitoring. Borehole 3450 (site 45-D) can be seen adjacent. A flow cell fitted with probes to measure electrical conductivity, Eh, pH, dissolved oxygen, and temperature was connected directly to borehole instrumentation to examine water's properties before its exposure to the atmosphere.

Plate 3.3. On-site waste treatment pond with the Con Shaft headframe and ore treatment plant beyond.

selected sites, including some new locations not previously sampled. Isolated samples were collected in September 1996 for isotopic analysis.

The water supply to the mine's environmental laboratory, taken directly from Yellowknife Bay on Great Slave Lake, was sampled monthly for the period July 1995-June 1996, and one precipitation sample was collected during a summer rainstorm.

3.1.3 Sample collection method

Samples taken in May 1995, and earlier, were simply collected in nalgene bottles with no preservation. Later sampling methods followed protocols appropriate to specific analyses to be done. These are detailed in Appendix 3.1.

3.1.4 Collection of field geochemical data

Field data were acquired at the time of sample collection. Where boreholes had been fitted with "Margo" plugs (packer and valve installations), a flow cell was used to monitor pH, Eh, electrical conductivity, dissolved oxygen, and temperature of emerging groundwater before its exposure to air (Plate 3.2). Final values were recorded once meter readings stabilised, this normally taking at least half an hour after flow commenced through the cell. Alkalinity titrations were performed on water from each of these sites as soon as it was brought to surface at the end of a day's underground shift. Titrations were made with a Hach digital titrator using 100 ml samples and 0.16N or 1.6N H_2SO_4 acid.

3.1.5 Analytical procedure

Samples were collected for geochemical, stable isotope and radiogenic isotope analysis.

Chemistry

Major cation analyses were performed at the Geological Survey of Canada by ICP-AES.

Anions chloride, sulphate, bromide, fluoride, and nitrate were analysed by HPLC (Dionex), in the geochemistry laboratory at the University of Ottawa. The extreme range of salinity of the set of samples required dilutions between x 1 and x 20,000 to bring individual ions into the calibration range of the instrument. HCO_3 was determined by titration with H_2SO_4, or CO_2 extraction (DIC) as indicated in Appendix 3.3.

Sulphide was determined by difference between sulphate concentration in CdAc preserved samples, where sulphide was precipitated as CdS, and a duplicate set treated with H_2O_2 to oxidise it to sulphate.

Isotopes

The following isotopes were analysed in the G.G. Hatch isotope laboratories in the Department of Geology at the University of Ottawa:

Oxygen-18 - 1 ml water samples were equilibrated with standard CO_2 at 25 ^{0}C for 6 hours where salinity was <10,000 mg/L, and for 48 hours for more saline water. Where TDS was >225,000 mg/L, 5 ml of water were used to raise the volume of oxygen to ensure an adequate signal/noise response from the mass spectrometer. After equilibration, the CO_2

was analysed on a triple collector VG SIRA 12 mass spectrometer. Analytical precision (2σ) was 0.10 ‰. Results are expressed relative to the Vienna Standard Mean Ocean Water (VSMOW). Further calculations were made to correct for reduced ^{18}O activity at high salinities using the method of Sofer and Gat (1972), according to the relationship:

$$\delta^{18}O_{corrected} = \left\{ \frac{(1.11m_{Mg} + 0.47m_{Ca} - 0.16m_{K})}{1000} \times (\delta^{18}O_{measured} + 1000) \right\} + \delta^{18}O_{measured}$$

where m is molality (moles of cation per kg of water).

Deuterium - Water samples were prepared by prefiltering over heated metal filters to remove salts at the point of vacuum distillation. Hydrogen was obtained by reduction of the resultant water in the presence of zinc at 500 °C, and analysed on a double collector VG 602E mass spectrometer. Results are normalised to VSMOW, and precision (2σ) is 1.5 ‰.

Sulphur-34 - Aqueous sulphate was converted to precipitated $BaSO_4$ by addition of excess $BaCl_2.2H_2O$ to water samples, acidified with HCl to pH 3-4 to prevent co-precipitation of $BaCO_3$. The barite was converted to SO_2 by combustion with copper oxide and quartz at 1,100 °C. The gas was analysed on a triple collector VG SIRA 12 mass spectrometer. Precision (2σ) is 0.20 ‰. Results are expressed relative to the Canyon Diablo Troilite (CDT) sulphur standard.

Oxygen-18 in sulphate was analysed at the Environmental Isotope Laboratory, University of Waterloo. The sulphates were first prepared at the University of Ottawa as described

for sulphur-34, a split from which was sent for oxygen-18 analysis. CO_2 was produced by combustion of sample with graphite in molybdenum foil, with oxidation of co-produced CO completed in a high voltage chamber. Method precision (2σ) is 0.5 ‰. Results are expressed relative to VSMOW.

Carbon-13 - dissolved inorganic carbon (DIC) in water samples was converted to CO_2 by reaction with phosphoric acid which was then analysed on a triple collector VG SIRA 12 mass spectrometer to determine isotopic composition of the DIC. Precision (2σ) was 0.10 ‰. Results are expressed relative to the Vienna Pee Dee Belemnite (VPDB) carbon standard.

Carbon-14 was determined by tandem accelerator mass spectrometry (TAMS) at Isotrace, University of Toronto on CO_2 gas samples extracted in the stable isotope laboratory at the University of Ottawa using the same method as for carbon-13 samples.

Tritium - Samples were analysed at the Environmental Isotope Laboratory, University of Waterloo by liquid scintillation counting after electrolytic enrichment. Results are precise to 0.8 TU.

3.2 Aqueous Geochemistry

3.2.1 Field data

pH, Eh, dissolved oxygen, electrical conductivity, and temperature, data are given in Appendix 3.2.

Values of pH are restricted to a relatively small range (mostly 6.3-7.7 units). There was no systematic variability with depth, TDS, or HCO_3. However, minor variation exists between pH measured in the flow cell on-site, and at surface. Samples from sites on 2300-3500 levels showed higher pH (0.2-0.3 units higher) when re-measured at surface. Exposure to air, and pressure change, may have allowed CO_2 loss. 4500 level sites showed little change, while in water from levels 4900-5300, pH values were up to 1 unit less at surface, consistent with ingassing of atmospheric CO_2 since collection at the borehole.

3.2.2 Major ions

Analytical results are given in Appendix 3.3. Where used, the term TDS (total dissolved solids) refers to the total of the major ion concentrations, including Ca, Na, Mg, K, Cl, SO_4, Br, HCO_3. Representative chemistry of sampling locations (June 1996 data) is shown on Table 3.1.

The range of groundwater salinity is from 1,000 mg/L to 290 g/L. There is a general log-linear increase in TDS with depth (Fig. 3.2), locally irregular where subsurface flow is controlled by fracture hydraulic conductivity. Geochemistry, in terms of the dominant species Ca, Na, Cl, and SO_4, is illustrated by Fig. 3.3 which highlights the main difference in geochemical facies between waters of different salinity.

The deepest saline waters and brines are Ca-Na:Cl type, recognised elsewhere at depth in the Canadian Shield (Frape *et al.*, 1984; Macdonald, 1986). Smellie *et al.* (1995) reported this type below 800 m in predominantly granitic-granodioritic rocks at Åspö, Sweden. However, the Con Mine waters have a much higher Br/Cl ratio than that seen at Åspö. Br dominates over SO_4 at TDS concentrations over 100 g/L.

Shallowest sites have one of two main signatures:

a) Na-Ca:Cl-SO_4, seen at sites 23-A, and 35-A, and

b) Ca-Na:SO_4-HCO_3-Cl.

Both signatures show highly variable SO_4 and HCO_3 concentrations dependent on location and local dissolution and precipitation of gypsum and calcite, respectively. One of the least affected sites is 35-B where the type is Na-Ca:HCO_3-Cl.

The relationships between TDS and Cl, Ca, Na, K, Br, are a function of mixing between shallow meteoric waters and brine as the dominant control on water composition. In the least saline waters with concentration <6,000 mg/L TDS, there is a higher rate of increase in Na and Cl concentration relative to TDS than is observed in more saline water (Fig 3.4) where brine completely dominates water composition.

TABLE 3.1

Representative major ion chemistry and water isotope content for subsurface locations

Sample	Ca	Na	Mg	K	Cl	SO_4	Br	HCO_3	TDS	$\delta^{18}O_{SMOW}$	$\delta^{2}H_{SMOW}$
23-A-4	612	1131	27	10	2177	1049	18	27	5093	-23.69	-187.0
23-B-4	616	699	57	12	1559	1130	11	273	4413	-21.08	-169.6
23-C-4	541	374	49	11	762	1108	6	356	3237	-20.21	-160.4
23-D-4	6075	8426	339	52	25731	9	161	10	40988	-20.18	-145.5
23-E-4	215	100	61	10	142	483	1	390	1450	-19.54	-155.5
23-F-4	215	146	60	11	199	491	2	388	1577	-19.63	-157.2
35-A-4	1671	2007	33	14	6389	581	43	24	10811	-20.73	-160.8
35-B-4	226	245	33	9	610	154	4	442	1771	-19.72	-159.4
35-D-4	925	872	73	12	3181	603	33	127	5859	-19.52	-158.6
39-A-4	15339	7593	102	54	53706	609	378		78041	-19.12	-140.1
45-A-4	4796	3683	77	25	15137	584	111	32	24549	-20.46	-157.5
45-B-4	2524	2480	43	17	7845	609	62	32	13667	-20.60	-162.0
45-C-4	11495	6919	132	47	40035	693	257	22	59813	-20.09	-151.4
45-D-4	14540	7202	145	55	41271	738	315	51	64743	-19.22	-143.6
45-E-4	19029	9252	159	70	57866	465	373	47	87605	-18.96	-135.4
45-F-4	48515	21669	257	170	141287	489	888		214097	-16.93	-100.4
45-G-4	38171	17284	231	133	90166	369	659	27	147701	-17.61	-115.4
49-A-4	27057	14801	248	100	77986	642	575	7	121930	-19.56	-133.6
49-B-4	53442	23113	195	191	139149	443	925	15	218347	-16.48	-97.4
53-A-4	62811	25664	188	230	185555	247	1228	12	276957	-14.45	-73.2
53-B-4	68817	28284	232	255	159890	229	1464	12	260316	-14.35	-68.8
53-C-4	73462	29753	287	272	185215	130	1336	15	291744	-13.55	-61.5
53-D-4	57562	24920	271	197	152589	271	982		237768	-15.70	-84.4

Notes:
- Ionic concentration and TDS in mg/L
- Isotopic values in $^{0}/_{00}$

By contrast, Mg, SO_4, and HCO_3 do not have a well established linear relationship with TDS (Fig. 3.5) because they are a consequence of local influences. HCO_3 concentration is 100 mg/L in surface water (e.g. Yellowknife Bay). In groundwater it is much higher (>400 mg/L) at locations having a recent meteoric water signature. Saline water, brine, and some brackish water contained HCO_3 concentrations as low as <10 mg/L.

Sulphate concentration, highest (>1,100 mg/L) in shallow waters, decreases gradually with increasing TDS (Fig. 3.5) until the latter exceeds 200 g/L and rapidly thereafter to much lower levels in the most saline brines. Sources of sulphate have apparently been unavailable to site 23-D where saline water contained the lowest concentrations seen (<10 mg/L).

There are high sulphate concentrations, comparable with the brackish shallow groundwaters, in Upper Pud Lake (sample SW-12-1), an on-site tailings pond.

Sulphate concentration is unusually low in the least saline water at site 35-B.

3.2.3 Mineral saturations

SOLMINEQ.88 was used for mineral saturation determinations. For saline waters and brines, it was necessary to use an option within the programme that calculates ionic activity coefficients using Pitzer equations (Pitzer, 1981; Harvie *et al.*, 1984) which account for inter-ion interference at salinities higher than 1 molal. Output from the

programme shows that groundwater samples from below the 4500 level exceed this salinity.

Calculations indicated that waters from most of the locations sampled were at or near calcite saturation (Appendix 3.3). This is corroborated by the presence of euhedral calcite observed in fractures at the 3500 level in the mine. Water from 23-A was the most undersaturated with respect to calcite. Gypsum was at saturation in waters from the 4900 and 5300 levels, and approached saturation in most other samples.

3.2.4 Trace elements

In addition to minor cations reported in Appendix 3.3, other trace elements were analysed for geochemical exploration purposes and have not been used in this study.

3.2.5 Redox conditions

Eh was recorded in a flow cell in the absence of air at sites with "Margo" plug installations. Results for these sites (Appendix 3.2), apart from inconsistency between sampling visits, indicate highest Eh values at the 5300 level, and lowest at the 4500 level. The maximum range of values for any mine visit was 179 mV (July 1995). Results from the sampling in May 1995 show Eh decreasing from the 2300 level to the 4500 and 4900 levels, and increasing slightly again by the 5300 level. However, later data do not show this influence. Eh decreased at most sites on the 2300, 3500, and 4500 levels during the

course of the sampling programme. Eh results using a platinum electrode are unreliable in high chloride solutions due to the development of complexes on the electrode surface.

Dissolved oxygen was very low, often less than standard meter errors (0.15 mg/L), apart from some individual values which appeared aberrant when compared with readings taken at the same locations during different visits. NO_3 was low to non-detectable. Mn, and Fe were present in concentrations up to 14 and 15 mg/L, respectively, irregularly distributed, but generally occurring at higher concentrations with increasing depth.

Samples were taken to establish the distribution of sulphate / sulphide species with a view to assessing redox conditions. Negligible dissolved sulphide was indicated in all samples (Appendix 3.4) suggesting the absence of sulphate reduction. All tests for H_2S by smell, by adding acid to water samples, were negative. However, in the presence of Fe^{2+}, sulphide would be precipitated as amorphous iron sulphide. Therefore, sulphate reduction cannot be ruled out.

Manganese and iron are in the reduced forms Mn^{2+} and Fe^{2+}, according to the stability fields indicated by Eh-pH relationships (Fig. 3.6). The field boundaries are defined for concentrations of 10 mg/L for both. The 700 m interval between the 2300 level and surface could not be sampled, but Fe^{2+} and Mn^{2+} in groundwater suggest that there may be precipitated Fe and Mn oxyhydroxide with the potential to act as redox buffers in the section towards the surface.

Plate 3.4 Precipitated salts and corrosion on electrical switch on the 4500 level.

The combined effect of atmosphere and discharging groundwater can be seen on subsurface installations (Plate 3.4).

3.3 Stable Isotopes

3.3.1 Water isotopes - ^{18}O and ^{2}H

A local meteoric water line (LMWL) for Yellowknife was calculated from monitoring data for the years 1989-1993:

$$\delta^2H = 6.75\,\delta^{18}O - 20.1$$

(Standard errors: Slope = 0.21; Intercept = 4.61. Regression was significant: F = 1057) and used to relate precipitation to surface and groundwater samples. The regression, with 95 % confidence limits is shown in Fig. 3.7 along with the monitoring data. The rain sample collected in June 1996 ($\delta^{18}O$ =-15.88 ‰; $\delta^{2}H$ =-125.4 ‰) plots close to this line. Following are basic statistical results for local precipitation, calculated from the precipitation data (all values in ‰):

	Max	Min	Range	Standard deviation	Precipitation-weighted mean
$\delta^{18}O$	-9.01	-32.08	23.07	5.10	-20.54
$\delta^{2}H$	-92.7	-228.6	135.9	35.0	-157.2

Mean weighted deuterium excess (d) = 7.1.

Mean Annual Air Temperature = -5.08 ^{0}C.

Precipitation-weighted mean of the isotopes was obtained by weighting the isotope

measurements according to the amount of rainfall associated with those measurements. The relationship between mean monthly $\delta^{18}O$ in precipitation, and air temperature for the period 1989-1993 is $\delta^{18}O = 0.23\,T - 20.58$, obtained by regression of the measured data for these variables.

Isotope values for surface waters (Appendix 3.5) plot on an evaporation trend towards enriched ^{18}O and depleted ^{2}H relative to the LMWL, reflecting the range of evaporative effect on the different water bodies sampled (Fig. 3.8). The intersection between this trend ($\delta^{2}H = 4.10\,\delta^{18}O - 71$) and the LMWL lies at $\delta^{18}O = -19.2$ ‰ and $\delta^{2}H = -150$ ‰. The set of monthly samples from Yellowknife Bay showed ^{18}O depletion through the addition of meltwater from the later stages of the summer thaw, with a minimum value of -16.87 ‰, 0.8 ‰ less than the average $\delta^{18}O$ of -16.05 ‰, and a maximum of -15.6 ‰ in winter while the lake was frozen over.

Groundwater isotope content (Appendix 3.6) from the shallowest levels (2300 and 3500) indicate a dominant component of meteoric water by plotting on the LMWL, or below (Fig. 3.9). Representative isotope results are listed in Table 3.1. Two distinct influences of meteoric water are present. The first is shown by waters that plot closest to modern precipitation values. These mostly have $\delta^{18}O$ between -19.3 ‰ and -19.7 ‰, around 1 ‰ enriched relative to the weighted mean of precipitation, and are depleted in ^{2}H, which could indicate the presence of snowmelt in recharge. The second meteoric water influence is seen in waters that plot in a range depleted in ^{18}O and ^{2}H relative to the mean of local precipitation. This indicates the existence of precipitation derived from colder climates of

the past, and/or the presence of glacial meltwater. However, temperatures since the last glacial retreat have been higher than present day values, and therefore recharge of the depleted water must date back at least as far as that time.

Deeper waters carry an excess of ^{2}H, with respect to ^{18}O, which makes them plot above the LMWL (Fig. 3.9), characteristic of Yellowknife area shield brines (Frape *et al.*, 1984). Most waters at the 4500 level, and deeper, plot more closely to a trend between the brines and the depleted meteoric waters than between brine and those with a modern groundwater signature.

Surface and groundwater isotope results fall into two separate groups suggesting that there is no flowpath connecting them (Fig. 3.9).

3.3.2 Sulphate isotopes ^{34}S and ^{18}O

The concentration and isotopic composition of sulphate are important indicators of sulphate origin, and are therefore useful tracers of groundwater flowpaths and mixing. This subject was reviewed by Fritz *et al.* (1994) for shield brines. Samples show a range of $\delta^{34}S$ values from +3.1 ‰ to +28.3 ‰, and $\delta^{18}O$ from -5.4 ‰ to +9.7 ‰ (Table 3.2). Results highlight three possible sources (Fig. 3.10).

The first is characterised by depleted ^{34}S and ^{18}O contents. The $\delta^{34}S$ is 3-4 ‰, expected for sulphate derived from oxidised sulphide, being within the range of results for pyrite

(+0.4 to +6.9 ‰) from the mine reported by Wanless *et al.* (1960). The most likely source is mining-related surface operations because similar isotope values were obtained from surface tailings ponds (Fig. 3.10), although oxidation of pyrite in mineralised zones is a potential source of sulphate, either at outcrop, or in the subsurface. The negative $\delta^{18}O$ is typical of sulphate derived from oxidation of sulphide, where oxygen in the sulphate comes from water (precipitation or groundwater having $\delta^{18}O$ of -20 ‰, or less), subject to fractionation (fractionation factor $\varepsilon^{18}O_{SO4\text{-}H2O}$ = +4.1 ‰), and air ($\delta^{18}O$ = +23.8 ‰). For given values of $\delta^{18}O$ in water and sulphate, proportionate contributions from the two sources have been calculated by van Everdingen *et al.* (1985). In the case of the isotopically depleted sulphates, oxygen is indicated to be derived in approximately equal amounts from each.

TABLE 3.2 Sulphate concentration and isotopes

Sample	Location	SO_4 (mg/L)	$\delta^{34}S$ ‰ VPDB	$\delta^{18}O(SO_4)$ ‰ VSMOW	$\delta^{18}O(H_2O)$ ‰ VSMOW	$\delta^{18}O(SO_4\text{-}H_2O)$ ‰ VSMOW
23-A	2300-14140-4	1049	22.95	9.73	-23.69	33.42
23-B	Y-5-2	1202	11.23	7.74	-20.74	28.48
23-C	Y-6-2	1150	10.23	7.98	-19.66	27.64
23-E	646-2	538	4.08	-5.35	-19.45	14.10
35-A	9362-2	662	26.26	8.97	-20.92	29.89
35-B	8906-2	135	10.46	1.66	-19.32	20.98
35-D	9452-3	726	17.53	6.21	-19.72	25.93
45-A	5316-2	484	23.32	7.64	-19.12	26.76
45-B	3457-2	658	23.78	8.71	-20.59	29.30
45-D	3450-4	738	20.53	6.19	-19.22	25.41
45-E	5318-2	512	19.7	5.41	-19.14	24.55
45-G	3362-2	489	21.64	6.64	-18.36	25.00
49-A	5310-2	744	25.62	8.24	-20.13	28.37
49-B	4900-15130-4	443	28.33	8.01	-16.48	24.49
53-A	7126-3	122	25.67	7.67	-14.36	22.03
53-B	5586-4	229	24.6	7.21	-14.35	21.56
sw-11-1	L. Pud Lake	687	4.31	-2.63	-15.59	12.96
sw-12-1	U. Pud Lake	1077	3.15	-3.88	-14.83	10.95

The second source has relatively enriched $\delta^{18}O$ (5.4-9.0 ‰) and $\delta^{34}S$ (19.7-28.3 ‰), associated with the $^{18}O/^{2}H$-depleted shallow brackish meteoric waters, and brines. A Devonian marine evaporite could be the source of this sulphate (Bottomley *et al.*, submitted), however none has been identified on site. The closest published data relating to gypsum from near Gypsum Point, 50 km southwest of Yellowknife (Fig. 2.1), show $\delta^{34}S$ of 15.1 ‰ and 22.6 ‰ (Claypool *et al.*, 1980).

Samples analysed during this project have intermediate composition, lying on a trend suggestive of mixing between sulphate derived from sulphide oxidation and from dissolved evaporites. The maximum $\delta^{18}O$ of sulphate is 9.7 ‰ (23-A) which is below the lower limit of the Devonian marine evaporite range, possibly due to this mixing. However, samples taken from sites on the 4500 level in 1980 produced values of up to 16.7 ‰ (Fritz *et al.*,1994). The intermediate depth (4500 level) sites show a more depleted influence than the shallow sampling points towards the south end of the mine. This suggests that water infiltrating to the 4500 level contains a greater proportion of sulphate from areas where sulphide oxidation is occurring.

At equilibrium, the fractionation factor between $^{18}O_{sulphate}$ and $^{18}O_{water}$ at ambient temperatures should be 32-35 ‰ (Lloyd, 1968; Mizutani and Rafter, 1969), much more than the difference (21.5 - 22 ‰) between the two seen in the brines (Fig. 3.11). Therefore $^{18}O_{sulphate}$ and $^{18}O_{water}$ are not at equilibrium at the measured temperatures. The rate at which equilibrium is reached is highly dependent on temperature and pH, and

exceeds 10^6 years at neutral pH and present temperatures (Chiba and Sakai, 1985). Higher temperatures, or lower pH, reduce the equilibration time. Measurements of current conditions suggest that sulphate was introduced to the brines within the last few million years and, therefore, that the sulphate observed is not indigenous to brines that are older. Alternatively, the fractionation could reflect equilibrium achieved at a shorter time into the past due to the existence of higher water temperatures than currently seen.

The third effect is seen only at sites 23-B and 23-C. They have an enriched ^{18}O ($\delta^{18}O$ = +8 ‰), but intermediate $\delta^{34}S$ (+10 to +11 ‰) (Fig. 3.9). Waters from these locations have some of the highest sulphate concentrations (>1,100 mg/L) amongst the samples collected. Their origin is not known. Hattori and Cameron (1986) observe that $\delta^{34}S$ in sulphate of magmatic/hydrothermal origin in Archean greenstones is mostly in the range +8 to +14 ‰. For such sulphate, $\delta^{18}O$ near +10 ‰ can be expected (Fritz *et al.*, 1994). The sulphate in samples could derive from such an origin, its slightly lower $\delta^{18}O$ (+8 ‰) explained by mixing with sulphate from pyrite oxidation. Alternatively, the ^{18}O content might be explained by oxidation of sulphide where the presence of atmospheric oxygen is dominant over that from water, as observed by van Everdingen *et al.* (1985), a conceivable situation in mine waste dumps on surface. In this case, some sample isotope values might be explained by the additional presence of isotopically enriched sulphate from dissolved evaporites, added through mixing in the groundwater flow system.

3.3.3 ^{13}C from Dissolved Inorganic Carbon (DIC)

Analytical results for $\delta^{13}C$ in dissolved inorganic carbon (DIC) are given in Appendix 3.6. A summary of results representative of sampled locations is given in Table 3.3. The groundwaters show a range of -18.5 ‰ (slightly lower, to -20.6 ‰, in early samples not preserved for $\delta^{13}C$ analysis) to -8 ‰. The trend in variation in DIC as meteoric water

TABLE 3.3 Representative HCO_3(DIC) concentration, DIC and calcite isotopes

Sample	Location / Borehole	HCO_3(DIC) (mg/L)	$\delta^{13}C$ ‰ VPDB	^{14}C (pmC)
Groundwater				
23-A-5	2300-14140	13.36	-16.56	38.16
23-B-3	Y-5	295.85	-15.89	62.24
23-C-3	Y-6	282.43	-15.05	
23-E-3	646	366	-14.09	
23-F-1	660	311.7	-12.16	
35-A-3	9362	12.56	-17.17	59.74
35-B-3	8906	363.71	-15.22	71.90
35-D-3	9452	54.60	-17.00	
45-A-3	5316	32.25	-12.37	
45-B-3	3457	20.80	-17.54	
45-D-1	3450	13.4	-19.08	
45-E-3	5318	38.63	-18.49	
45-G-3	3362	31.80	-14.60	
49-A-3	5310	2.26	-10.66	
53-A-3	7126	4.64	-8.00	
Surface water				
sw-1-1	Yellowknife Bay	49	-3.35	
sw-2-1	Rat Lake	89.9	-6.17	
sw-4-1	Kam Lake	71.3	-3.85	
sw-10-1	Pumphouse faucet	41.4	-4.46	
Fracture carbonate				
Sample		$\delta^{18}O$ ‰ VSMOW	$\delta^{13}C$ ‰ VPDB	
YKN-SS1	S of Negus Point	11.21	-3.04	
YKN-SS2	S of Negus Point	11.34	-3.12	
YKN-SS3	S of Negus Point	9.16	-1.58	
YKN-US1	3500L shear zone	12.42	-3.3	
YKN-US2	3500L 15750 (Negus F)	9.11	-3.63	
YKN-US3	3500L near 35-B (Angel F)	12.95	-15.42	

infiltrates from surface is illustrated by the relationship between $\delta^{13}C$ and Cl concentration (Fig.3.12). Waters are differentiated by the relationship between $\delta^{13}C$ and HCO_3 concentration (Fig. 3.13). $\delta^{13}C$ measured in surface waters ranges from -3 ‰ to -6 ‰. These relatively high values are caused by exchange with atmospheric CO_2 (-6 to -7 ‰), with input from organically derived CO_2 (-23 to -25 ‰) after recharge at the ground surface. Fractionation between CO_2 gas and DIC ($\varepsilon^{13}C_{DIC\text{-}CO2}$), reaching approximately +9 ‰ at the sampling temperature (15 °C approx.) and pH (>7.3), is integrated in the actual $\delta^{13}C$ measured in groundwaters.

Most of the shallowest recent meteoric groundwaters have $\delta^{13}C$ values of approximately -14 to -16 ‰, and high DIC concentrations, e.g. 35-B (up to >400 mg/L HCO_3). Dissolution of soil CO_2 (estimated $\delta^{13}C$ of -23 to -25 ‰) from organic carbon oxidation in the shallow subsurface during recharge is the reason for the ^{13}C depletion relative to surface water. The very high DIC concentrations indicate that significant amounts of soil CO_2 are dissolved during recharge, or that large amounts of DOC accompany recharge and are oxidised in the subsurface. The soil CO_2 decreases pH causing calcite dissolution which adds ^{13}C-enriched DIC (-3.6 to -1.6 ‰ in collected fracture calcites).

More brackish, and saline waters (e.g. 23-A, 35-A) have similar, or lower, $\delta^{13}C$ values and much lower HCO_3 concentrations, but are still saturated with respect to calcite. Infiltrating meteoric water with high DIC concentrations (eg. 35-B) can evolve to these compositions by precipitating calcite on encountering high Ca concentrations in saline groundwater. The decrease in DIC is accompanied by a decrease in $\delta^{13}C$ from 35-B to 23-

A and 35-A close to the amount that may be explained by a Rayleigh distillation process (Appendix 3.7), where ^{13}C is preferentially removed by calcite precipitation. The extent of the decrease in $\delta^{13}C$ due to this process is limited by the small fractionation (<1 ‰) between calcite and HCO_3 in solution at neutral pH and temperatures of 15 ^0C or less (Appendix 3.7).

Five of the six fracture calcites from local surface and subsurface rock samples collected have $\delta\ ^{13}C$ values in the range -3.6 to -1.6 ‰ (Table 3.3). The remaining one, collected from the Angel fault close to the 35-B location on the 3500 level gave a value of $\delta^{13}C$ = -15.42 ‰, close to that of borehole 35-B water (-15.66 to -15.22 ‰). It suggests that the calcite could be precipitated from groundwater currently found in the Angel fault, consistent with fractionation of ^{13}C between calcite and DIC ($\varepsilon^{13}C_{CaCO3\text{-}HCO3}$) which ranges from +0.41 ‰ at 15 ^0C to -0.11 ‰ at 5 ^0C (Clark and Fritz, 1997).

Brine samples are characterised by enriched $\delta^{13}C$ values and very low DIC concentrations. Borehole 53-A on the 5300 level had a $\delta^{13}C$ value of -8 ‰, possibly indicating DIC predominantly from an original volcanic or hydrothermal source mixed with a meteoric water component diminishing with depth.

3.4 Radiogenic isotopes

3.4.1 Tritium

Very high levels of atmospheric tritium were generated by nuclear bomb testing during the 1950's and early 1960's, reaching a peak in 1963. Monitoring records since the early 1950's for the Ottawa area (Brown, 1989) illustrate the relative variation with time (Fig. 3.14). Tritium levels in precipitation at that time were high enough to be detected in groundwater for up to 40-50 years after recharge. As atmospheric levels decline through decay (half-life 12.43 years), and absorption in oceanic water, this detection period is also declining. Thus, measurable tritium in discharging groundwater indicates the presence of "modern" recharge, constraining the circulation time of at least a component of that water to less than a few decades. Prior to bomb testing, atmospheric tritium levels were much lower and would now be undetectable due to decay.

During this study, tritium was measured to assess the contribution of modern recharge to groundwaters at all levels in the mine, and determine rates of circulation. Results are given in Appendix 3.6.

Precipitation monitoring data from Yellowknife for 1989-1993 (IAEA database) show seasonal variation from less than 10 TU in winter to almost 40 TU in summer (Fig. 3.15), with a weighted mean of 20 TU. Surface lakes off-site showed tritium content slightly below this average. However, the two tailings ponds sampled on-site contained 30 TU

which may reflect the composition of water recharged since the early 1960's and pumped from the mine in the past few years.

Tritium was measured (>0.8 TU) at all underground sites analysed except one. It was below detection at site 23-D where the borehole is not associated with any of the three main faults, and currently produces approximately 0.01L/min. The absence of detectable tritium 38 years after the borehole was drilled helps to constrain surface-depth hydraulic parameters at this location. Tritium bordered on the detection limit at the sites at the deepest level (5300). The effect of dilution of tritium content, introduced in recently recharged meteoric water, by mixing with untritiated groundwater, reduces its detectable concentration, especially at greater depths. The presence of tritium indicates that modern recharge is being transported by active surface to depth groundwater flow and has a maximum mean residence time of the order of 40-50 years before discharging at depths of at least 1,615 m (5300 level).

Residence times of modern meteoric waters at the 4500 level are estimated to be in the range of 6-20 years. Reported values from previous sampling in 1981 and 1985 (Frape and Fritz,1981; Macdonald, 1986) for three locations, 45-B, 45-D, and 45-G, are much higher than results from the recent sampling, therefore closer to the 1963 bomb peak. Monitoring of sites 45-B and 45-G since 1980 shows that the 1963 peak passed those locations in the early to mid-1980's. These sites showed low tritium content, corrected for dilution by tritium-free groundwater (glacial water and brine components calculated in the mixing model below), in 1980 of 11.1 and 8.3 TU, increasing by 1981 to 85 and 89.8

TU, respectively, remaining high in 45-B in 1985 (86.4 TU), and dropping back to 19.4 and 23.2 TU at the two sites by 1996(Table 3.4). Results indicate a 20 year maximum mean residence time for a modern recharge component of the groundwater discharging from those boreholes. The results from the new sampling are lower than would be expected by decay alone of the previous levels, indicating that it is post-bomb recharge. The levels of tritium in meteoric water recharge since bomb testing have been attenuated, in addition to decay, by absorption of atmospheric tritium in ocean water.

The tritium content of samples (Table 3.4) falls in a limited range, in a few cases exceeding the weighted mean (20.8 TU) from monitoring data for 1989-1993 (Fig.3.16). On the assumption that modern recharge has been diluted by untritiated groundwater according to the mixing model calculations below, tritium content has been calculated for "undiluted" modern meteoric water (Table 3.4) as a step towards a standardised comparison of tritium content in modern meteoric waters across the study area. Some water samples from Negus fault intersections contain tritium levels higher than the weighted mean of the monitoring data (Fig. 3.16). This suggests that these waters were recharged before 1989, have a mean residence time of >6 years, and originate from higher atmospheric tritium levels of the 1980's and 1970's (Fig. 3.14).

Angel and Pud fault waters contain less tritium. The significance of this is equivocal. It could be a result of less tritiated younger recharge along a more conductive flowpath, as Angel faults are likely to be, given their high associated inflow rates and orientation

TABLE 3.4 Tritium results, and calculated tritium corrected for dilution of modern meteoric water

Sample	Fault	1980		1981		1985		Jul-95		Nov-95		Jun-96	
		measured	*calc*	measured	*calc*	measured	*calc*	measured	*calc*	measured	*calc*	measured	*calc*
23-A	Pud												
23-B	Angel											11.9	*24.8*
23-C	Angel							19.6	*24.2*				
23-D	n/a							21.2	*22.6*	19.6	*22.0*		
23-E	Negus											<0.8	
35-A	Pud?							26	*26.8*	23.9	*24.9*		
35-B	Angel							16.4	*21.6*	15.4	*20.3*	17.9	*23.2*
35-D	Negus							19.3	*19.7*	21	*22.3*		
45-A	Pud/Negus									24.6	*28.3*		
45-B	Negus/?	3	*11.1*	34	*85*	57	*86.4*	10.7	*18.1*				
45-D	Negus	47	*71.2*			45	*70.3*	18.7	*24.6*	14.2	*18.7*	15.1	*19.4*
45-E	Angel/Negus											17.2	*26.9*
45-G	Angel/Negus	3	*8.3*	44	*89.8*			21.2	*29.9*				
49-A	Pud/Negus							11.8	*22.3*	13.3	*26.1*	8.8	*23.2*
49-B	Angel							4	*9.3*			4.4	*16.3*
53-A	Angel/Pud											2.4	*30.0*
53-B	Pud									<0.8		0.9	
53-C	Angel											1	*7.7*
										1.1		1.4	

parallel to the principal regional stress direction. Alternatively, it could be the effect of dilution of tritium by submodern and older untritiated recharge, dating from the early years of mine operations, or before, discharging from less conductive faults. Those having the NW-SE Pud orientation are normal to the current principal regional stress direction and, consequently, can be expected to have relatively low conductivity. Given the persistence of glacial water associated with the Pud, it is reasonable to assume that submodern meteoric water could also still be present. Very low tritium levels in water from boreholes 45-G and 45-B (3 TU) about six months after drilling in 1980, suggest that contamination that may have been expected from drillwater had already been mostly purged. What remained was either left over from drilling or evidence of influx of only a minor component of modern recharge.

3.4.2 ^{14}C from Dissolved Inorganic Carbon(DIC)

Four samples were selected for ^{14}C analysis. Results are given in Table 3.3. Three of the most depleted (^{18}O and ^{2}H) water samples, 23-A-5, 23-B-3 and 35-A-3, were selected on the assumption that the depletion implies paleo-recharge of glacial meltwater. These gave measured a^{14}C of 38.16, 62.24 and 59.74 pmC, respectively. One further sample, 35-B-3, was selected as being most representative of ^{14}C content in modern recharge because it was one of the least saline waters, and its isotopic content was similar to that of modern precipitation. In this sample a^{14}C was measured to be 71.90 pmC. Uncorrected apparent "ages", or mean residence times (MRT), have been calculated for these mixed waters (Appendix 3.9). These are minimum ages for the paleowater component, considering the

^{14}C input from recently recharged meteoric water which acts to reduce apparent age. However, mass balance calculations (Appendix 3.9), using the recent and glacial water fractions derived from the mixing model described later, suggest that virtually all of the ^{14}C is contributed by recent meteoric water, while that in the glacial component is very low (<3 pmC in 23-A-5 and 35-A-3). Therefore, the ages calculated based on ^{14}C content in diluted recent recharge have no meaning.

4. DISCUSSION

4.1 Water type

4.1.1 Identification of water types

Review of geochemical and isotope data suggests that salinity trends are due to specific water types. The presence of three end-members was indicated by a principal components analysis (PCA). This statistical approach was used to combine data from ten variables providing an objective illustration of relative water signature. Laaksoharju (1995) described the use of PCA to identify end-members in mixed groundwater inflow at the Åspö hardrock research laboratory in Sweden. In the Con Mine waters, it showed the presence of three clearly distinct influences, but also indicated association between mixed samples by their relative positioning in trends or groups (Fig. 4.1). Factor scores for individual samples are listed in Table 4.1. By inspection it can be seen that the most saline waters plot together at the end of one trend indicating the brine influence. It can also be seen from the elements in Factor 1 that the influence is strongest in samples where $\delta^{18}O$ and $\delta^{2}H$ have the highest relative values, and where sulphate concentration is lowest.

A second influence is seen in the point plotting furthest from the most saline and fresh waters. This is controlled mostly by its depleted ^{18}O, the signature of glacial water as defined in the mixing model below, and high sulphate content.

TABLE 4.1 Principal Component Analysis factor scores (Based on May 1995 data)

Location	Factor1	Factor2
23-A	-1.826	1.057
23-B	-0.413	-1.019
23-C	-0.207	-1.624
23-E	-0.085	-1.339
23-F	-0.100	-1.330
35-A	-0.991	0.354
35-B	0.312	-2.055
35-C	-0.465	-0.255
39-A	-0.306	0.677
45-A	-0.268	1.114
45-B	-0.840	0.432
45-C	-0.571	0.538
45-D	-0.407	0.575
45-E	-0.373	0.382
45-G	0.068	0.771
49-A	-0.480	1.180
49-B	0.679	0.764
53-A	1.973	0.374
53-B	1.860	0.559
53-C	2.345	0.606

Thirdly, the freshest meteoric waters with the isotopic signature of present day precipitation fall towards the end of a trend at right angles to the brine influence. Their position is determined by the dominant effect of bicarbonate, shown by its large negative loading coefficient in Factor 2 (Fig. 4.1).

Certain waters fall around the intersection of the trends showing, by their relative position, which influences are strongest in each, and which sites are most closely related, for example 35-A and 45-B.

4.1.2 Brine

Apart from its high salinity, brine is distinguished from meteoric water by its very enriched deuterium and depleted ^{18}O relative to meteoric water. The most extreme brine influence is indicated by maximum $\delta^{18}O$ = -13.5 ‰, and $\delta^{2}H$ = -56 ‰ at site 53-C. By comparison, a theoretical "pure" brine end-member is expected to have a $\delta^{18}O$ of -10 to -12 ‰, and $\delta^{2}H$ of -20 to -50 ‰(Frape *et al.*, 1984), this being the area of convergence of ^{18}O/deuterium regression lines for several sites across the Canadian Shield. Pearson (1987) calculated a value for $\delta^{18}O$ of -9±2 ‰ based on extrapolation to halite saturation.

Salinity reaches a maximum TDS of 290 g/L with chemistry completely dominated by the Ca-Na-Cl composition.

4.1.3 Glacial water

Water from certain sites, most obviously the samples from the south end of the 2300 level drift, with minimum $\delta^{18}O$ = -23.9 ‰ and $\delta^{2}H$ = -187 ‰, is depleted in ^{18}O (by 3.5 ‰) and ^{2}H (by 30 ‰) relative to the mean of present day precipitation. It also plots slightly below the LMWL for the district, calculated earlier. It indicates the presence of water of glacial origin. This type of water was found only as a component of bulk groundwater mixed with components from other sources. Additionally, this water has tritium indicating that it is a mixture containing recent recharge, implying the presence of a component more depleted than the composite sample value of -24 ‰, therefore closer to glacial influence.

About 10,000-9,000 years BP, during glacial regression, proglacial lakes, including Lake McConnell which covered the area on and around that now occupied by Great Slave Lake, developed at the margin of the retreating ice sheet. The lake water probably consisted in roughly equal proportions of glacial meltwater and precipitation, according to work done on Lake Agassiz in northern Manitoba (Teller,1990). Assuming for modelling purposes that it approximated the isotopic composition of a mixture of precipitation and meltwater recharging a water table within the retreating ice sheet, and assuming that glacial ice at that time had $\delta^{18}O$ of about -30 to -35 ‰, comparable with similarly aged Pleistocene ice from Dye-3, Greenland (Dansgaard, 1982), and that precipitation was close to -20 ‰, as today, water available for recharge could have been near $\delta^{18}O$ of -27 to -28 ‰.

The waters showing a glacial influence have a Na-Ca:Cl-SO_4 composition, unlike the recent groundwater component. Sulphate concentration is unusually high, and HCO_3 is very low. Mineral saturation calculations show calcite to be undersaturated, and gypsum to be marginally undersaturated.

4.1.4 Modern meteoric water

The LMWL calculated from precipitation monitoring data intersects the surface water evaporation regression line at $\delta^{18}O$ of -19.0 ‰, and $\delta^{2}H$ of -151 ‰. The least saline

groundwater samples have $\delta^{18}O$ in the range -19.3 to -19.7 ‰ and $\delta^{2}H$ of -150 to -160 ‰. This is in good agreement with the intersection, and suggests that they are recently recharged meteoric waters that have $\delta^{18}O$ close to the mean annual value for local precipitation.

The waters are brackish, mostly Ca-Na:SO_4-HCO_3-Cl with TDS in the range 1,000-2,000 mg/L, and $CaCO_3$ saturated.

4.1.5 Submodern meteoric water

Although it has not been distinguished by PCA, submodern recharge, identified by its lack of detectable tritium (not included in the PCA), can be present as an otherwise invisible component of infiltrating meteoric water. Such water has a circulation time >40-50 years. The early years of mining from 1937 onwards can be expected to have induced surface to depth flow. Therefore, for modelling purposes, it is assumed that much of the submodern meteoric water is mining-related, and it has been combined with modern meteoric water in the "recent" end-member.

Water from borehole 23-D has a salinity of <30,000 mg/L, an order of magnitude less than the deeper brines, and therefore contains a dominant component of meteoric water. Its isotopic composition is more closely related to current precipitation than to the most depleted meteoric water, suggesting dominance of meteoric water with current precipitation signature. However, having no detectable tritium, it is therefore >40-50 year

old recharge. By similar reasoning, water from borehole 45-G also contained submodern meteoric water when sampled soon after it was drilled in 1980. However, it contained very low tritium (3 TU) which could have derived either from drilling contamination or from minor modern influx.

4.2 Mixing

4.2.1 Introduction

Water composition can be represented as a result of mixing of brine, glacial water, and recent meteoric water within the groundwater flow system. A possible explanation for the presence of a mixture of water types at diagrammatically represented borehole inflow locations is illustrated in Fig. 4.7 (during mining panel). Further, more complex mixing occurs where a borehole has intersected more than one fault, each with its own distinct water type, as is the case at sites 45-B, 45-A, and 45-E.

4.2.2 Geochemical composition as an indicator of mixing

In the shallow, least saline waters there is evidence of active geochemical processes, primarily dissolution by meteoric water of calcite, and probably gypsum, producing Ca-SO_4 to Ca-HCO_3 composition water which can raise TDS up to 3,000-5,000 mg/L, and precipitation of low temperature secondary minerals, such as calcite, in faults. These processes preclude observation of end-member mixing in geochemical data for these waters. The chemical composition of waters showing huge salinity increases from

brackish to saline water and brine is completely dominated by Cl, Ca, and Na, the proportions of which change little. A linear relationship between these can be seen (Fig. 3.4) above Cl concentrations of 1,000-2,000 mg/L as the brackish waters infiltrate to depth. The linearity is an indication of predominant simple dilution of saline water and brine due to rapid influx of meteoric water to depth, such that the effects of active, but relatively slow, rock-water chemical processes are not seen.

4.2.3 Water isotopes as indicators of mixing

Mixing is evident from the $\delta^{18}O/\delta^{2}H$ relationships. A trend can be seen between meteoric water and brine (Fig. 3.9). Mixing also takes place between recent meteoric water and glacial meltwater. Sites 23-A and 35-A are the best examples of such mixing. By contrast, water sampled at site 23-D, having undetectable tritium, demonstrates the existence of water that could range from submodern to older. Although it plots above the LMWL due to the influence of brine, site 23-D water apparently contains both untritiated submodern, and glacial meteoric waters.

4.2.4 Sulphate isotopes as indicators of mixing

Sulphate input derives from two main sources, one at surface producing sulphate depleted in ^{34}S and ^{18}O, the other supplying sulphate with enriched ^{34}S and ^{18}O as seen in meteoric water having a glacial component, for example in 23A water samples. As water infiltrates to depth there is mixing of the two (Fig. 3.11). An apparent "mixing" trend exists (Fig. 3.10) reflecting the proportional contribution from each source. However, it is not a

quantitative indicator of overall water mixing since it takes no account of meteoric water with low sulphate concentration as seen in Angel fault flow at site 35-B. Nor is there sufficient knowledge about the actual distribution of sulphate sources to allow estimation of water input from specific flow paths using sulphate data.

As was seen earlier, sulphate is a qualitative indicator of influx of meteoric water as it migrates to depth and mixes with brine.

4.2.5 ^{13}C as an indicator of mixing

In samples with Cl > 30,000 mg/L, $\delta^{13}C$ shows enrichment from a minimum of -18 ‰, as Cl concentration increases, to $\delta^{13}C$ = -8 ‰, as DIC from shallower groundwater mixes with that of possibly volcanic or hydrothermal origin in saline waters and brine (Fig 3.12). Where Cl < 30,000, $\delta^{13}C$ content is controlled by changes in DIC content as infiltrating meteoric water is exposed to soil CO_2 and associated fractionation.

4.2.6 Definition of end-members for mixing model

Theoretical end-members have been used to generate an analytical solution for the influences that are indicated by PCA. For the three influences indicated, the characteristics of end-member waters were most simply defined in terms of the two variables, $\delta^{18}O$ and chloride concentration (Fig. 4.2), both of which can be considered as conservative in the context of the short-term period investigated by this study.

They are as follows:

	$\delta^{18}O$	Cl
1) Brine	-10.0 ‰	230,000 mg/L
2) Glacial water	-28.0 ‰	4,800 mg/L
3) Recent meteoric water	-19.2 ‰	10 mg/L

For the brine, $\delta^{18}O$ of -10 ‰ is consistent with the ranges -10 to -12 ‰, and -9+/-2 ‰, identified by Frape *et al.* (1984) and Pearson (1987), respectively. Pearson estimated the end-member brine at halite saturation to have a Cl concentration of 230,000 mg/L. The glacial water was defined by a $\delta^{18}O$ of -28 ‰, estimated above for Lake Agassiz, and chloride adjusted to twice the maximum concentration obtained from that site to compensate for dilution of glacial water by an approximately equal proportion of fresh precipitation water.

The $\delta^{18}O$ for recent meteoric water was taken as the value (-19.2 ‰) at the intersection of the surface water evaporation trend and the LMWL (Fig. 3.9), and the chloride concentration was arbitrarily selected as 10 mg/L, less than the lowest sample value.

4.2.7 Calculation of mixing ratios

The composition of individual samples can be expressed in terms of mixing ratios of the three end-members. The results show the relative distribution of each water type across the study area, and how they change through time. Component fractions are relatively

insensitive to the precision of estimated end-members, but distorted, or negative, values can occur where one component is completely dominant or very low.

Starting with the assumption that the three components combined represent 100 % of a sample, $\delta^{18}O$ and chloride concentration proportions were calculated by solving the following equations:

$$C_T = C_B + C_G + C_R \qquad (1)$$

where C_T is the sum (=1) of the brine component C_B, the glacial water component C_G, and the recent meteoric water component C_R, and by mass balance equations for $\delta^{18}O$ and Cl:

$$C_T \delta^{18}O_T = C_B \delta^{18}O_B + \delta^{18}O_G C_G + C_R \delta^{18}O_R \qquad (2)$$

$$C_T Cl_T = C_B Cl_B + C_G Cl_G + C_R Cl_R \qquad (3)$$

followed by substitution in equation (2) for C_R from equation (1), and rearrangement, to obtain:

$$C_B = \{C_T(\delta^{18}O_T - \delta^{18}O_R) - C_G(\delta^{18}O_G - \delta^{18}O_R)\} / (\delta^{18}O_B - \delta^{18}O_R)$$

and substitution in equation (3) for C_B from equation (1) to obtain:

$$C_R = \{C_T(Cl_T - Cl_B) - C_G(Cl_G - Cl_B)\} / (Cl_R - Cl_B).$$

There is a unique solution for C_G when $C_T = 1$. The other two components are calculated by back-substitution. Results of calculations indicating water composition in terms of end-member fractions are shown in Appendix 4.1. Representative results (Table 4.2) are used to illustrate relative component distribution, spatially, in Figs 4.3, 4.4, and 4.5.

4.3 Distribution of water types across the study area

4.3.1 Spatial distribution

The hydraulic conditions in the past could have resulted in a general distribution of water types as shown in Fig. 4.7. At this time, brine is the dominant component of water only at the sampled locations at the 5300 level (Fig. 4.3). Recent meteoric water is present at all sites but shows a marked reduction below level 4900 (Fig. 4.4). The glacial water influence is seen across the study area, most evident towards the south end of all drifts

Table 4.2 Groundwater composition in terms of end-member fractions

Sample	Date collected	Recent	Glacial	Brine
23-A-3	Nov-95	0.45	0.54	0.00
23-B-3	Nov-95	0.74	0.25	0.01
23-C-3	Nov-95	0.89	0.11	0.00
23-D-3	Nov-95	0.61	0.27	0.12
23-E-3	Nov-95	0.96	0.04	0.00
23-F-3	Nov-95	0.96	0.04	0.00
35-A-3	Nov-95	0.76	0.21	0.03
35-B-3	Nov-95	0.94	0.06	0.00
35-D-3	Nov-95	0.87	0.09	0.03
43-A-3	Nov-95	0.49	0.24	0.26
43-B-3	Nov-95	0.75	0.17	0.08
43-C-3	Nov-95	0.56	0.32	0.12
45-A-3	Nov-95	0.56	0.25	0.19
45-B-3	Nov-95	0.76	0.19	0.05
45-C-3	Nov-95	0.56	0.27	0.18
45-D-3	Nov-95	0.63	0.19	0.18
45-E-3	Nov-95	0.71	0.15	0.14
45-F-4	Jun-96	0.01	0.38	0.61
45-G-3	Nov-95	0.51	0.21	0.27
49-A-3	Nov-95	0.32	0.39	0.29
49-B-3	Nov-95	0.18	0.33	0.49
53-A-3	Nov-95	-0.07	0.28	0.79
53-B-3	Nov-95	-0.05	0.27	0.78
53-C-3	Nov-95	-0.08	0.24	0.84
53-D-4	Jun-96	0.05	0.29	0.66

down to the 4900 level, closest to Pud-related flow (Fig. 4.5). This may imply segregation of water type by fault, or it could simply result from older holes having produced larger volumes allowing glacial water to be replaced by modern meteoric water.

The depths currently reached by meteoric water are certainly due to the influence of mining on the groundwater flow system. However, there was a significant volume of glacial water already in the system, demonstrated by its present rate of inflow (2 L/min) at site 23-A, and historic production at site 45-B since the borehole was drilled in 1980. Prior to the commencement of mining, infiltrating fresh and brackish glacial water may have been restricted in migrating to depth by the density contrast between it and the underlying brine, which could have been over 20 %.

The fault system provides pathways for movement of waters between points of surface recharge, or local subsurface occurrence of fracture minerals able to affect the chemical composition of groundwater, and discharge points in the mine openings. Site 23-D does not intersect any of the main faults, and its flow rate of 0.01 L/min and high salinity for its depth of 42,000 mg/L suggest a tight fracture system poorly connected, if at all, with the primary water-conducting faults.

4.3.2 Association of water type with the Negus Fault

In boreholes intersecting the Negus fault, water composition was seen to evolve toward lower proportions of recent meteoric water with depth (Fig. 4.6a). At the 4500 level, the brine component was relatively uniform, while the glacial water influence strengthened

southwards. This might be a consequence of either mixing along flow towards an area having a resident body of glacial water, or influx of groundwater with a component of glacial water to the southern area of the mine. However, tritium is generally higher in Negus fault water than in Angel and Pud flow (Fig. 3.16).

Input of recent meteoric water from another fault pathway is clear at site 45-B (Fig. 4.6a). Although a separate fault has not been previously distinguished in the borehole, one is strongly indicated by the anomalously high recent component. The identity of faults on this other pathway is unknown. Mixing of water from two faults in the borehole simulates the effect of meeting of separate fracture flows at fault plane intersections. The composition of the resultant flow is controlled by that of the separate flows, and the proportion in which they are mixed, which is in turn dependent on the relative hydraulic characteristics of the faults and flow.

4.3.3 Association of water type with Angel-type faults

The Angel-type faults are associated with the highest proportions of recent meteoric water inflow to boreholes at the 3500, 4500, and 5300 levels, and the least saline. Site 35-B with TDS of 1,300 mg/L, produces water at up to 8 L/min with exceptionally low salinity for its depth. It has an exceptionally low sulphate concentration compared with other meteoric groundwaters. The Angel-type fault intersected at this site is clearly not the same one identified in the boreholes at the shallower sites 23-B and 23-C where discharging water has much higher sulphate concentrations.

4.3.4 Association of water type with the Pud Fault

Boreholes intersecting a Pud-type fault produce a significant component of glacial water, with the exception of 53-B where the brine influence is very dominant. This suggests that the Pud fault is connected with a groundwater reservoir where glacial water has been stored since it was recharged thousands of years ago. The inflow with the greatest proportion of glacial water is that at location 23-A, at the extreme south end of the 2300 drift, within the block bounded by the Pud and Negus faults. The high glacial component at site 49-A suggests that it is similarly remote from recent meteoric water influence. In contrast, 35-A water, with its intermediate depletion and significant tritium, clearly receives additional modern input from surface through a fault more conductive than the Pud. In character it most closely resembles site 45-B, and the most recently (June 1996) sampled 45-A water. In overall character 49-A and 45-A were most closely associated with each other in July 1995, although since then their isotopic content has evolved in opposite directions, 49-A towards a greater brine influence and 45-A to increased recent meteoric water.

4.4 Temporal variation

4.4.1 Introduction

An objective of this project was to determine if the groundwater system has changed, and continues to change, as a result of mine excavation. Inferences have been drawn about groundwater behaviour before mining started, and local disturbance to distribution of end-member water types near points of groundwater inflow (Fig. 4.7). The original

distribution of waters in the mine cannot be determined from sample data because of the unknown extent of disturbance created by earlier mine excavation. The extent of actual changes in groundwater composition can only be assessed for the period since dedicated samples for chemistry and isotope analysis were first collected in 1980. Data obtained during this study, and results from those earlier samples have shown considerable change within time scales of as little as one year. The period of monitoring at the 4500 level spans sixteen years since the first of the sampled boreholes was drilled, while sites sampled at the deeper 5300 level were not drilled until 1988 and later.

4.4.2 Pre-mining situation

There is no information about regional groundwater flow but water could have entered the fault system in the area of the mine by lateral migration from outside the area, or by infiltration from surface locally, or a combination of the two.

The presence of a persistent ^{18}O depletion, supported by ^{14}C content, shows the existence of a reservoir of glacial water. Warmer climatic conditions than those today, with ^{18}O content similar to, or higher than current values, have prevailed since deglaciation in the Yellowknife region. Thus, the ^{18}O depletion cannot derive from recharge occurring since the last deglaciation. Therefore, this water had remained in place in a relatively stable hydrodynamic environment for at least 9,000-10,000 years prior to the mine being opened. There are indications (Section 4.1.5) of meteoric water recharge up to submodern time (site 23-D), which could predate the mine, but are more likely to have infiltrated as a

result of early mine operations. Snowmelt and storm runoff can be expected to infiltrate surface faults locally. Groundwater discharge other than that within the mine has not been identified.

4.4.3 Groundwater flow system change during the early mining period (1937-)

Mine shaft excavation started in 1937, but not until 1946 did it reach approximately 750 m (2,500 ft), and in 1974 the Robertson shaft was sunk to 1,890 m (6,200 ft). Further mining activity, drift opening, and borehole drilling would have increasingly disturbed the groundwater system, inducing flow towards the openings.

Evidence for infiltration of recently recharged water is given by the presence of tritium in groundwater, detected (>0.8 TU) in all but one (23-D) water analysed down to the 5300 level. This is "bomb" tritium in water recharged since nuclear bomb testing in the 1950's to 1960's. Tritium was reported in water from sites on the 4500 level in 1980, 1981 (Fritz and Frape, 1982), and 1985 (Macdonald, 1986). Early mine excavation would have created a surface to depth flow of water which would no longer have detectable tritium. The presence of such submodern recharge may be indicated at sites 23-D and 45-G as discussed earlier.

4.4.4 Groundwater composition change during monitoring (July 1980-June 1996)

Changes in the chemistry and isotope composition of groundwater since 1980, and continuing during the period of this study, have been significant at several sites,

especially at the 4500 level. The predominant change below the 2300 level was towards increased salinity, except at borehole 45-A.

Pressure monitoring (Intera, 1997) indicates hydraulic connection between all sites on the 4500 level, regardless of which faults have been intersected, and with sites on the deeper 4900 and 5300 levels. Consequently, hydraulic pressure change at any site could affect all locations with the effect of altering flow conditions and the balance of individual fault contributions to the overall groundwater flow mixture. Increased pressure could open less conductive, poorly connected faults releasing trapped water. The increased Cl concentration observed in June 1996 (Fig. 4.10), following 6-month shut-in periods for all boreholes, except 45-A and 45-E (found open in June 1996), and 53-A and 53-C (found with plugs blown out in June 1996), could be a consequence of borehole shut-in, especially where the faults intersected are not conduits for flow passing to other discharge points. However, the trend towards more saline discharge is clearly also a function of another, wider influence. This is apparent from the increasing salinity of water samples collected directly from Angel Fault seepage at location 49-B (Fig. 4.16) prior to the six-month shut-in of boreholes, and continuing until June 1996. Three conceptual flowing boreholes on the "during mining" panel on Fig. 4.7 show how different waters might contribute to mixed sample water. Coning of the interfaces between water types, if caused by flowing boreholes, should decay when flow is shut-in, and result in more saline discharge later because the flow of recent meteoric water from surface would be reduced.

Levels 2300-3500

Sites at the shallower levels, 2300 and 3500, were sampled from May 1995 to June 1996. The minor variability in composition of samples during regular sampling from July 1995 onwards is illustrated by Cl concentration (Fig. 4.8). The reason for the exceptionally dilute reconnaissance samples taken at 23-B and 23-C in May 1995 is not known.

Borehole 35-B was drilled to intersect the Angel fault in 1995 and sampled within weeks. It immediately produced modern meteoric water which did not change over the following year, indicating that it had tapped into an active surface to depth flowpath. Borehole 35-A, likewise, also produced water from the time of drilling that has so far remained very constant, apart from the first sample which was slightly more dilute than the others, with an isotopic signature intermediate between glacial and recent meteoric water. Borehole 35-D was first sampled only weeks after drilling. Subsequent sampling six months later showed a salinity drop of 50 %.

Level 4500

On the 4500 level, significant changes were seen at most sites, illustrated by deuterium (Fig. 4.9) and chloride concentration (Fig. 4.10). Variation in overall isotopic character of the water is shown for the four locations exhibiting the greatest change (Fig. 4.11).

After borehole shut-in, a shift was observed in 45-G (Fig. 4.12) and 45-E (Fig. 4.13) samples towards a relative increase in brine influence, or decrease in meteoric water. From 1995 to 1996, the Cl concentration at 45-E doubled, and by June 1996 site 45-G

had shifted towards the highest salinity seen since 1980 (Fig. 4.10), soon after drilling. This is a significant departure for a site where the water character in 1995 had changed little since 1981. The common behaviour, supported by the existence of pressure communication (Intera, 1997), confirms a physical link between the two holes which both intersect the Angel fault. The increased salinity is a plausible consequence of reduced flow of recent meteoric water from surface during borehole shut-in (flow control valve closed), while, at the same time, glacial water and brine distribution can change back towards the pre-mining state.

An increased influence of recent meteoric water was seen in borehole 45-B water sampled during previous work in 1980-1985 (Fig. 4.14), and in the most recently sampled 45-A water (Fig. 4.15). This is attributed to inflow from the Pud fault because glacial water was still significant, however, communication with surface via a more complex pathway involving another fault cannot be excluded. It can be explained as a drawing down of recently recharged water from surface after prolonged continuous discharge at the sampling sites 45-B and 45-A. When data were first obtained on 45-B in 1980 (Frape and Fritz, 1981), within a few months of drilling, composition indicated that discharge consisted of predominantly glacial water. Most of the glacial water was replaced by recently recharged water within five years, by 1985 (Fig. 4.14). It suggests good communication with surface. Drilling of 45-B appears to have drained a reservoir of predominantly glacial water which had lain in the local fault system between brine below and modern meteoric water above.

Site 45-A water changed significantly during the sampling programme, towards a higher component of recent meteoric water at the expense of the brine component (Fig. 4.15). The proportion of glacial water remained relatively unchanged. The borehole intersects the Negus and Pud faults. Whereas the water mixture, in terms of end-members, seemed to be consistent with Negus in November 1995 (Fig. 4.6a), it had changed by June 1996 to be very similar in composition to site 45-B water (Fig. 4.6b). This is attributed to a shift in the balance of contributions to borehole mixing away from Negus in favour of Pud inflow. Cl concentration in water from borehole 45-A decreased by 70 % during the study (Fig. 4.10).

Site 45-D composition was virtually unchanged during 1995-1996, although data from 1985 sampling (Macdonald, 1986) indicate that there has been a shift towards recent meteoric water since then. In spite of being in very good hydraulic pressure communication with borehole 45-E, it does not show the same change in composition towards increased brine at the latest sampling. Therefore, it is more remote from the source of the incoming brine.

As at the shallower levels, the 4500 level holes were shut-in after the November 1995 sampling.

Levels 4900-5300

From 1995 to 1996 there was a shift towards a brine isotopic signature at both 4900 level sites, borehole 49-A, and at the copiously dripping Angel fault where it intersects the drift at the 49-B sampling site (Fig. 4.16), especially after Nov 1995 when all the monitored boreholes were shut-in.

Less change was seen at 5300 level sites where high salinity brines persisted throughout the study. An increase in sulphate occurred with the effect of increasing calculated (SOLMINEQ.88) gypsum to marginal saturation, although no mineralisation was identified in the area of the boreholes.

5 CONCLUSIONS

Groundwater types: Groundwaters at the Con Mine are composed of mixtures of three primary water-types. These are:

1) Shield brine having high salinity up to 290 g/L,

2) a combined glacial meltwater and Early Holocene precipitation with ^{18}O and ^{2}H content depleted relative to present day precipitation, and

3) recent meteoric water with an isotopic signature close to that of present day precipitation, consisting of submodern (tritium-free) and modern recharge (tritium detectable).

Flow paths: At salinities of over 2,000-6,000 mg/L TDS, the composition of mine inflow is controlled by dilution of brine by meteoric water. Individual groundwater flow paths cannot be differentiated due to overall similarity of geochemical facies. However, salinity can be sufficiently different between faults that the effect of merging of flows from additional faults can sometimes be seen. Isotopic composition of dissolved sulphate (^{34}S, ^{18}O), and DIC (^{13}C), while indicating several possible origins, did little to differentiate fault flows. However, there are some subtle local spatial variations, and differences between discharge from separate faults, in isotopic (^{18}O, ^{2}H, ^{3}H) content of the water, according to the history of environmental conditions and timing of recharge specific to meteoric water components. Isotopic composition of sampled surface water bodies is unlike that of groundwaters, suggesting absence of a flow path between them.

Origin of sulphate and DIC: Sulphate isotopes indicate sulphate derivation from three possible origins: marine evaporite, atmospheric oxidation of sulphide, and local influence of a possible Archean magmatic / hydrothermal source.

The isotopic content of dissolved inorganic carbon (DIC) in groundwater suggests derivation from biogenic (soil) CO_2. In brines, DIC is from a probable hydrothermal origin.

Groundwater provenance: The spatial composition of inflow demonstrates that surface recharge follows vertical hydrodynamic gradients towards discharge in mine excavations. Glacial water lying in the fault system between brine below, and surface, has also been mobilised to flow to discharge points. Brine becomes the increasingly dominant component of groundwater mixtures with depth, but it is locally exceptionally high at the shallowest sampled depth where contained in an area with poor hydraulic connection to the main water-carrying faults. Sulphate isotopes were able to distinguish water from area(s) where sulphide oxidation was an important source of sulphate, from water from areas where it was not.

Circulation times: Tritiated modern precipitation is found in discharge down to 1,615 m, indicating circulation times of less than 40-50 years. Bomb tritium was observed in samples from 1,372 m during the early 1980's, constraining residence times to 20 years or less. Glacial meltwater likely infiltrated the fault system at least to the 4500 level (1,372m) during deglaciation in the region between 9,000 and 10,000 years ago under the

influence of high hydraulic gradients at the margin and base of the receding ice sheet, envisaged as the mechanism for recharge. This water cannot be dated by ^{14}C because activities would have been very low in the environment of the ice sheet due to the paucity of organic activity, and virtually all of the ^{14}C content can be attributed to recent recharge. Residence times for the brines are very long compared with those for meteoric water, and beyond the context of this study.

Temporal change: The presence of glacial water suggests that the groundwater system has been slow-moving, or stagnant, under the influence of very low hydraulic gradients, with minimal deep circulation, from the retreat of the Laurentide ice sheet until disturbed when mining commenced about 60 years ago. Sub-modern meteoric water in mine inflow is probably recharge dating from the early years of mine excavation. Groundwater composition since initial sampling in 1980, expressed in terms of end-member water type, shows a change towards increasing modern precipitation in discharge at some locations, signifying increased surface to depth groundwater flow, and demonstrating disturbance to the natural groundwater flow system caused by mining. Locally, significant change in the composition of water inflow can occur immediately following drilling of boreholes, or after boreholes have been shut-in.

Redox : At the levels sampled, Mn and Fe are present as the reduced forms Mn^{2+} and Fe^{2+}, suggesting that there may be precipitated oxyhydroxides, having the potential to act as redox buffers, in the 700 m interval between the shallowest sampling points and

surface. Sulphate is also present, and dissolved sulphide is virtually absent. However, sulphide would be precipitated as iron sulphide in the presence of Fe^{2+}. Thus, reduction of sulphate could be taking place.

Relevance to a nuclear waste disposal facility: The southern part of the Con Mine provided access to drifts up to 40-50 years old at depths of 700 to 1600 m with no overhead excavation. These conditions parallel those in a conceptual deep (500 to 1000 m) nuclear waste disposal site at the end of its envisaged 50 year operating life. Disturbance to groundwater flow can be considered to be at a maximum at this time because it is the point at which the facility would be backfilled and sealed, allowing water to return to dewatered areas in and around excavations initiating a return to natural regional hydraulic gradients.

6 REFERENCES

Bard, E., Hamelin, B., Fairbanks, R.G., and Zindler, A., 1990. Calibration of the ^{14}C timescale over the past 30,000 years using mass spectrometric U-Th ages from Barbados corals, *Nature*, **345**, 405.

Brown,R.M., 1989. Tritium in the environment. *Marko symposium on radiation protection: Past and Future. 1989 Mar 20-22. Chalk River, Ontario.*

Bottomley, D.J., Douglas, M., Katz, A., Chan, L., and Raven, K.G., 1997. Possible Devonian brines in Archean volcanic rocks of the Yellowknife greenstone belt, Slave province, Northwest Territories, Canada. Submitted to *Geochimica et Cosmochimica Acta.*

Bottomley, D.J., Gregoire, D.C., and Raven, K.G., 1994. Saline groundwaters and brines in the Canadian Shield: Geochemical and isotopic evidence for a residual evaporite brine component. *Geochimica et Cosmochimica Acta,* **58**, No.5, 1483-1498.

Campbell, N., 1948. West Bay Fault. In Structural geology of Canadian ore deposits. *Canadian Institute of Mining and Metallurgy Jubilee Volume*, 244-259.

Canmet, 1996. Ground stress determinations at the Miramar Con Mine, Yellowknife, N.W.T.

Chiba,H., and Sakai,H., 1985. Oxygen isotope exchange rate between dissolved sulphate and water at hydrothermal temperatures. *Geochimica et Cosmochimica Acta,* **49**, 993-1000.

Christiansen, E.A., Genzwill, D.J., and Menely, W.A., 1982. Howe Lake: A hydrodynamic blowout structure. *Canadian Journal of Earth Sciences*, **19**, 1122-1139.

Clark,I.D., and Fritz, P.,1997. Environmental Isotopes in Hydrogeology. CRC Lewis Publishers, New York. 345 pp.

Claypool, G.E., Holser, W.T., Kaplan, I.R., Sakai, H., and Zak, I., 1980. The age curves of sulphur and oxygen isotopes in marine sulphate and their mutual interpretation. *Chemical Geology*, **28**, 199-260.

Craig, B.G., 1965. Glacial Lake McConnell, and the surficial geology of parts of Slave River and Redstone River map-areas, District of Mackenzie; Geological Survey of Canada, Bulletin 122, 33pp.

Cunningham,M.P., and St. J. Lambert,R., 1988. Petrochemistry of the Yellowknife Greenstone Belt at Yellowknife, N.W.T. *Canadian Journal of Earth Sciences*, **26**, 1630-1647.

Dansgaard, W., Clausen, H.B., Gundestrup, N., Hammer, C.U., Johnsen, S.J., Kristinsdottir, P.M., and Reeh, N., 1982. A new Greenland deep ice core. Science, **218**, 1273-1277.

Dyke, A.S., and Dredge, L.A., 1989. Quaternary geology of the northwestern Canadian Shield; in Chapter 3 of Quaternary Geology of Canada and Greenland, R.J. Fulton (ed.); Geological Survey of Canada, Geology of Canada, no.1 (also Geological Society of America, The Geology of North America, v. K-1).

Frape, S.K., Fritz, P., and McNutt, R.H., 1984. Water-rock interaction and chemistry of groundwaters from the Canadian Shield. *Geochimica et Cosmochimica Acta,* **48**, 1617-1627.

Frape, S.K., and Fritz, P., 1981. A preliminary report on the occurrence and geochemistry of saline groundwaters in the Canadian Shield. *Atomic Energy of Canada Limited Technical Record, TR-136.*

Fritz,P. Frape,S.K., Drimmie,R.J., Appleyard,E.C. and Hattori,K., 1994. Sulphate in brines in the crystalline rocks of the Canadian Shield. *Geochimica et Cosmochimica Acta,* **58**, 57-65.

Fritz, P., Frape, S.K., Drimmie, R.J., and O'Shea, K., 1987. The isotopic composition of precipitation and groundwater in Canada. *International symposium on the use of isotope techniques in water resources development,* IAEA-SM-299, 539-550.

Fritz, P., and Frape, S.K., 1982. Saline groundwaters in the Canadian Shield - a first overview: *Chemical Geology,* **36**,179-190.

Gascoyne, M., and Cotzer, T., 1995. Isotopic methods in hydrogeology and their application to the Underground Research Laboratory, Manitoba. *Report AECL-11370.*

Gascoyne, M., and Kamineni, D.C., 1994. The hydrogeochemistry of fractured plutonic rocks in the Canadian shield. *Appied Hydrogeology* **2**, 43-49.

Harvie, C.E., Møller, N., and Weare, J.H., 1984. The prediction of mineral solubilities in natural waters: the Na-K-Mg-Ca-Cl-SO_4-H_2O system from zero to high concentration at 25 ^{0}C. *Geochimica et Cosmochimica Acta,* **48**, 723-751.

Hattori, K., and Cameron, E.M., 1986. Archean magmatic sulphate. *Nature* **319**, no.6048, 45-47.

Helmstaedt, H., and Padgham, W.A., 1986. A new look at the stratigraphy of the Yellowknife Supergroup at Yellowknife, N.W.T. - implications for the age of gold-

bearing shear zones and Archean basin evolution. *Canadian Journal of Earth Sciences*, 23, no.4, 454-475.

Henderson, J. F., and Brown, I. C., 1966. Geology and structure of the Yellowknife Greenstone Belt, District of Mackenzie. *Geological Survey of Canada*, Bulletin 141, 87pp.

Intera Consultants Ltd, 1997. Hydrogeological and hydrogeochemical study of the Miramar Con Mine, Yellowknife, NWT. Report prepared for the Atomic Energy Control Board of Canada.

Laaksoharju, M., (Ed.), 1995. Sulphate reduction in the Åspö HRL tunnel. SKB Technical Report 95-25, Swedish Nuclear Fuel Waste Management Co., Stockholm, Sweden.

Lloyd, R.M., 1968. Oxygen-isotope behaviour in the sulphate-water system. *Journal of Geophysics Research*, 73, 6099-6110.

Lindberg, P.A., 1987. An investigation of the Pud and Negus Fault offsets of the Campbell Shear Zone, Con Mine, Yellowknife, Northwest Territories. Report prepared for Nerco Minerals Company.

Macdonald, I.M., 1986. Water-rock interaction in felsic rocks of the Canadian Shield. *MSc thesis, University of Waterloo.*

McDonald, D.W., Duke, N.A., and Hauser, R.L., 1993. Geological setting of the NERCO Con Mine and the relationship of gold mineralisation to metamorphism, Yellowknife, N.W.T. *Exploration Mining Geology,* **2,** No.2, 139-154.

Mizutani, Y., and Rafter, T.A., 1969. Oxygen isotopic composition of sulphates Pt.3, Oxygen isotope fractionation in the bisulphate ion-water system. *New Zealand Journal of Science,* **12,** 54-59.

Natural Resources, Canada, 1995. Canada Permafrost, In: The National Atlas of Canada, 5th Edition.

Nordstrom, D.K., Ball, J.W., Donahoe, R.J., and Whittemore, D., 1989. Groundwater geochemistry and water-rock interactions at Stripa. *Geochimica et Cosmochimica Acta,* **53,** 1727-1740.

Pitzer, K.S., 1981. Characteristics of very concentrated aqueous solutions. In Chemistry and geochemistry of solutions at high temperatures and pressures. Physics and Chemistry of the Earth, 13-14, 249-272.

Pearson, F.J., Jr, 1987. Models of mineral controls on the composition of saline groundwaters in the Canadian Shield. In Saline waters and gases in crystalline rocks, Editors: Fritz, P. and Frape, S.K.; *Geological Association of Canada Special Paper 33*, 39-51.

Raven, K.G., and Clark, I.D., 1993. Survey of geoscientific data on deep underground mines in the Canadian shield. Atomic Energy Control Board Report 92-012.

Smellie, J.A.T., Laaksoharju, M., Wikberg, P., 1995. Åspö, SE Sweden: a natural groundwater flow model derived from hydrogeochemical observations. *Journal of Hydrology* **172**(1995),147-169.

Sofer, Z., and Gat, J.R., 1972. Activities and concentrations of oxygen-18 in concentrated aqueous salt solutions: analytical and geophysical implications. *Earth Planet. Sci. Lett.*, **15**, 232-238.

Teller, J. T., 1990. Volume and routing of late-glacial runoff from the southern Laurentide ice sheet. *Quaternary Research*, **34**, 12-23.

van Everdingen, R.O., Shakur, M.A., and Michel, F.A., 1985. Oxygen- and sulfur-isotope geochemistry of acidic groundwater discharge in British Columbia, Yukon, and District of Mackenzie, Canada. *Canadian Journal of Earth Sciences*, **22**, 1689-1695.

Wanless, R.K., Boyle, R.W., and Lowden, J.A.,1960. Sulphur isotope investigation of the gold-quartz deposits of the Yellowknife district. *Economic Geology*, **55**, 1591-1621.

APPENDIX 2.1

Sample location - Physical Data

Sample site	Depth (m)	Level	Northing	Borehole Number	Borehole Drill Date	Fault(s) identified (core and mapping)	Flow Rate (L/min) Current	Flow Rate (L/min) While drilling
23-A	701	2300	14140	seep		?	2	
23-B	701	2300	15053	Y-5	Jan-70	angel	<0.5	insignificant
23-C	701	2300	15053	Y-6	Dec-69	angel	<0.2	insignificant
23-D	701	2300	16673	B-654	Apr-58	B-101 shear	0.01	insignificant
23-E	701	2300	16848	B-646	Apr-58	negus	2	insignificant
23-F	701	2300	17300	B-660	May-58	negus	<3	high pressure flow
35-A	1067	3500	14700	B-9362	Apr-95	?	20	16
35-B	1067	3500	15386	B-8906	Apr-95	angel	4	16
35-C	1067	3500	15410	seep		angel		
35-D	1067	3500	15800	B-9452	Sep-95	negus	<2	1
39-A	1189	3900	17060	seep		?		
43-A	1311	4300	21098	B-1912	Jun-70	westbay		
43-B	1311	4300	25500	K-134	Apr-81	?		
43-C	1311	4300	26200	seep				
45-A	1372	4500	15000	B-5316	Sep-87	pud/neg	2	insignificant
45-B	1372	4500	15110	B-3457	Mar-80	negus/ ?	5	90
45-C	1372	4500	15110	B-3618	Feb-81	negus	0.5	insignificant
45-D	1372	4500	15115	B-3450	Feb-80	negus	10	157
45-E	1372	4500	15200	B-5318	Sep-87	ang/neg	max 45;(1-2 in 1994-5)	insignificant
45-F	1372	4500	15286	B-3316	1979	pud/angel		
45-G	1372	4500	15360	B-3362	Dec-79	angel/negus	1	90
49-A	1494	4900	14905	B-5310	Sep-87	pud/negus	1	insignificant
49-B	1494	4900	15130	seep		angel		
53-A	1615	5300	15100	B-7126	Mar-91	angel/pud	2	high pressure flow
53-B	1615	5300	15395	B-5586	Jun-88	pud	0.3	insignificant
53-C	1615	5300	15400	B-6709	Jul-90	angel	0.5	insignificant
53-D	1615	5300	15800	B- ?	n/a			

APPENDIX 3.1 Summary of Field Sampling Protocols.

ANALYTE	CONTAINER	FILTERING	PRESERVATION
Cations	60 ml, nalgene	0.45 μm	120 μl ultrapure HNO_3, stored cool
Anions	60 ml, nalgene	0.45 μm	stored cool
Alkalinity	nalgene		Analysed same day
Sulphate	60 ml, nalgene	0.45 μm	a few grains CdAc, stored cool
Total Sulphur	60 ml, nalgene	0.45 μm	0.5 ml 30% H_2O_2, stored cool
^{18}O and ^{2}H	60 ml, nalgene		stored cool
^{34}S and ^{18}O in sulphate	0.5-1 L, nalgene	0.45 μm	a few grains CdAc
^{13}C in DIC	250 ml, brown glass	0.45 μm	3 drops saturated solution of $HgCl_2$, stored cool
^{14}C in DIC	1L, brown glass	0.45 μm	6 drops saturated solution of $HgCl_2$, stored cool
^{3}H	0.5-1 L, nalgene		

APPENDIX 3.2 Field Chemistry Data

Sample	Borehole	Date	pH	Eh (mV) (measured)	Eh (mV) (corrected)	D.O. (mg/L)	Conductivity (mS)	Temperature (deg C)	Alkalinity (mg/L HCO_3)	Notes
41-1(4300L)	ditch	Feb-94	7.2				72			
41-2 (45-A)	B-5316	Feb-94	6.6				140			
41-3(45-B)	B-3457	Feb-94	7.4				32			
41-4(4900L)	ditch	Feb-94	6.2				400			
41-5(39-A)	seep	Feb-94	6.8				166			
41-6	Rob shaft	Mar-94	7.7				23			
41-7(35-C)	seep	Feb-95								
41-8(45-F)	B-3316	Feb-95								
41-9(45-B)	b-3457	Feb-95								
41-10(49-B)	seep	Feb-95								
41-11(53-A)	B-7126	Feb-95								
41-12(5300L)	4 holes	Feb-95								
23-A-1	seep	May-95								
23-B-1	Y-5	May-95	6.3	-161	52	0.26	2.55	11.1		
23-C-1	Y-6	May-95	6.95	-75	142	5.29	2.25	10.8		
23-E-1D	B-646	May-95								
23-E-1	B-646	May-95	7.09	-40	174	0.25	5.7	11.4		Duplicate
23-F-1	B-660	May-95								
35-A-1	B-9362	May-95	2.87	-71	132	0.05	15.1	16.9		
35-B-1	B-8906	May-95	6.5	-100	117	0.05	2.25	16.9		
35-C-1	seep	May-95								
39-A-1	seep	May-95	6.83				113			
45-A-1	B-5316	May-95	5.85	-198	10	0.14	100	21.6		
45-B-1	B-3457	May-95	5.35	-233	-28	0.04	32	21.4		
45-C-1	B-3618	May-95								
45-D-1	B-3450	May-95								
45-E-1	B-5318	May-95	1.96?	-174	31	0.04	70	21.1		
45-G-1	B-3362	May-95	6.27	-170	35	0.27	127	21.5		
49-A-1	B-5310	May-95	6.5	-206	3	0.12	115	23		
49-B-1	seep	May-95								
53-A-1	B-7126	May-95	6.81	-133	70	0.9	326	25		
53-B-1	B-5586	May-95								
53-C-1	B-6709	May-95	6.55	-123	77	0.5	350	24.2		

Sample	Borehole	Date	pH	Eh (mV) (measured)	Eh (mV) (corrected)	D.O. (mg/L)	Conductivity (mS)	Temperature (deg C)	Alkalinity (mg/L HCO_3)	Notes
23-A-2	seep	Jul-95	5.7				8.21			
23-B-2	Y-5	Jul-95	6.75	-186	26	0.07	5.33	11.1	262.3	
23-C-2	Y-6	Jul-95	6.5	-85	127	1.2	4.66	11.1	361.12	
23-E-2	B-646	Jul-95	6.74	-56	156	0.6	2.46	11.4	400.16	
23-F-2	B-660	Jul-95	6.97				1.76			
35-A-2	B-9362	Jul-95	7.38	-125	83	2.53	15.21	17.4	19.52	
35-B-2	B-8906	Jul-95	6.93	-167	41	0.08	1.82	16.8	411.14	
45-A-2	B-5316	Jul-95	6.48	-214	40	0.03	90.9	21.8	35.01	
45-B-2	B-3457	Jul-95	5.97	-220	-9	0.03	27.5	21.6	28.06	
45-B-2D	B-3457	Jul-95	6.77	-188	36	0.07	21.5	21.5		Duplicate
45-C-2	B-3618	Jul-95								
45-E-2	B-5318	Jul-95	6.31	-169	-19	0.05	75	21.5	51.24	
45-E-2A	B-5318	Jul-95	6.62	-165	-15	0.11	70.9	21.2	57.34	Negus
45-E-2B	B-5318	Jul-95	6.67	-182	17	0.02	77	21.4	57.34	Angel
45-G-2	B-3362	Jul-95	5.64	-171	34	0.03	136.3	21.7	33.67	
49-A-2	B-5310	Jul-95	7.23	-226	-23	0.1	126.2	23.1	12.81	
49-B-2	seep	Jul-95	6.4				175.5			
23-A-3	seep	Nov-95								
23-B-3	Y-5	Nov-95	6.91	-190	23		9.12	10	269.62	
23-C-3	Y-6	Nov-95	7.24	40	252		4.93	11.5	289.14	No flow cell
23-D-3	B-654	Nov-95								
23-E-3	B-646	Nov-95	7.17	-231	-21	0.03	2.03	13.1	445.3	
23-F-3	B-660	Nov-95								
35-A-3	B-9362	Nov-95	7.74	-169	38	0.02	15.75	18.6	23.79	
35-B-3	B-8906	Nov-95	7.18	-197	10	0.05	1.89	18	405.04	
35-D-3	B9452	Nov-95	7.01	-100	107	0.05	17.14	18.5	101.26	
43-A	B-1912	Nov-95	6.55	6			118		28.06	
43-B	K-134	Nov-95	7.5	-110			41.5		24.03	
43-C	seep	Nov-95							62.22	
45-A-3	B-5316	Nov-95	6.57	-234	-33		79.2	26.3	39.04	
45-B-3	B-3457	Nov-95	7.29	-231	-27	0.04	24.6	22.7	30.5	
45-C-3	B-3618	Nov-95								
45-D-3	B-3450	Nov-95							1.95	
45-E-3	B-5318	Nov-95	6.62	-193	9		61.5	25.9	51.24	
45-G-3	B-3362	Nov-95	6.4	-209	-5	0.06	110.5	22.8	39.04	

Sample	Borehole	Date	pH	Eh (mV) (measured)	Eh (mV) (corrected)	D.O. (mg/L)	Conductivity (mS)	Temperature (deg C)	Alkalinity (mg/L HCO_3)	Notes
49-A-3	B-5310	Nov-95	7.33	-184	19	0.12	133.8	24	11.83	
49-B-3	seep	Nov-95								
53-A-3	B-7126	Nov-95	6.87	-135	67		522	25	16.47	
53-B-3	B-5586	Nov-95	6.82	-66	137		520	23.5		
53-C-3	B-6709	Nov-95	6.73	-94	108		562.5	24.5	19.52	
23-A-4	seep	Jun-96	6.4							
23-B-4	Y-5	Jun-96	6.94	-217	-5	0.35	6.47	11.2	27.45	
23-C-4	Y-6	Jun-96	7.06	-210	2	0.34	11.9	11.1	273.28	
23-D-4	B-654	Jun-96	5.95						356.24	
23-E-4	B-646	Jun-96	7.19	-185	26	0.32	1.97	12.1	9.76	
23-F-4	B-660	Jun-96	7.19						390.4	
35-A-4	B-9362	Jun-96	7.6	-218	-11	0.25	16.2	17.6	387.96	
35-B-4	B-8906	Jun-96	7.28	-230	-22	0.27	2.58	17.2	24.4	
35-D-4	B9452	Jun-96	7.02	-222	-15	0.29	9.92	17.6	441.64	
39-A-4	seep	Jun-96					114.8		126.88	
45-A-4	B-5316	Jun-96	7.09	-274	-71		38.3	24	31.72	
45-B-4	B-3457	Jun-96	7.31	-240	-35		24	22	31.72	
45-C-4	B-3618	Jun-96							21.96	
45-D-4	B-3450	Jun-96	6.31	-106	99		87.6	22	51.24	
45-E-4	B-5318	Jun-96	6.35	-227	-22		124	22	46.97	
45-F-4	B-3316	Jun-96					197.7			
45-G-4	B-3362	Jun-96	6.36	-268	-63		174.6	22	26.84	
49-A-4	B-5310	Jun-96	7.2	-218	-14	0.29	140.1	23.3	7.32	
49-B-4	seep	Jun-96	6.5						15.006	
53-A-4	B-7126	Jun-96	6.64	-153	48		476	26	11.956	
53-B-4	B-5586	Jun-96							11.59	
53-C-4	B-6709	Jun-96	6.5	-112	90		484	25	14.64	
53-D-4	B- ?	Jun-96					350			

Sample	Borehole	Date	pH	Eh (mV) (measured)	Eh (mV) (corrected)	D.O. (mg/L)	Conductivity (mS)	Temperature (deg C)	Alkalinity (mg/L HCO_3)	Notes
sw-1-1, YK Bay		Jul-95	8.08			10.39	0.174	14.5	58.56	
sw-2-1, Rat Lake		Jul-95	7.33	-78	129	2.83	0.44	18.6	117.12	
sw-3-1, Rat Lake		Jul-95								
sw-4-1, Kam Lake		Jul-95	8.58	136	344	8.15	0.529	16.5	96.38	
sw-5-1, Frame L		Jul-95								
sw-6-1, Jackfish L		Jul-95								
sw-7-1, YK River		Jul-95								
sw-8-1, Prosperous L		Jul-95								
sw-10-1,pumphouse tap		Jul-95	7.6	747	956			14.7	58.56	
sw-11-1,L Pud Lake		Jul-95	8.08	133	341			16.8	59.78	
sw-12-1, U.Pud L		Jul-95	8.11	240	447			17.2	39.04	
sw-13-1,U.Pud L		Jul-95								
sw-14, bog W of Pud L		Jul-95								
sw-15, bog W of Pud L		Jul-95								
sw-16-1,Envir Lab intake		Jul-95								

Eh (corrected) is Eh (measured) corrected for Ag-AgCl electrode at sampling temperature

45-E-2 samples A, B were from hole intervals separated by a packer (Solinst). The seal was not complete.

APPENDIX 3.3 Geochemistry Data

Sample	Date collected	Ca	Na	Mg	K	Si	Sr	B	Al	Fe	Mn	Ba	Li
Mine groundwaters													
41-1	Feb-94	7800	4300	260	45		230						<.2
41-2 (45-A)	Feb-94	18000	8900	270	91		380						0.41
41-3(45-B)	Feb-94	2900	2600	51	15		41						0.19
41-4	Feb-94	50000	18000	200	150		930						0.83
41-5(39-A)	Feb-94	18000	10000	120	100		330						0.56
41-6	Feb-94	2250	2100	300	16		46						0.17
41-7(35-C)	Feb-95	180	190	30	2.7	9.1	3.6	0.56	<.2		0.21	<.2	0.02
41-8(45-F)	Feb-95	43060	21150	260	160	2.5	730	1.5	3.9		3.4	2.6	2.50
41-9(45-B)	Feb-95	2900	2800	55	14	7.6	57	1.6	1.2		0.52	0.26	0.34
41-10(49-B)	Feb-95	44020	21700	200	160	2.5	720	1.4	3.7		4.5	3	2.70
41-11(53-A)	Feb-95	70510	31490	230	270	0.94	1130	1.5			7.6	9	4.10
41-12	Feb-95	62220	27030	260	260	1.1	1060	2.3			9.8	12	4.00
23-A-1	May-95	650	1010	30	4.1	4.4	10	2.1		3.1	<.2		0.09
23-B-1	May-95	480	120	29	3.3	4.5	4.8				0.27		0.03
23-C-1	May-95	470	58	26	3.5	4.5	4.2				0.24		0.02
23-E-1D	May-95	250	160	66	4.7	8.2	3.6	0.46			<.2		0.04
23-E-1	May-95	250	170	67	4.7	8.1	3.6	0.43			<.2		0.04
23-F-1	May-95	220	130	63	4.5	8.3	3	0.43			<.2		0.02
35-A-1	May-95	1640	1870	37	8.6	6.6	30	1.8			0.26		0.18
35-B-1	May-95	210	200	32	3.1	9.5	4.4	0.54			0.22		0.07
35-C-1	May-95	210	180	32	3.2	9.4	4.1	0.57			<.2		0.03
39-A-1	May-95	19530	10070	130	63	5.1	330				1.6		1.30
45-A-1	May-95	17990	10330	300	73	4.4	410			3.3	5.7		0.83
45-B-1	May-95	4060	2850	87	17	7.3	87	1.5			1.2		0.29
45-C-1	May-95	10340	6440	130	38	6.3	190				1.2		0.72
45-D-1	May-95	13710	7590	150	50	6.1	250				1.9		0.84
45-E-1	May-95	11910	6210	140	43	10	210			4.6	1.4		0.73
45-G-1	May-95	25750	12740	210	93	5	460			15	2.8		1.40
49-A-1	May-95	20530	12690	200	75		400			1.8	3.2		1.40
49-B-1	May-95	42050	20170	180	150		710			1.1	3.9		2.50
53-A-1	May-95	60310	26000	200	250		1000				6.4		3.60
53-B-1	May-95	63820	27960	230	250		1080				7		3.50
53-C-1	May-95	70860	30550	290	270		1250				12		3.30

Sample	Date collected	Ca	Na	Mg	K	Si	Sr	B	Al	Fe	Mn	Ba	Li
23-A-2	Jul-95	690	1210	33	5	6.1	11	2.3		0.095	<.2	<.2	0.10
23-B-2	Jul-95	720	950	76	7.9	6.1	11	1.3		0.67	0.62	<.2	0.12
23-C-2	Jul-95	590	410	56	5	6.2	7.5	0.78		6.3	0.54	<.2	0.08
23-E-2	Jul-95	250	190	67	4.4	11	3.6	0.54		<.003	<.2	<.2	0.05
23-F-2	Jul-95	220	150	66	4.1	11	3.1	0.61		<.003	<.2	<.2	0.04
35-A-2	Jul-95	2010	2380	42	10	9.6	37	1.8		0.058	0.32	<.2	0.22
35-B-2	Jul-95	200	210	33	3.1	12	4	0.62			0.25	<.2	0.05
45-A-2	Jul-95	20020	11110	330	80	6.4	440	1.4		11	6.2	2.4	0.92
45-B-2	Jul-95	3830	3250	71	17	11	75	1.8		1.6	0.78	0.39	0.34
45-B-2D	Jul-95	3650	3140	64	16	11	68	1.7		0.78	0.62	0.23	0.33
45-C-2	Jul-95	12040	7160	150	47	9.3	210	1.5		2.2	1.4	0.79	0.86
45-E-2	Jul-95	13920	7050	150	53	13	240	1.8		0.73	1.5	0.8	0.90
45-E-2A	Jul-95	12650	6380	150	48	13	220	1.7		0.67	1.4	0.77	0.81
45-E-2B	Jul-95	14080	7140	150	54	13	240	1.7		0.9	1.6	0.88	0.91
45-G-2	Jul-95	27720	13440	210	99	7	480	1.6		2.3	2.8	1.4	1.50
49-A-2	Jul-95	22750	13700	220	83	5.1	430	1.4		3.7	3.5	2	1.50
49-B-2	Jul-95	45760	21140	190	170	3.3	750	1.7		0.5	4.2	2.9	2.70
23-A-3	Nov-95	643	1190	28.99	10.41	4.61	9.37	2.13	0.31	0.19	0.19	0.02	0.07
23-B-3	Nov-95	756	1060	73.46	13.24	4.19	11.85	1	0.26	0.43	0.51	0.07	0.11
23-C-3	Nov-95	567	464	57.29	10.97	3.83	7.71	1	0.28	0.31	0.27	0.03	0.07
23-D-3	Nov-95	5980	8361	342.89	51.4	2.49	150.49	1.51	0.26	-0.02	3.65	25.39	0.7
23-E-3	Nov-95	260	180	66	5	9.5	3.6	0.52		0.04	0.2	0.2	0.03
23-F-3	Nov-95	209	133	60.72	9.95	8.36	2.33	0.65	0.4	0.04	0.15	0.14	0.02
35-A-3	Nov-95	1738	2138	33.92	15.11	7.68	30.77	2.18	0 03	0.16	0.3	0.06	0.2
35-B-3	Nov-95	173	172	29.55	8.2	9.46	2.87	0.72	0.07	0.03	0.26	0.03	0.02
35-D-3	Nov-95	2167	1852	141.2	16.6	8.4	45.15	1.87	0.25	0.9	0.72	0.14	0.16
43-A-3	Nov-95	18612	13682	792.52	102.68	2.43	533.13	1.05	0.45	-0.05	13.28	92.04	0.95
43-B-3	Nov-95	5934	5100	126.97	28.05	4.75	115.81	1.07	0.27	0	1.12	0.15	0.25
43-C-3	Nov-95	9633	6491	365.59	45.64	6.74	211.89	1.06	0.09	-0.01	1.97	0.61	0.34
45-A-3	Nov-95	14543	8552	247.77	60.47	4.88	304.94	1.75	0.24	11.02	4.65	1.33	0.83
45-B-3	Nov-95	3661	3201	63.59	20.69	7.85	70.7	1.77	0.18	1.25	0.76	0.36	0.34
45-C-3	Nov-95	12860	7599	142.57	50.41	6.94	223.49	1.73	0.31	2.54	1.46	0.79	0.95
45-D-3	Nov-95	15047	7692	143.69	55.6	8.38	255.28	1.97	0.38	1.24	1.71	0.86	0.99
45-E-3	Nov-95	11655	6039	133.83	46.13	10.76	198.41	1.79	0.39	0.35	1.26	0.66	0.8
45-G-3	Nov-95	23946	12130	266.59	90.73	5.14	443.09	1.89	0.31	5.2	4.38	1.45	1.39
49-A-3	Nov-95	23483	14022	239.28	86.47	3.83	443.32	1.46	0.34	4.53	4.49	2.57	1.6
49-B-3	Nov-95	43442	20380	184.52	155.13	2.79	706.41	2	0.36	0.69	4.64	3.1	2.82
53-A-3	Nov-95	66321	28182	204.44	240.7	1.28	1060.61	2.35	0.26	2.78	7.5	8.6	4.01
53-B-3	Nov-95	66532	28522	232.64	244.3	1.6	1073.97	2.4	0.29	2.83	8.37	9.44	3.97
53-C-3	Nov-95	70294	29626	283.43	258.07	1.08	1187.13	2.75	0.5	2.42	13.37	17.25	3.71

Sample	Date collected	Ca	Na	Mg	K	Si	Sr	B	Al	Fe	Mn	Ba	Li
23-A-4	Jun-96	612	1131	26.99	10.46	4.58	8.87	2.04	-0.06	0.17	0.19	0.02	0.06
23-B-4	Jun-96	616	699	57.44	12.41	4.69	8.65	1.22	0.2	1.12	0.58	0.06	0.06
23-C-4	Jun-96	541	374	49.2	11.06	4.56	6.05	0.8	0.13	6.69	0.63	0.05	0.02
23-D-4	Jun-96	6075	8426	338.79	51.77	2.69	153.57	1.26	0.13	1.05	3.68	22.29	0.72
23-E-4	Jun-96	215	100	60.55	10.38	8.44	2.18	0.35	0.13	0.51	0.18	0.14	0
23-F-4	Jun-96	215	146	59.84	10.81	8.41	2.34	0.54	0.09	0.06	0.16	0.13	0
35-A-4	Jun-96	1671	2007	32.75	14.16	8.11	29.67	1.94	0.03	0.18	0.32	0.07	0.19
35-B-4	Jun-96	226	245	32.81	8.82	10.28	4.17	0.71	0.03	0.04	0.3	0.04	-0.01
35-D-4	Jun-96	925	872	73.29	12.17	9.39	17.57	1.69	0.15	1.18	0.4	0.04	0.1
39-A-4	Jun-96	15339	7593	102.16	53.74	3.86	251.56	1.4	0.13	0.16	1.45	0.73	1.09
45-A-4	Jun-96	4796	3683	76.58	25.45	7.75	91.86	1.79	0.12	1.73	1.06	0.33	0.39
45-B-4	Jun-96	2524	2480	42.61	17.29	8.75	44.35	1.94	0.24	0.5	0.41	0.12	0.23
45-C-4	Jun-96	11495	6919	131.55	47.42	7.04	199.56	1.83	0.14	1.8	1.36	0.71	0.9
45-D-4	Jun-96	14540	7202	145.45	55.42	9.73	246.18	1.98	0.08	1.02	1.65	0.82	0.98
45-E-4	Jun-96	19029	9252	159.03	69.61	9.74	326.47	1.99	0.19	1.04	1.91	0.88	1.24
45-F-4	Jun-96	48515	21669	256.64	170.03	2.25	807.14	2.27	0.4	0.13	3.95	2.77	3.07
45-G-4	Jun-96	38171	17284	230.95	133.37	4.98	644.96	1.97	0.18	1.13	3.72	2.12	2.39
49-A-4	Jun-96	27057	14801	247.75	100.47	3.73	493.91	1.8	0.11	5.03	4.94	2.38	1.87
49-B-4	Jun-96	53442	23113	195.49	190.95	2.14	855.61	2.35	0.26	0.96	5.43	4.32	3.5
53-A-4	Jun-96	62811	25664	187.74	230.19	1.08	996.12	2.12	0.12	3.28	7.28	8.42	3.95
53-B-4	Jun-96	68817	28284	231.79	255.4	1.6	1102.82	2.42	0.19	2.97	8.8	9.9	4.29
53-C-4	Jun-96	73462	29753	287.42	271.61	1.05	1230.32	2.83	0.08	2.66	14.14	18.77	4.07
53-D-4	Jun-96	57562	24920	270.83	197.21	1.72	953.48	2.51	0.5	0.58	6.91	6.67	3.55
Surface waters													
sw-1-1	Jul-95	23	6.8	5.3	1.1	0.85	0.12	<.016		<.003	<.2	<.2	0.00
sw-2-1	Jul-95	59	13	12	9.5	0.59	0.18	0.085		0.014	<.2	<.2	0.01
sw-3-1	Jul-95												
sw-4-1	Jul-95	57	33	12	3.7	0.2	0.6	0.048		0.019	<.2	<.2	0.01
sw-5-1	Jul-95												
sw-6-1	Jul-95												
sw-7-1	Jul-95												
sw-8-1	Jul-95												
sw-10-1	Jul-95	21	6.3	5.3	1.1	0.93	0.1	<.016		<.003	<.2	<.2	0.00
sw-11-1	Jul-95	1790	990	61	27	0.94	29	0.54		<.003	<.2	0.21	0.04
sw-12-1	Jul-95	1840	960	70	29	0.6	27	0.57		<.003	<.2	0.21	0.03
sw-13-1	Jul-95												
Negus Pond	Nov-95	495	50	280.76	20.84	30.64	0.9	0.03	12.2	8.97	7.49	0.05	0.35

Data from previous Con Mine groundwater studies (Frape et al, 1984; Macdonald, 1986)

Sample	Date collected	Ca	Na	Mg	K	Si	Sr	B	Al	Fe	Mn	Ba	Li
45-B	Jul-80	12900	10900	268	111		671					7.6	0.78
45-D	Jul-80	15700	9420	250	110		314					11.3	0.4
45-G	Jul-80	54400	35800	1340	483		1570					300	1.58
45-B	Apr-81	10500	8050	209	53.1		237					2.53	0.52
45-G	Apr-81	23400	13600	468	109		617					10	0.6
45-B	85	4217	2970	73	22.3		77.9					2.73	0.15
45-D	85	14330	6970	162	62.3		251.3					11.9	0.26

Sample	Cl	SO4	Br	F	NO3	HCO3	HCO3(DIC)	TDS	meq cat	meq anion	error	SI(calcite)	SI(gypsum)
Mine groundwaters													
41-1	22000	460	100	0.06	220	31.1		35446	600	631	-3		
41-2 (45-A)	50000	210	220	0.07	380	17.1		78469	1312	1416	-4		
41-3(45-B)	8900	300	31	0.12	93	15.9		14947	263	257	1		
41-4	110000	57	570	0.06	1100	9.8		181018	3303	3107	3		
41-5(39-A)	47000	290	290	0.06	510	18.3		76659	1347	1334	1		
41-6	7400	880	130	0.05	16	79.3		13218	229	228	0		
41-7(35-C)	328	118	3.3	<.05	<.1			865	20	12	26		
41-8(45-F)	105000	330	1036	<.05	<.1			171742	3098	2978	2		
41-9(45-B)	10000	658	71	<.05	<.1			16567	272	296	-4		
41-10(49-B)	101400	537	1027	<.05	<.1			169782	3165	2880	5		
41-11(53-A)	147000	18	1595	<.05	<.1			252266	4921	4161	8	-0.55	-1.08
41-12	146500	58	578	<.05	<.1			237995	4315	4135	2		
23-A-1	2098	1037	18.49	<.05	<.1			4867	79	81	-1	-1.23	-0.08
23-B-1	166	925	1.7	<.05	0.3			1735	32	24	14	-0.34	-0.06
23-C-1	48	951	0.51	<.05	0.8		421.5	1988	28	28	0	0.23	-0.04
23-E-1D	228	518	2.28	<.05	0.4		190.3	1432	25	20	10		
23-E-1	226	514	2.45	<.05	0.2		319.6	1566	26	22	7	0.15	-0.49
23-F-1	123	496	1.54	<.05	<.1		311.7	1361	22	19	8		
35-A-1	3853	602	52	<.05	<.1		9.52	8111	167	122	16	-0.54	-0.13
35-B-1	428	129	17.9	<.05	<.1		386.7	1421	22	21	1	0.59	-1.12
35-C-1	381	128	3.33	<.05	<.1			952	21	13	22		
39-A-1	49954	564	428	<.05	<.1			81077	1427	1424	0		
45-A-1	48630	441	443	<.05	<.1		10.3	78642	1376	1385	0	-1.43	-0.14
45-B-1	11283	562	104	<.05	<.1		14.34	19075	335	331	1	-0.49	-0.09
45-C-1	26772	502	246	<.05	6.7			44673	809	768	3		
45-D-1	34326	452	307	<.05	<.1		13.4	56857	1029	980	2		
45-E-1	29413	460	272	<.05	<.1			48675	878	842	2	-0.37	-0.13
45-G-1	59979	424	605	<.05	<.1		7.56	100293	1861	1706	4	-1.10	-0.13
49-A-1	59245	660	485	<.05	<.1		2.87	94294	1597	1689	-3	-1.24	0.08
49-B-1	105545	465	993	<.05	<.1			170271	2998	2995	0		
53-A-1	156100	225	1443	<.05	<.1		4.27	245542	4169	4420	-3	-0.46	0.06
53-B-1	154810	208	1264	<.05	<.1			249633	4432	4381	1		
53-C-1	170900	83	1646	<.05	<.1			275864	4902	4836	1	-0.45	-0.26

Sample	Cl	SO4	Br	F	NO3	HCO3	HCO3(DIC)	TDS	meq cat	meq anion	error	SI(calcite)	SI(gypsum)
23-A-2	2406	1306	19.18	<.05	<.1			5689	90	95	-3		
23-B-2	1692	1202	16.5	<.05	<.1		285.8	4970	84	78	4		
23-C-2	689	1150	12.7	<.05	7.7		375.6	3317	52	50	2		
23-E-2	263	538	1.91	<.05	<.1		406.3	1736	26	25	2		
23-F-2	156	512	2.32	<.05	<.1			1125	23	15	21		
35-A-2	5930	662	54	<.05	<.1		10.2	11147	208	182	7		
35-B-2	323	135	3.06	<.05	<.1		428.6	1353	22	19	7		
45-A-2	47045	484	465	<.05	<.1		17.8	80020	1514	1341	6		
45-B-2	10201	658	91	<.05	<.1		19.3	18228	339	303	6		
45-B-2D	8583	631	89.5	<.05	<.1			16256	325	256	12		
45-C-2	29700	558	258	<.05	0.9			50140	927	851	4		
45-E-2	33130	512	290	<.05	<.1			55364	1016	948	4		
45-E-2A	28917	474	278	<.05	<.1		29.8	49165	924	828	5		
45-E-2B	32561	467	300	<.05	<.1		30.6	55042	1028	931	5		
45-G-2	63650	489	592	<.05	<.1		16.8	106713	1990	1811	5		
49-A-2	53060	744	497	<.05	<.1		4.6	91506	1754	1516	7		
49-B-2	101200	541	912	<.05				170678	3227	2873	6		
23-A-3	2398	1150	26.0	0.6	6.8			5470	87	92	-3		
23-B-3	2467	1155	24.4	<5	5.0		295.85	5869	90	99	-4		
23-C-3	971	1189	7.9	<5	<5		282.43	3564	54	57	-3		
23-D-3	28800	7	176	<5	<25			28983	692	814	-8		
23-E-3	322	558	2.29	<1	<5		366	1773	26	27	-1		
23-F-3	193	525	1.37	<1	<5			719	22	16	14		
35-A-3	7319	648	49.6	<5	<5		12.56	11995	183	220	-9		
35-B-3	391	147	2.88	<5	<5		363.71	1300	19	20	-3		
35-D-3	7680	726	61.2	<5	7		54.60	12764	201	233	-7		
43-A-3	61432	<10	601	<0.2	<1			95865	1594	1738	-4		
43-B-3	19575	1469	164.4	<5	7			32528	530	584	-5		
43-C-3	28641	885	263	<1	16			46563	796	829	-2		
45-A-3	43948	536	305	<1	<5		32.25	68554	1121	1253	-6		
45-B-3	12967	623	87	<1	<5		20.80	20727	328	380	-7		
45-C-3	41345	532	260	<1	<5			63027	987	1179	-9		
45-D-3	41720	501	306	<20	<5			65736	1100	1189	-4		
45-E-3	32682	491	224	<1	<5		38.63	51524	858	934	-4		
45-G-3	63766	454	514	<1	<5		31.80	101662	1749	1813	-2		
49-A-3	67994	698	507	<1	<5		2.26	107493	1806	1936	-3		
49-B-3	112935	478	804	<1	<5			179102	3078	3201	-2		
53-A-3	183368	122	1264	<5	<5		4.64	280793	4565	5184	-6		
53-B-3	179489	153	1271	<1	<5			277548	4592	5075	-5		
53-C-3	194225	93	1474	<10	<50		4.71	297487	4833	5492	-6		

Sample	Cl	SO4	Br	F	NO3	HCO3	HCO3(DIC)	TDS	meq cat	meq anion	error	SI(calcite)	SI(gypsum)
23-A-4	2177	1049	18	6	<1.25	27.5	20	5093	82	84	-1	-1.8	-0.1
23-B-4	1559	1130	11	2	36	273.3		4413	66	72	-4		
23-C-4	762	1108	6	5	6	356.2		3237	48	50	-3	0.37	-0.02
23-D-4	25731	9	161	<.25	<1.25	9.8		40988	700	727	-2	-1.75	-1.93
23-E-4	142	483	1	9	27	390.4		1450	20	20	0	0.3	-0.55
23-F-4	199	491	2	7	47	388.0		1577	22	22	0		
35-A-4	6389	581	43	9	<1.25	24.4		10811	174	193	-5	0.09	-0.18
35-B-4	610	154	4	7	26	441.6		1771	25	28	-5	0.54	-1.05
35-D-4	3181	603	33	2	<1.25	126.9		5859	91	105	-7	0.11	-0.22
39-A-4	53706	609	378	<1	<1.25			78041	1107	1530	-16		
45-A-4	15137	584	111	<.25	<1.25	31.7		24549	407	440	-4	0.02	-0.07
45-B-4	7845	609	62	<.25	<1.25	31.7		13667	238	235	1	0.07	-1.04
45-C-4	40035	693	257	<.25	<1.25	22.0		59813	888	1146	-13		
45-D-4	41271	738	315	<.25	163	51.2		64743	1054	1183	-6		
45-E-4	57866	465	373	<1	<1.25	47.0		87605	1369	1645	-9	-0.23	-0.08
45-F-4	141287	489	888	<1	<5			214097	3394	4001	-8		
45-G-4	90166	369	659	<1	<5	26.8		147701	2683	2556	2	-0.35	-0.1
49-A-4	77986	642	575	<1	<1.25	7.3		121930	2020	2217	-5	-0.12	0.1
49-B-4	139149	443	925	<1	<5	15.0		218347	3698	3941	-3	-0.27	0.25
53-A-4	185555	247	1228	<1	<5	12.0		276957	4278	5248	-10	0.25	0.29
53-B-4	159890	229	1464	<1	<5	11.6		260316	4696	4527	2		
53-C-4	185215	130	1336	<1	<5	14.6		291744	4998	5237	-2	0.22	0.04
53-D-4	152589	271	982	<1	<5			237768	3989	4316	-4		
23-A-5							13.36						
Surface waters													
sw-1-1	4.69	15	<.05	<.05	<.1		49	106	2	1	21		
sw-2-1	27.75	64	<.05	<.05	<.1		89.9	276	5	4	14		
sw-3-1													
sw-4-1	73.94	37	0.82	<.05	<.1		71.3	290	5	4	14		
sw-5-1													
sw-6-1													
sw-7-1													
sw-8-1													
sw-10-1	6.8	15	<.05	<1	0.2		41.4	98	2	1	21		
sw-11-1	4031	687	42.29	<1	60		31.9	7751	138	129	4		
sw-12-1	3708	1077	38.23	<1	67.8		36.59	7855	140	128	5		
sw-13-1													
Negus Pond	109	2649	<5	<5	4.1			3669	51	58	-7		

Data from previous Con Mine groundwater studies (Frape et al, 1984; Macdonald, 1986)

Sample	Cl	SO4	Br	F	NO3	HCO3	HCO3(DIC)	TDS	meq cat	meq anion	error	SI(calcite)	SI(gypsum)
45-B	37100	746	358	5.74	3	28		63099	1144	1065	4		
45-D	31900	198	324			69		58297	1218	907	15		
45-G	135000	1	1150		33	2		230081	4401	3817	7		
45-B	29400	715	304	2.88	5	34		49513	894	847	3		
45-G	60200	715	647		5	48		99820	1803	1719	2		
45-B	18000	723	165	0.7	<10	34.5		26286	347	524	-20		
45-D	38590	214	306			107.8		61006	1035	1095	-3		

Note : All concentrations in mg/L

APPENDIX 3.4 Calculated sulphide concentrations

Sample	sulphate + oxidised sulphide	sulphate alone	calculated sulphide	sulphide %
23-B	1120.6	1115.9	4.7	0.4
23-C	1085.2	1065.3	19.9	1.8
23-E	467.1	463.0	4.1	0.9
35-A	619.3	610.9	8.4	1.4
35-B	125.9	114.9	10.9	8.7
45-A	436.3	444.1	-7.8	-1.8
45-B	598.9	602.8	-3.9	-0.6
45-B	606.5	604.8	1.7	0.3
45-E	465.0	470.2	-5.1	-1.1
45-E	460.1	468.5	-8.4	-1.8
45-E	462.4	468.0	-5.6	-1.2
45-G	436.7	432.3	4.4	1.0
49-A	702.4	699.2	3.2	0.5

APPENDIX 3.5 Surface water isotope determinations

Sample	Location	Date collected	$\delta^{18}O$ ‰ VSMOW	$\delta^{2}H$ ‰ VSMOW	$\delta^{13}C$ ‰ VPDB	^{3}H (TU)	$\delta^{34}S$ ‰ CDT	$\delta^{18}O$(sulph ‰ VSM
sw-1-1	YK Bay	Jul-95	-16.22	-135.9	-3.35			
sw-2-1	Rat Lake	Jul-95	-12.55	-126.3	-6.17	16.2		
sw-3-1	Rat Lake	Jul-95	-12.54	-125.2				
sw-4-1	Kam Lake	Jul-95	-13.77	-129.3	-3.85	19		
sw-5-1	Frame L	Jul-95	-11.06	-115.9				
sw-6-1	Jackfish L	Jul-95	-12.94	-114.2				
sw-7-1	YK River	Jul-95	-14.83	-134.3				
sw-8-1	Prosperous L	Jul-95	-14.66	-135.9				
sw-10-1	pumphouse tap	Jul-95	-16.28	-137.1	-4.46	29.9		
sw-11-1	L Pud Lake	Jul-95	-15.59	-135.1		31.7	4.3	-2
sw-12-1	U.Pud L	Jul-95	-14.83	-131.1		29.2	3.2	-3
sw-13-1	U.Pud L	Jul-95	-14.86	-124.0				
sw-14-1	bog W of Pud L	Jul-95	-15.52	-139.6				
sw-15-1	bog W of Pud L	Jul-95	-16.12	-143.1				
sw-16-1	Envir Lab intake	Jul-95	-16.48	-133.0				
Negus Pond		Nov-95	-12.66	-129.7				
SW-16-2		Aug-95	-16.87	-139.1				
SW-16-3		Sep-95	-16.23	-135.9				
SW-16-4		Oct-95	-15.67	-138.5				
SW-16-5		Nov-95	-15.86	-135.7				
SW-16-6		Dec-95	-15.60	-132.5				
SW-16-7		Jan-96	-15.61	-137.5				
SW-16-8		Feb-96	-15.93	-138.5				
SW-16-9		Mar-96	-16.02	-136.7				
SW-16-10		Apr-96	-15.79	-137.4				
SW-16-12		May-96	-16.52	-137.5				
rain R-4		Jun-96	-15.88	-125.4				

All SW-16 samples collected at the intake to the mine environmental laboratory (pumped from Yellowknife Bay

APPENDIX 3.6 Groundwater isotopes

Sample	Date collected	$\delta^{18}O$ ‰ VSMOW	$\delta^{2}H$ ‰ VSMOW	$\delta^{13}C$ ‰ VPDB	^{3}H (TU)	$\delta^{34}S$ ‰ CDT	$\delta^{18}O$(sulphate) ‰ VSMOW	^{14}C (pmC)
41-2 (45-A)	Feb-94	-19.19	-133.9					
41-3 (45-B)	Feb-94	-20.49	-159.4					
41-5 (39-A)	Feb-94	-19.08	-139.5					
41-6	Feb-94	-12.33	-130.5					
41-7 (35-C)	Feb-95	-19.27	-156.8	-15.06				
41-8 (45-F)	Feb-95	-17.15	-103.4					
41-9 (45-B)	Feb-95	-20.40	-160.5	-17.51				
41-10 (49-B)	Feb-95	-17.64	-110.5	-19.44				
41-11 (53-A)	Feb-95	-14.47	-68.7	-10.39				
41-12	Feb-95	-14.10	-67.2	-8.59				
23-A-1	May-95	-23.51	-182.4					
23-B-1	May-95	-19.16	-145.0					
23-C-1	May-95	-19.04	-156.8					
23-E-1	May-95	-19.33	-148.7					
23-E-1	May-95	-19.38	-147.3	-11.98				
23-F-1	May-95	-19.29	-151.6	-12.16				
35-A-1	May-95	-20.78	-159.1					
35-B-1	May-95	-19.26	-159.8	-15.35				
35-C-1	May-95	-19.28	-155.5					
39-A-1	May-95	-19.13	-137.8					
45-A-1	May-95	-19.21	-137.4	-17.06				
45-B-1	May-95	-20.29	-156.5	-19.79				
45-C-1	May-95	-19.99	-148.4					
45-D-1	May-95	-19.51	-144.8	-19.08				
45-E-1	May-95	-19.12	-145.8					
45-G-1	May-95	-18.36	-130.3	-20.60				
49-A-1	May-95	-20.12	-139.6					
49-B-1	May-95	-17.60	-105.7					
53-A-1	May-95	-14.61	-68.0					
53-B-1	May-95	-14.56	-73.4					
53-C-1	May-95	-13.58	-56.0					
23-B-2	Jul-95	-20.74	-167.2		19.6	11.2	7.74	
23-C-2	Jul-95	-19.65	-158.5	-16.23	21.2	10.2	7.98	
23-E-2	Jul-95	-19.45	-152.2	-13.87	26	4.1	-5.35	
35-A-2	Jul-95	-20.92	-162.8		16.4	26.3	8.97	
35-B-2	Jul-95	-19.32	-156.0	-15.66	19.3	10.5	1.66	
45-A-2	Jul-95	-19.12	-139.4	-15.19	10.7	23.3	7.64	
45-B-2	Jul-95	-20.59	-164.9		18.7	23.8	8.71	
45-B-2D	Jul-95	-20.66	-163.5					
45-E-2	Jul-95	-19.14	-142.9		21.2	19.7	5.41	
45-E-2A	Jul-95	-19.22	-146.5	-18.03				
45-E-2B	Jul-95	-18.98	-144.9	-17.76				
45-G-2	Jul-95	-18.36	-135.2		11.8	21.6	6.64	
49-A-2	Jul-95	-20.13	-140.9	-11.31	4	25.6	8.24	
23-A-3	Nov-95	-23.94	-185.3					
23-B-3	Nov-95	-21.33	-166.3	-15.89				
23-C-3	Nov-95	-20.10	-162.4	-15.05	19.6			62.24 ± 0.44
23-D-3	Nov-95	-20.42	-145.8					
23-E-3	Nov-95	-19.50	-158.1	-14.09	23.9			
23-F-3	Nov-95	-19.56	-154.8					
35-A-3	Nov-95	-20.77	-163.2	-17.17	15.4			
35-B-3	Nov-95	-19.70	-154.8	-15.22	21			59.74 ± 0.45
35-D-3	Nov-95	-19.72	-155.8	-17.00	24.6	17.5	6.21	71.90 ± 0.48

Sample	Date collected	$\delta^{18}O$ ‰ VSMOW	$\delta^{2}H$ ‰ VSMOW	$\delta^{13}C$ ‰ VPDB	^{3}H (TU)	$\delta^{34}S$ ‰ CDT	$\delta^{18}O$(sulphate) ‰ VSMOW	^{14}C (pmC)
43-A-3	Nov-95	-18.90	-134.0					
43-B-3	Nov-95	-19.90	-155.4					
43-C-3	Nov-95	-20.92	-160.0					
45-A-3	Nov-95	-19.70	-145.6	-12.37				
45-B-3	Nov-95	-20.38	-160.0	-17.54	14.2			
45-C-3	Nov-95	-19.92	-152.0					
45-D-3	Nov-95	-19.26	-139.9					
45-E-3	Nov-95	-19.25	-144.4	-18.49				
45-G-3	Nov-95	-18.55	-134.7	-14.60	13.3			
49-A-3	Nov-95	-19.97	-139.0	-10.66				
49-B-3	Nov-95	-17.59	-112.6					
53-A-3	Nov-95	-14.36	-74.1	-8.00	<.8	25.7	7.67	
53-B-3	Nov-95	-14.47	-71.5					
53-C-3	Nov-95	-13.53	-63.9		1.1			
23-A-4	Jun-96	-23.69	-187.0	-17.60	11.9	23.0	9.73	
23-B-4	Jun-96	-21.08	-169.6					
23-C-4	Jun-96	-20.21	-160.4					
23-D-4	Jun-96	-20.18	-145.5		<0.8			
23-E-4	Jun-96	-19.54	-155.5					
23-F-4	Jun-96	-19.63	-157.2					
35-A-4	Jun-96	-20.73	-160.8		17.9			
35-B-4	Jun-96	-19.72	-159.4					
35-D-4	Jun-96	-19.52	-158.6					
39-A-4	Jun-96	-19.12	-140.1					
45-A-4	Jun-96	-20.46	-157.5					
45-B-4	Jun-96	-20.60	-162.0		15.1			
45-C-4	Jun-96	-20.09	-151.4					
45-D-4	Jun-96	-19.22	-143.6		17.2	20.5	6.19	
45-E-4	Jun-96	-18.96	-135.4					
45-F-4	Jun-96	-16.93	-100.4					
45-G-4	Jun-96	-17.61	-115.4		8.8			
49-A-4	Jun-96	-19.56	-133.6		4.4			
49-B-4	Jun-96	-16.48	-97.4		2.4	28.3	8.01	
53-A-4	Jun-96	-14.45	-73.2		0.9			
53-B-4	Jun-96	-14.35	-68.8		1	24.6	7.21	
53-C-4	Jun-96	-13.55	-61.5		1.4	26.1		
53-D-4	Jun-96	-15.70	-84.4					
23-A-5	Sep-96			-16.56				38.16 ± 0.32

Data from previous groundwater studies (Frape et al, 1984; Macdonald, 1986)

45-B	Jul-80	-22.84	-163.0		3		11.80	
45-D	Jul-80	-19.70	-145.0	-15.40	47			
45-G	Jul-80	-14.30	-82.0		3	19.9	7.30	
45-B	Apr-81	-22.27	-162.0		34		7.90	
45-G	Apr-81	-19.00	-133.0		44		8.50	
45-B	85	-20.81	-159.2		57	27.5		
45-D	85	-19.34	-135.3		45	23.1		

APPENDIX 3.7 Evolution of DIC concentration and $\delta^{13}C$ between two samples

Calcite precipitating from solution in a closed groundwater system causes a decrease in $\delta^{13}C$ of DIC remaining in the solution due to temperature dependent fractionation between calcite and DIC. $\delta^{13}C$ is dependent on the fraction (f) of the original DIC remaining, according to the equation:

$$\delta^{13}C_{DIC\ remaining} = \delta^{13}C_{DIC\ original} + \varepsilon_{calcite\text{-}DIC} \times \ln f$$

where ε is the fractionation factor between DIC, essentially all HCO_3 at neutral pH, and precipitated calcite. $\varepsilon_{calcite\text{-}HCO3}$ is +0.41 $^0/_{00}$ at 15 ^{0}C (Clark and Fritz, 1997).

Comparison of 35-B-3 (364 mg/L HCO_3; $\delta^{13}C$ = -15.22 $^0/_{00}$) with 35-A-3 (12.6 mg/L HCO_3; $\delta^{13}C$ = -17.17 $^0/_{00}$), which is an order of magnitude more saline, indicates that most of the difference between the two waters can be explained by Rayleigh distillation as calcite precipitates out of solution as DIC-rich infiltrating meteoric water mixes with saline waters with high Ca concentrations. The table below shows that $\delta^{13}C$ would decrease by about 1.5 $^0/_{00}$ while DIC decreased by the difference between the two waters.

δ_{DIC}	$\delta_{0\ DIC}$	ε	ln f	f	DIC (mg/L)
-15.22	-15.22	0.41	0	1	364
-15.31	-15.22	0.41	-0.22	0.8	291.2
-15.43	-15.22	0.41	-0.51	0.6	218.4
-15.60	-15.22	0.41	-0.92	0.4	145.6
-15.88	-15.22	0.41	-1.61	0.2	72.8
-16.16	-15.22	0.41	-2.30	0.1	36.4
-16.45	-15.22	0.41	-3.00	0.05	18.2
-16.73	-15.22	0.41	-3.69	0.025	9.1

This suggests a possible common source of DIC for the two samples. Both waters are calculated to be saturated with respect to calcite.

APPENDIX 3.8 Fracture carbonate isotopes

Sample	Location	$\delta^{18}O$ ‰ VSMOW	$\delta^{13}C$ ‰ VPDB
YKN-SS1	S of Negus Point	11.21	-3.04
YKN-SS2	S of Negus Point	11.34	-3.12
YKN-SS3	S of Negus Point	9.16	-1.58
YKN-US1	3500L shear zone	12.42	-3.30
YKN-US2	3500L 15750 (Negus fault)	9.11	-3.63
YKN-US3	3500L near 35-B (Angel fault)	12.95	-15.42

APPENDIX 3.9

1. ^{14}C age determination (uncorrected):

$$A_{meas} = A_o e^{-\lambda t}, \qquad \text{Equation A.1}$$

assuming A_o = 110 pmC, where A_{meas} is the ^{14}C activity, or concentration, measured in the sample, and A_o is the ^{14}C activity estimated (Bard et al, 1990) for the atmosphere assuming infiltration occurred 9,000-10,000 years ago, during glacial retreat, λ is the ^{14}C decay constant, and t is the decay time.

a) Sample 35-A-3

A_{meas} = 59.74 pmC ; $\lambda = \ln 2 / t_{1/2}$; $t_{1/2}$ for ^{14}C = 5730 years

Rearranging equation A.1:

$$t = -8267 \times \ln (A_{meas} / A_0) \qquad \text{Equation A.2}$$

$$= -8267 \times \ln (59.74 / 110) = 5047 \text{ years}$$

b) Sample 23-B-3

A_{meas} = 62.24 pmC ;

$$t = -8267 \times \ln (62.24 / 110) = 4708 \text{ years}$$

c) Sample 23-A-5

A_{meas} = 38.16 pmC ;

$$t = -8267 \times \ln (38.16 / 110) = 8752 \text{ years}$$

2. Calculation of apparent glacial ^{14}C, and sensitivity to water component fractions

The mass balance equation:

$$^{14}C_{meas} \times 1 = {}^{14}C_{recent} \times (1-f) + {}^{14}C_{glacial} \times f$$

has been used to calculate glacial ^{14}C in the scenarios below.

Sample	^{14}C(pmC)	Recent fraction (1-f)	Glacial fraction (f)	Recent ^{14}C (pmC)	Glacial ^{14}C (pmC)
a) Assuming 35-B-3 was 100 % recent meteoric water:					
23-A-5	38.16	0.47	0.53	71.9	8.24
23-B-3	62.24	0.75	0.25	71.9	33.26
35-A-3	59.74	0.76	0.24	71.9	21.23
35-B-3	71.9	0.92	0.08		
b) ^{14}C recalculated after correcting for dilution of recent water by glacial (0.08%) in 35-B-3:					
23-A-5	38.16	0.47	0.53	78.15	2.70
23-B-3	62.24	0.75	0.25	78.15	14.51
35-A-3	59.74	0.76	0.24	78.15	1.44
c) Adjusting model recent and glacial component fractions to find values when glacial ^{14}C approximates to zero:					
23-A-5	38.16	0.49	0.51	78.15	-0.26
23-B-3	62.24	0.795	0.205	78.15	0.54
35-A-3	59.74	0.765	0.235	78.15	-0.19

The sensitivity of ^{14}C calculation in relation to recent and glacial water component values can be seen in 23-B-3 where it decreases from 14.5 pmC to 0 for a change in glacial component from 0.25 to 0.20. The very low calculated values, corrected for dilution by recent meteoric water, for glacial ^{14}C in 23-A-5 and 35-A-3 support the validity of the mixing model component ratios.

APPENDIX 4.1 Groundwater composition by end-member fraction

Sample	Date collected	Recent	Glacial	Brine
41-2 (45-A)	Feb-94	0.56	0.22	0.22
41-3(45-B)	Feb-94	0.78	0.18	0.04
41-5(39-A)	Feb-94	0.60	0.20	0.20
41-6	Feb-94	1.70	-0.74	0.04
41-7(35-C)	Feb-95	0.99	0.01	0.00
41-8(45-F)	Feb-95	0.30	0.24	0.45
41-9(45-B)	Feb-95	0.78	0.18	0.04
41-10(49-B)	Feb-95	0.28	0.28	0.44
41-11(53-A)	Feb-95	0.23	0.13	0.64
41-12	Feb-95	0.28	0.08	0.64
23-A-1	May-95	0.50	0.49	0.00
23-B-1	May-95	1.00	0.00	0.00
23-C-1	May-95	1.02	-0.02	0.00
23-E-1	May-95	0.98	0.02	0.00
23-F-1	May-95	0.99	0.01	0.00
35-A-1	May-95	0.79	0.19	0.01
35-B-1	May-95	0.99	0.01	0.00
35-C-1	May-95	0.99	0.01	0.00
39-A-1	May-95	0.57	0.22	0.21
45-A-1	May-95	0.57	0.22	0.21
45-B-1	May-95	0.78	0.17	0.05
45-C-1	May-95	0.68	0.21	0.11
45-D-1	May-95	0.66	0.19	0.15
45-E-1	May-95	0.75	0.12	0.13
45-G-1	May-95	0.57	0.18	0.26
49-A-1	May-95	0.38	0.37	0.25
49-B-1	May-95	0.25	0.29	0.46
53-A-1	May-95	0.14	0.19	0.68
53-B-1	May-95	0.15	0.17	0.67
53-C-1	May-95	0.12	0.14	0.74
23-B-2	Jul-95	0.81	0.18	0.01
23-C-2	Jul-95	0.94	0.05	0.00
23-E-2	Jul-95	0.97	0.03	0.00
35-A-2	Jul-95	0.76	0.22	0.02
35-B-2	Jul-95	0.98	0.01	0.00
45-A-2	Jul-95	0.59	0.20	0.20
45-B-2	Jul-95	0.76	0.20	0.04
45-B-2D	Jul-95	0.76	0.20	0.04
45-E-2	Jul-95	0.71	0.14	0.14
45-E-2A	Jul-95	0.74	0.13	0.12
45-E-2B	Jul-95	0.74	0.12	0.14
45-G-2	Jul-95	0.53	0.19	0.27
49-A-2	Jul-95	0.43	0.34	0.23
23-A-3	Nov-95	0.45	0.54	0.00
23-B-3	Nov-95	0.74	0.25	0.01
23-C-3	Nov-95	0.89	0.11	0.00
23-D-3	Nov-95	0.61	0.27	0.12
23-E-3	Nov-95	0.96	0.04	0.00
23-F-3	Nov-95	0.96	0.04	0.00
35-A-3	Nov-95	0.76	0.21	0.03
35-B-3	Nov-95	0.94	0.06	0.00
35-D-3	Nov-95	0.87	0.09	0.03

Sample	Date collected	Recent	Glacial	Brine
43-A-3	Nov-95	0.49	0.24	0.26
43-B-3	Nov-95	0.75	0.17	0.08
43-C-3	Nov-95	0.56	0.32	0.12
45-A-3	Nov-95	0.56	0.25	0.19
45-B-3	Nov-95	0.76	0.19	0.05
45-C-3	Nov-95	0.56	0.27	0.18
45-D-3	Nov-95	0.63	0.19	0.18
45-E-3	Nov-95	0.71	0.15	0.14
45-G-3	Nov-95	0.51	0.21	0.27
49-A-3	Nov-95	0.32	0.39	0.29
49-B-3	Nov-95	0.18	0.33	0.49
53-A-3	Nov-95	-0.07	0.28	0.79
53-B-3	Nov-95	-0.05	0.27	0.78
53-C-3	Nov-95	-0.08	0.24	0.84
23-A-4	Jun-96	0.48	0.51	0.00
23-B-4	Jun-96	0.78	0.22	0.00
23-C-4	Jun-96	0.88	0.12	0.00
23-D-4	Jun-96	0.66	0.23	0.11
23-E-4	Jun-96	0.96	0.04	0.00
23-F-4	Jun-96	0.95	0.05	0.00
35-A-4	Jun-96	0.77	0.20	0.03
35-B-4	Jun-96	0.94	0.06	0.00
35-D-4	Jun-96	0.94	0.05	0.01
39-A-4	Jun-96	0.54	0.23	0.23
45-A-4	Jun-96	0.73	0.21	0.06
45-B-4	Jun-96	0.78	0.19	0.03
45-C-4	Jun-96	0.55	0.28	0.17
45-D-4	Jun-96	0.64	0.19	0.18
45-E-4	Jun-96	0.52	0.23	0.25
45-F-4	Jun-96	0.01	0.38	0.61
45-G-4	Jun-96	0.38	0.23	0.39
49-A-4	Jun-96	0.27	0.39	0.33
49-B-4	Jun-96	0.08	0.32	0.60
53-A-4	Jun-96	-0.11	0.30	0.80
53-B-4	Jun-96	0.13	0.17	0.69
53-C-4	Jun-96	0.00	0.20	0.80
53-D-4	Jun-96	0.05	0.29	0.66

Samples from previous Con Mine groundwater studies
(Frape et al, 1984; Macdonald, 1986)

45-B	Jul-80	0.27	0.58	0.16
45-D	Jul-80	0.66	0.20	0.14
45-G	Jul-80	0.36	0.06	0.59
45-B	Apr-81	0.40	0.48	0.12
45-G	Apr-81	0.49	0.25	0.26
45-B	85	0.66	0.26	0.08
45-D	85	0.64	0.19	0.17

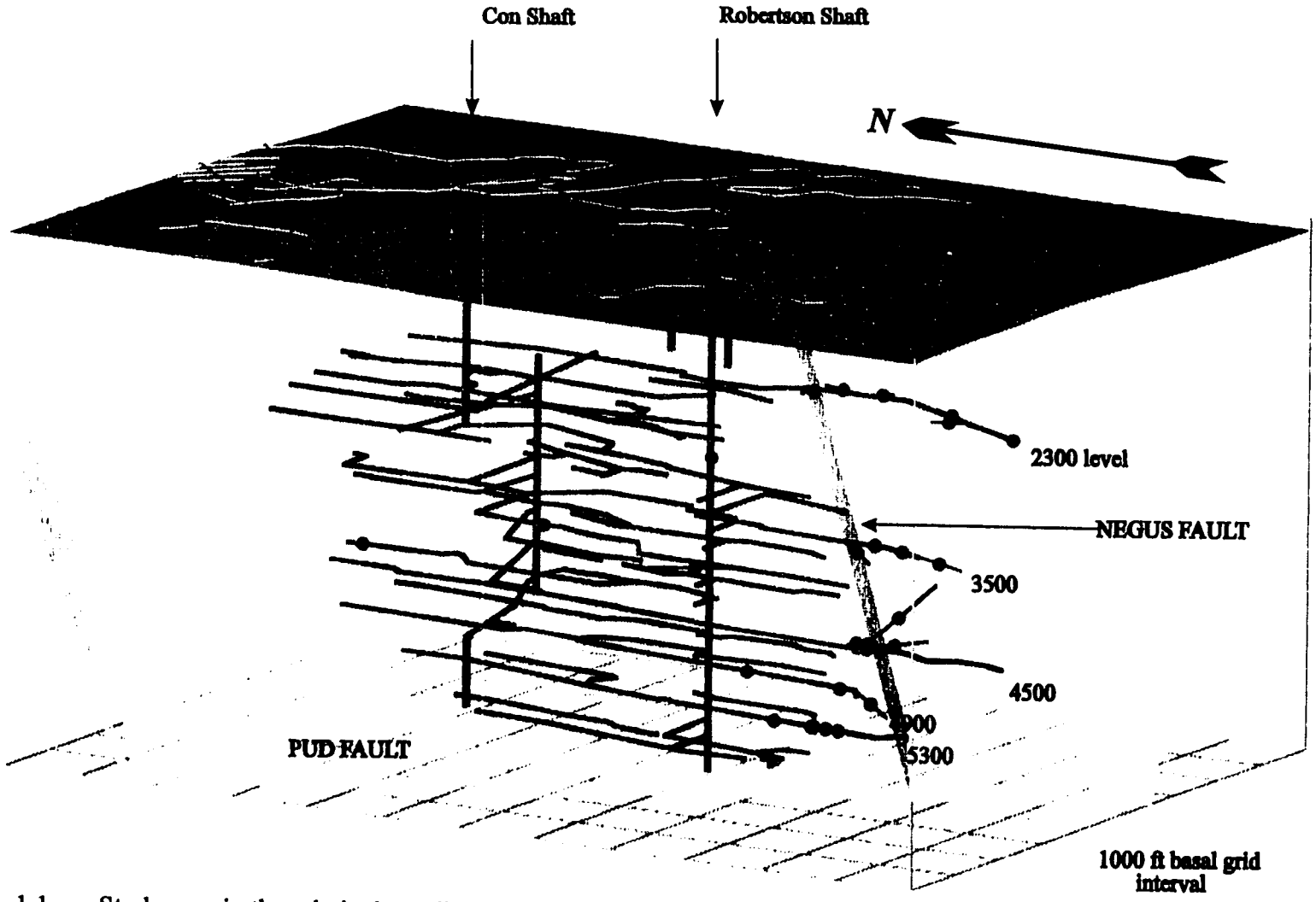

Fig. 1.1. Study area in the relatively undisturbed south end of the Con Mine. The position of the Negus fault in relation to intersecting boreholes (blue), and drifts (green), can be seen. Where they penetrate SW of the Pud fault these appear darker. Angel-type faults (E-W; sub-vertical) have been omitted for clarity. Sampled locations are indicated by red circles.

Fig. 2.1. Geographical context of study area.

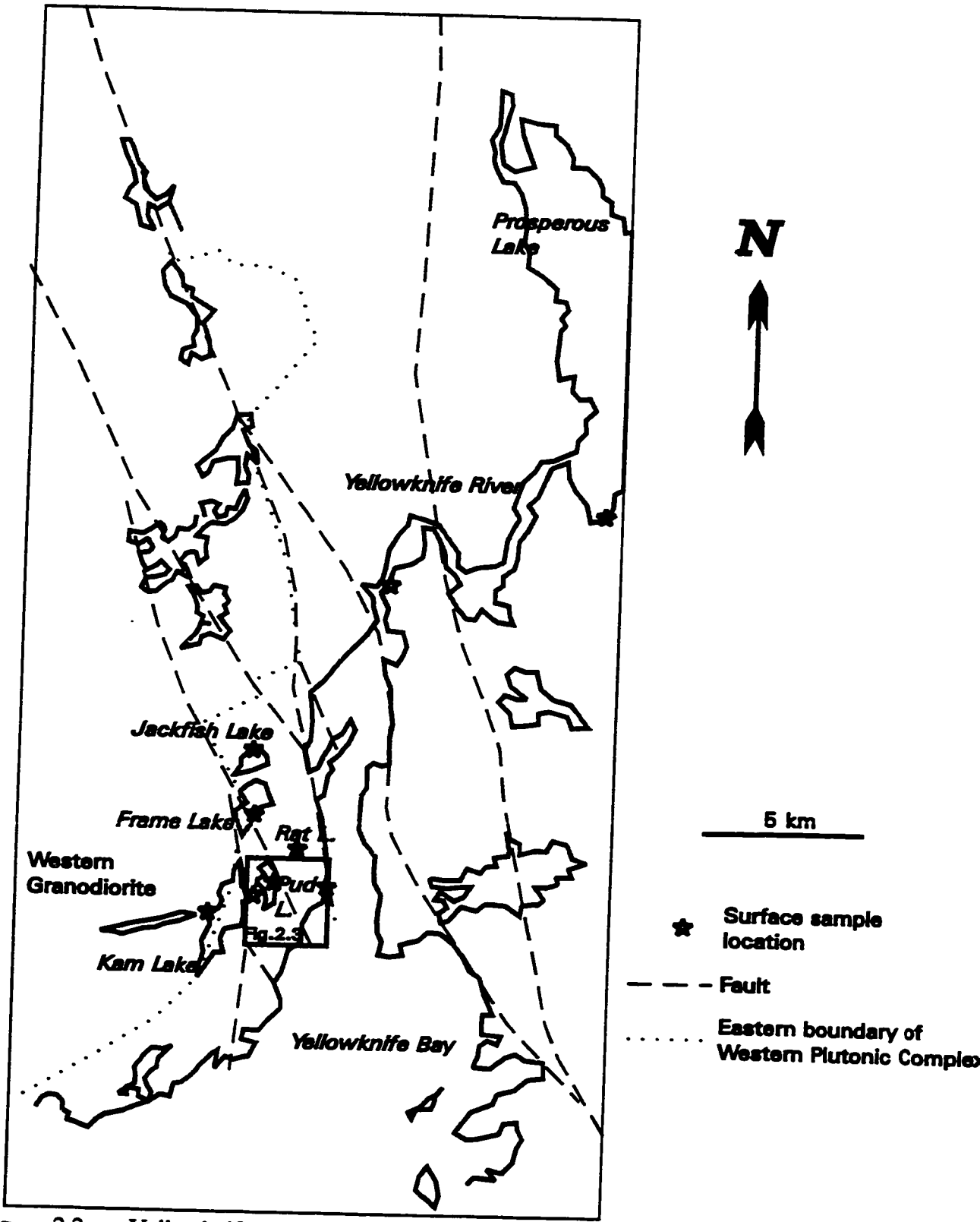

Fig. 2.2. Yellowknife district showing surface water sample locations and regional faulting.

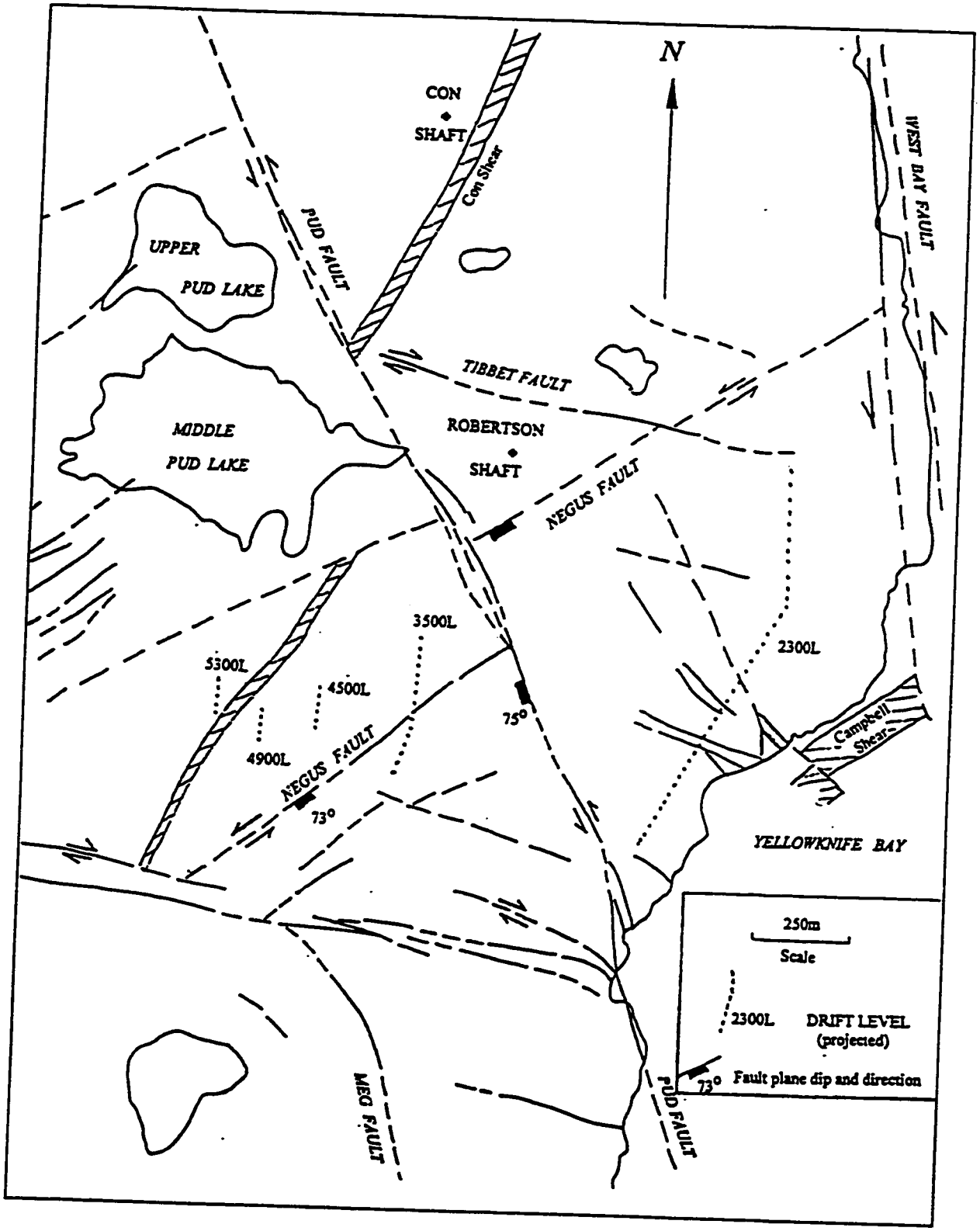

Fig. 2.3. Surface detail showing mineralised shear zones, faults, and surface water bodies in the area sampled. The projected drift sections represent the north-south limits between regular sampling locations at each level, and illustrate the westerly offset of drifts with increasing depth.

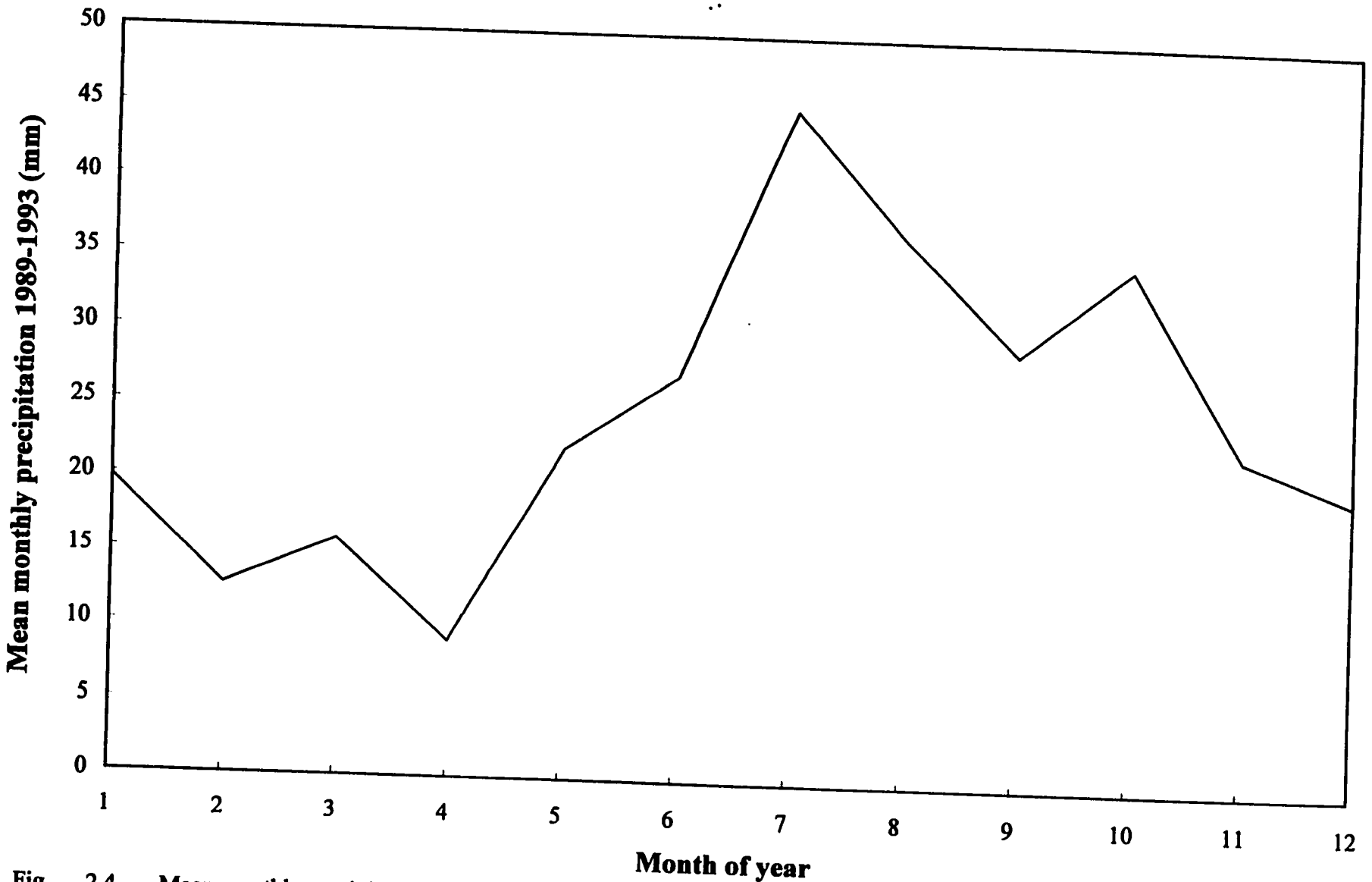

Fig. 2.4 Mean monthly precipitation at Yellowknife for 1989-1993.

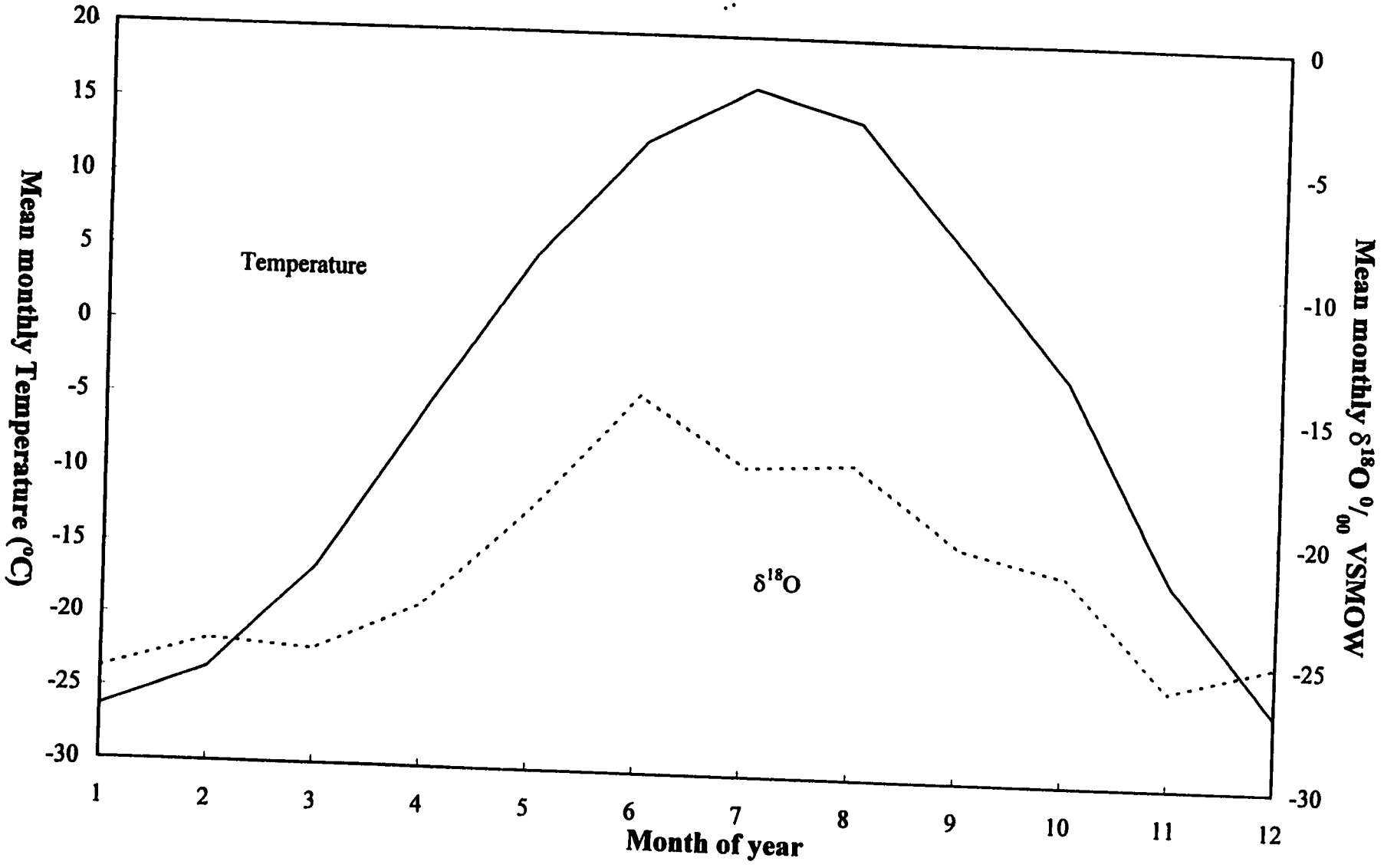

Fig. 2.5 Mean monthly temperature and $\delta^{18}O$ in precipitation at Yellowknife for the period 1989-1993.

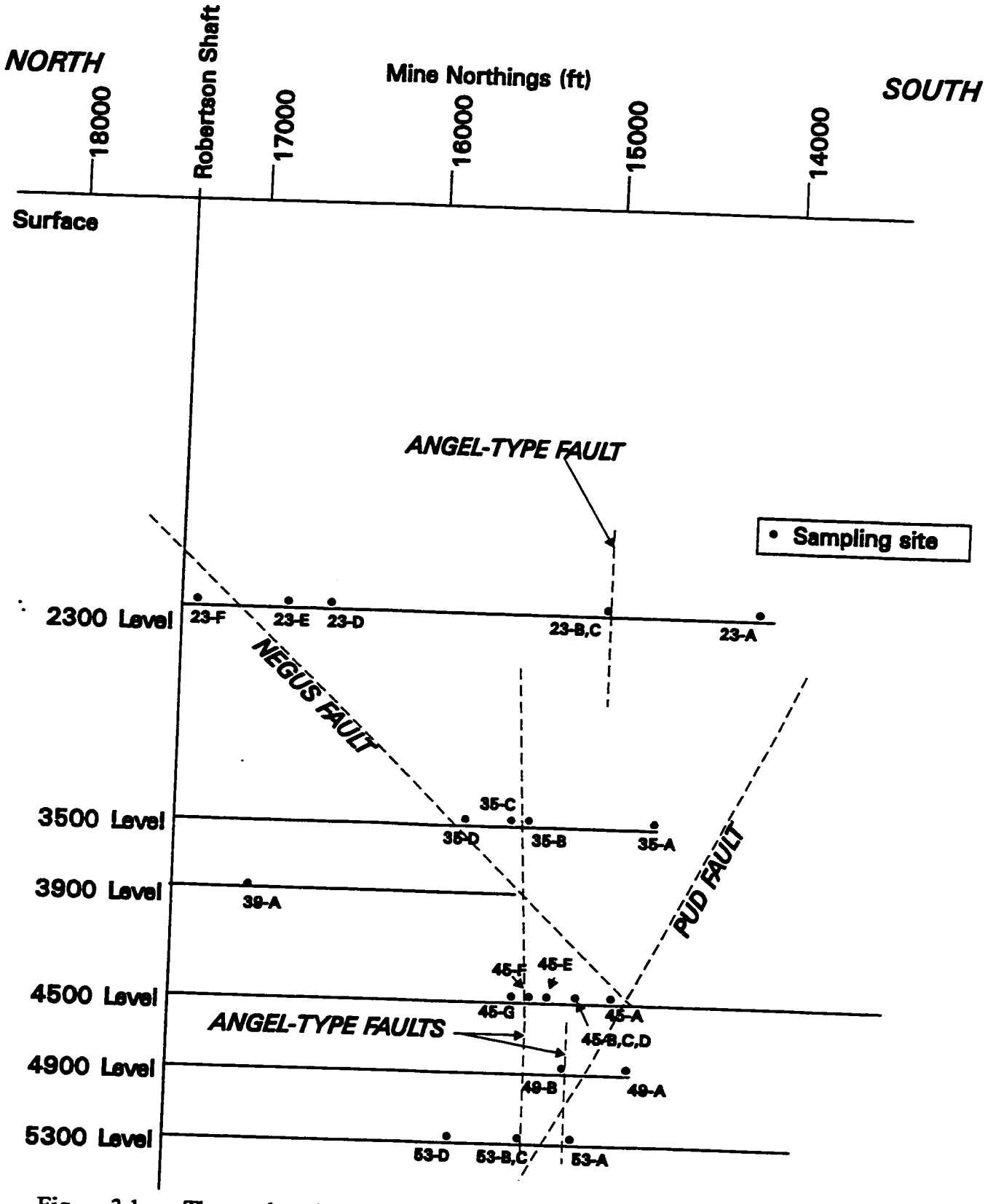

Fig. 3.1. The south end of the mine showing drifts with sample locations and their relationship to faults, projected to this vertical cross-section.

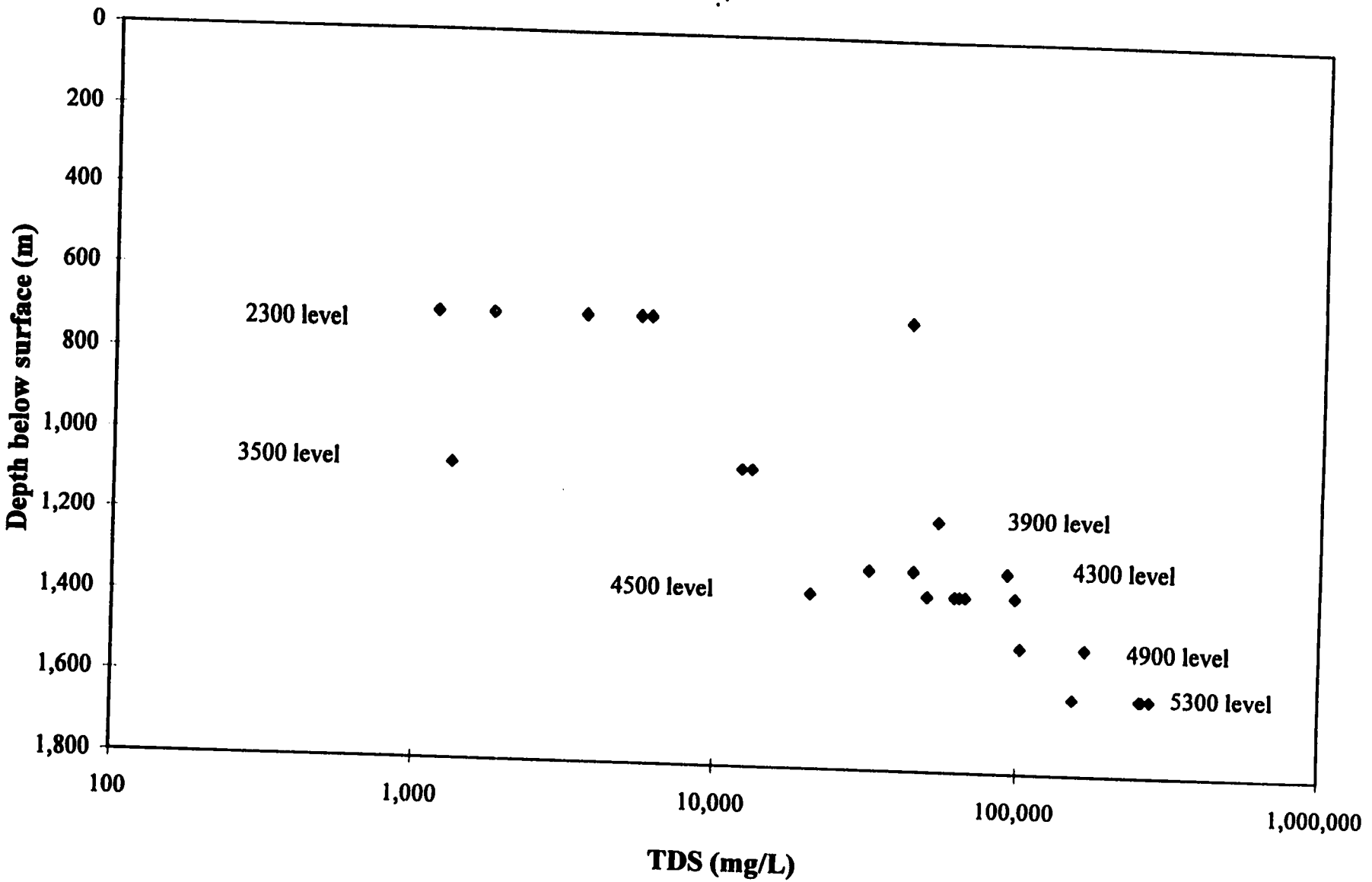

Fig. 3.2. Relationship of Total Dissolved Solids and sampling depth (Nov 95 data).

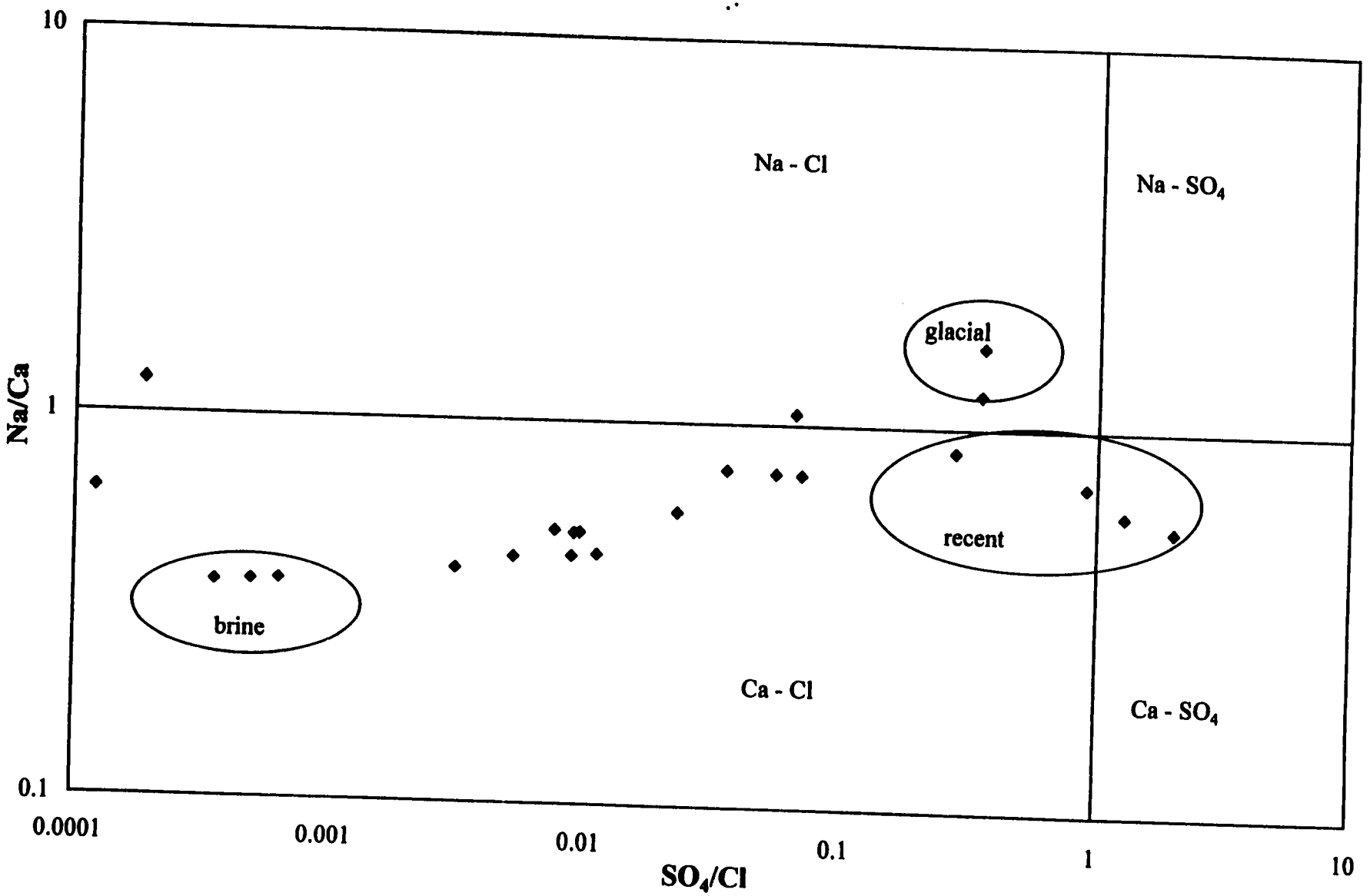

Fig. 3.3. Comparison of Na/Ca and SO_4/Cl ratios (using meq/L) (Nov 95 data).

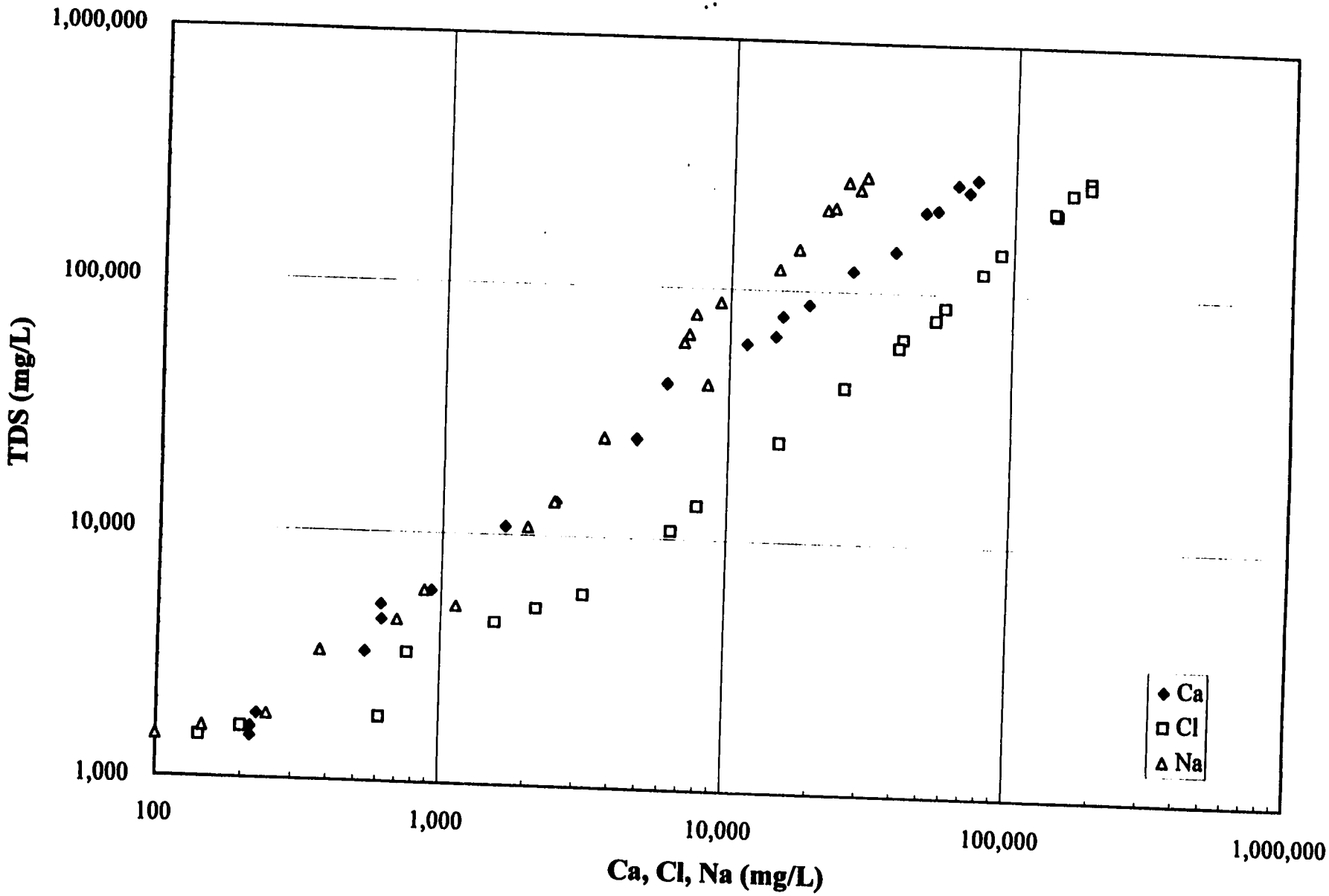

Fig. 3.4. Relationship of TDS and the dominant ions Cl, Ca, and Na (June 96 data).

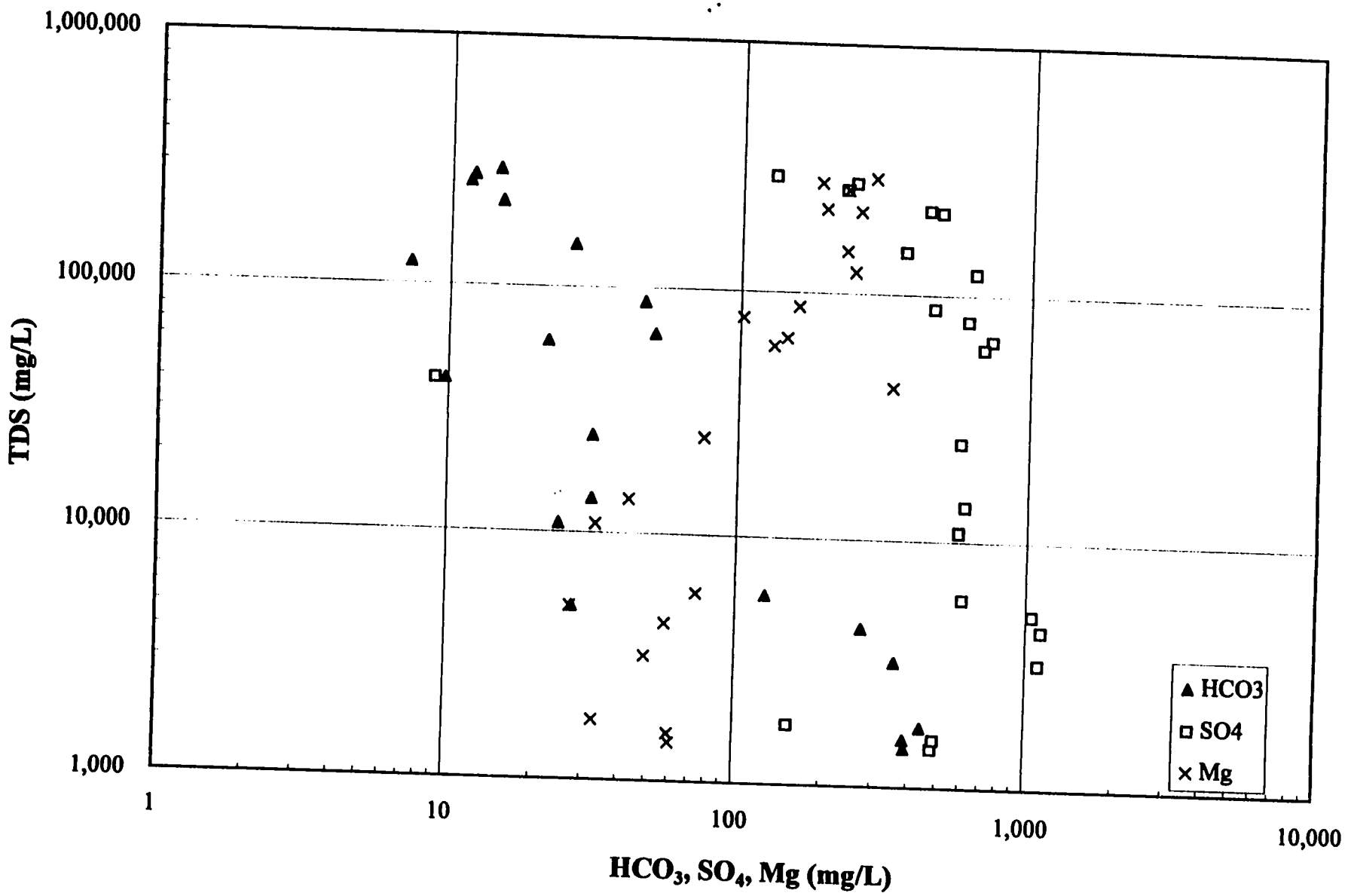

Fig. 3.5. Relationship of TDS and Mg, SO_4, and HCO_3 (June 96 data).

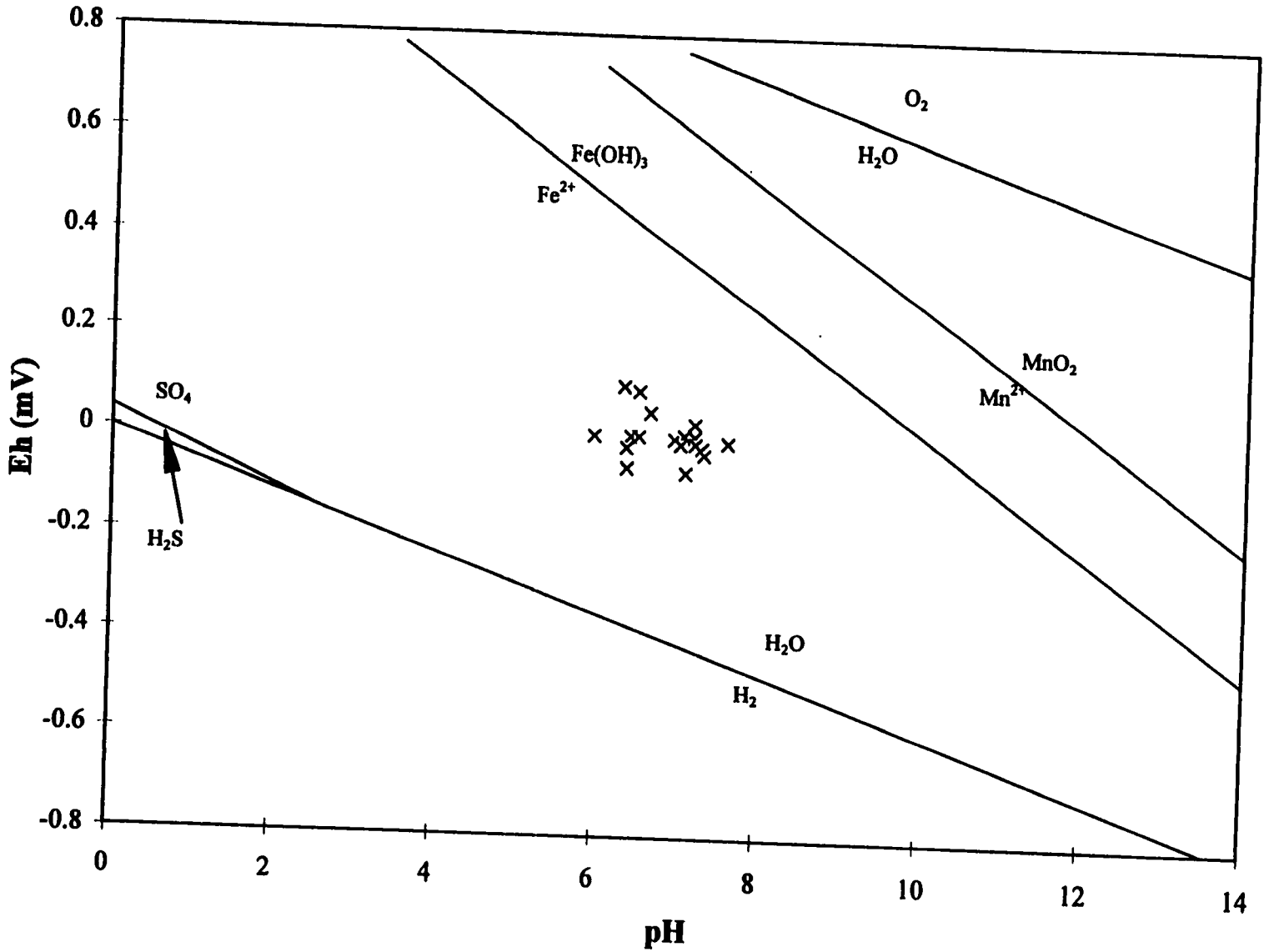

Fig. 3.6 Eh/pH relationship for samples (June 96). The Mn and Fe field boundaries are defined for Mn^{2+} and Fe^{2+} concentrations of 10 mg/L.

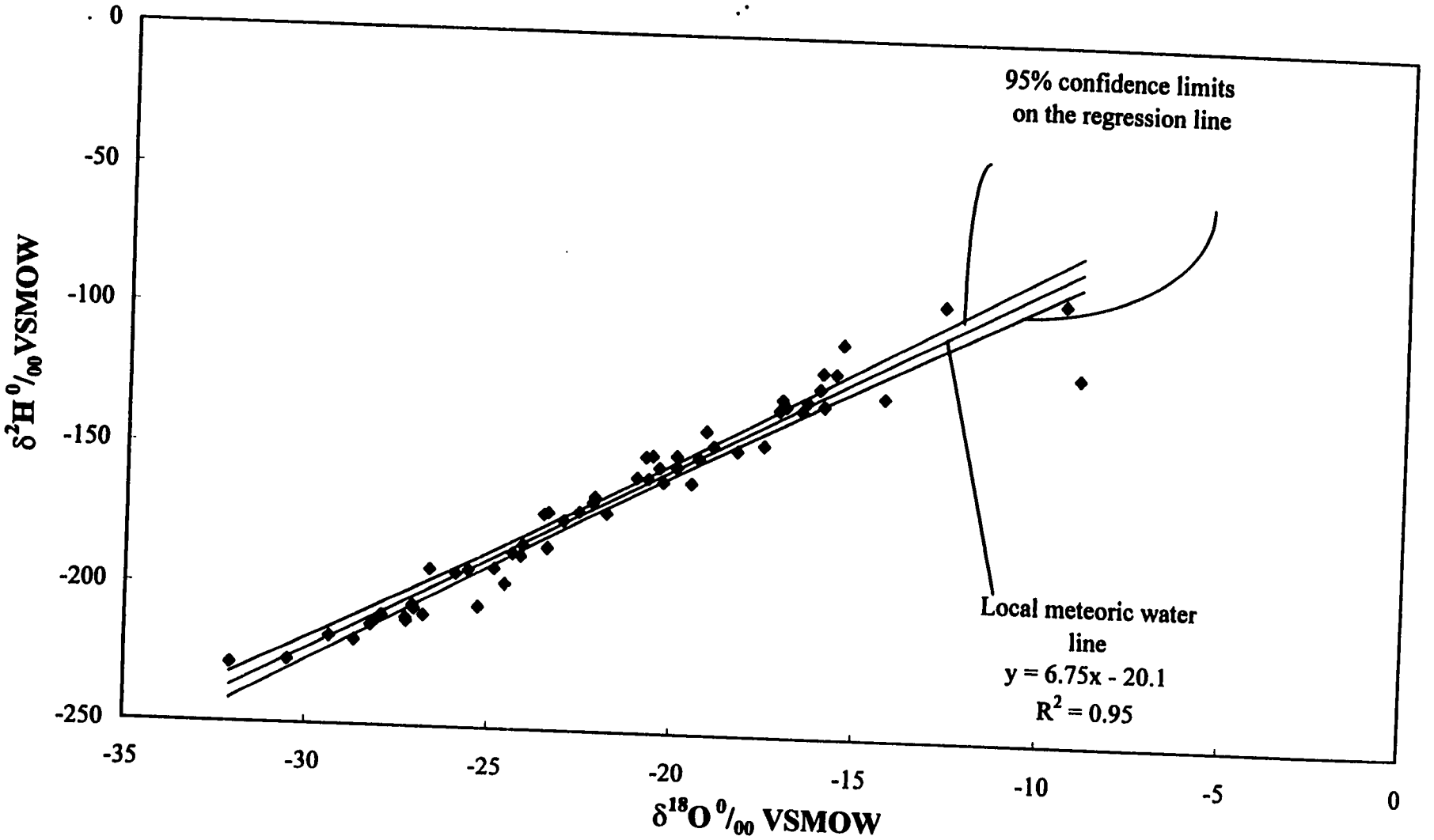

Fig. 3.7 Relationship of $\delta^{18}O$ and $\delta^{2}H$ for Yellowknife precipitation for the period 1989-1993. Regression of these data produced the trendline and equation shown, and is used as the Local Meteoric Water Line (LMWL). The 95 % confidence limits on the regression are shown.

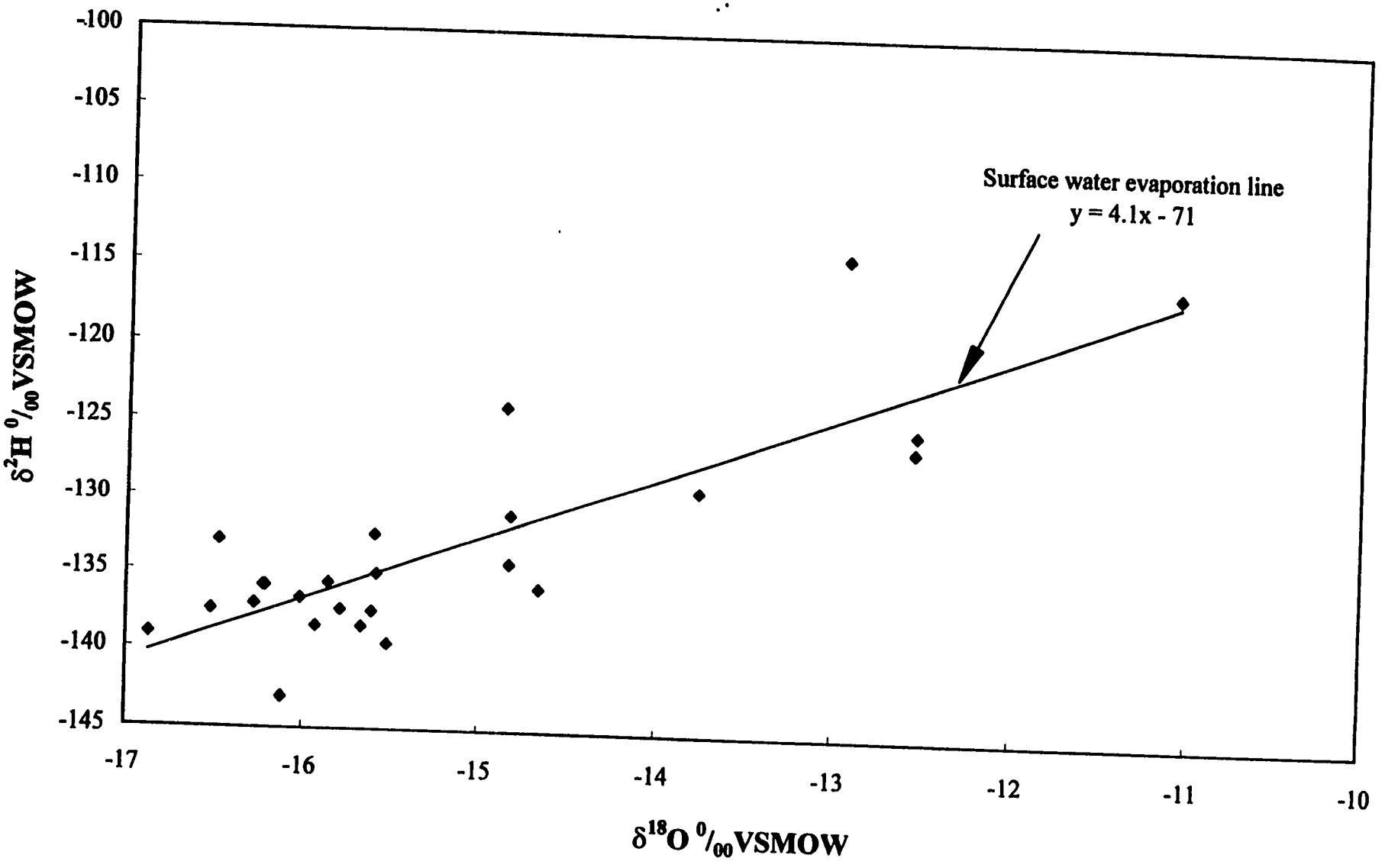

Fig. 3.8. Relationship of $\delta^{18}O$ and $\delta^{2}H$ for surface waters. Regression of this data produced the trendline and equation shown, and represents the surface water evaporation line.

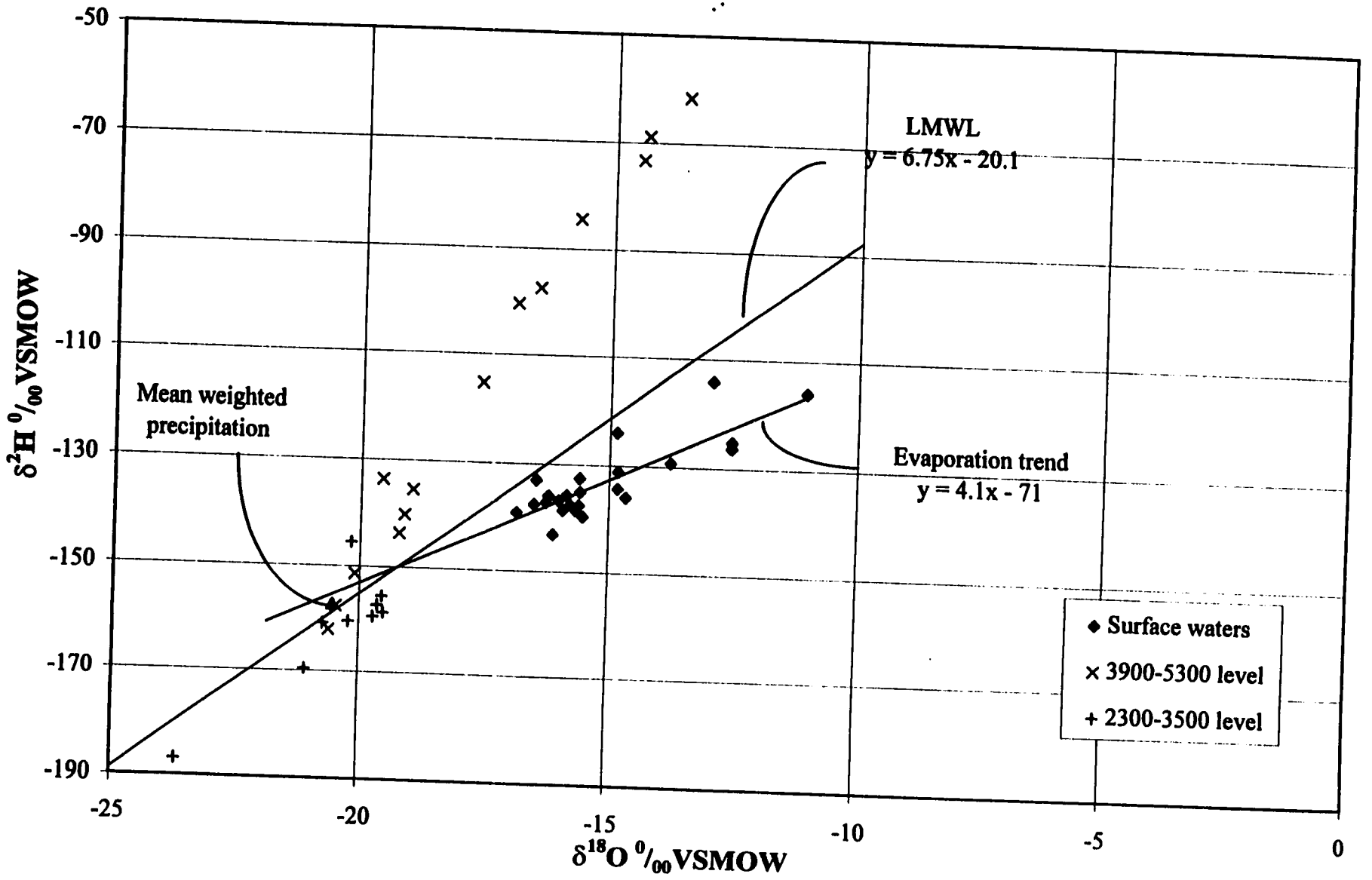

Fig. 3.9. Relationship of water isotopes $\delta^{18}O$ and $\delta^{2}H$, including all surface water data, and June 1996 groundwaters.

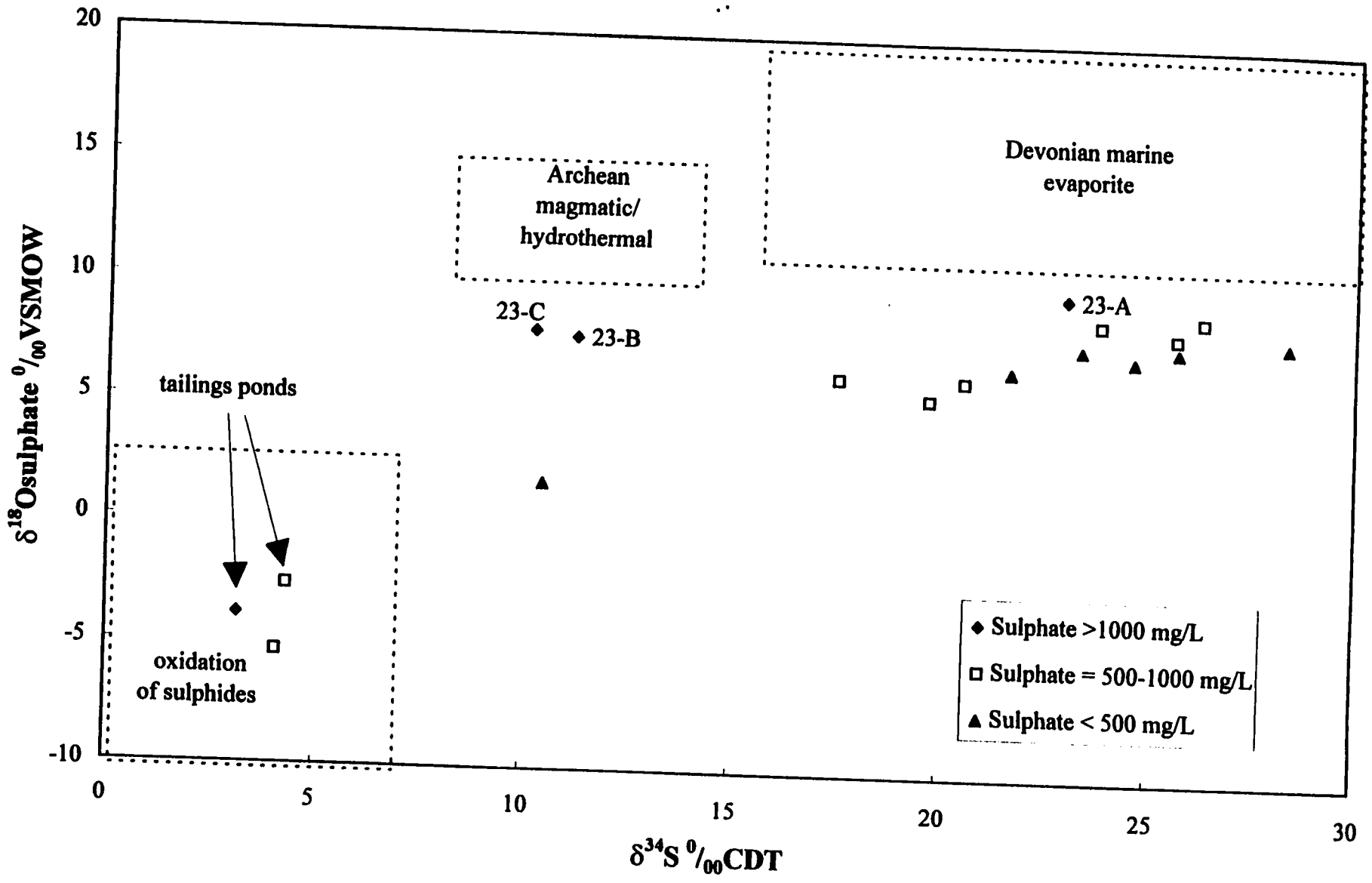

Fig. 3.10. Relationship of the sulphate isotopes $\delta^{18}O$ and $\delta^{34}S$.

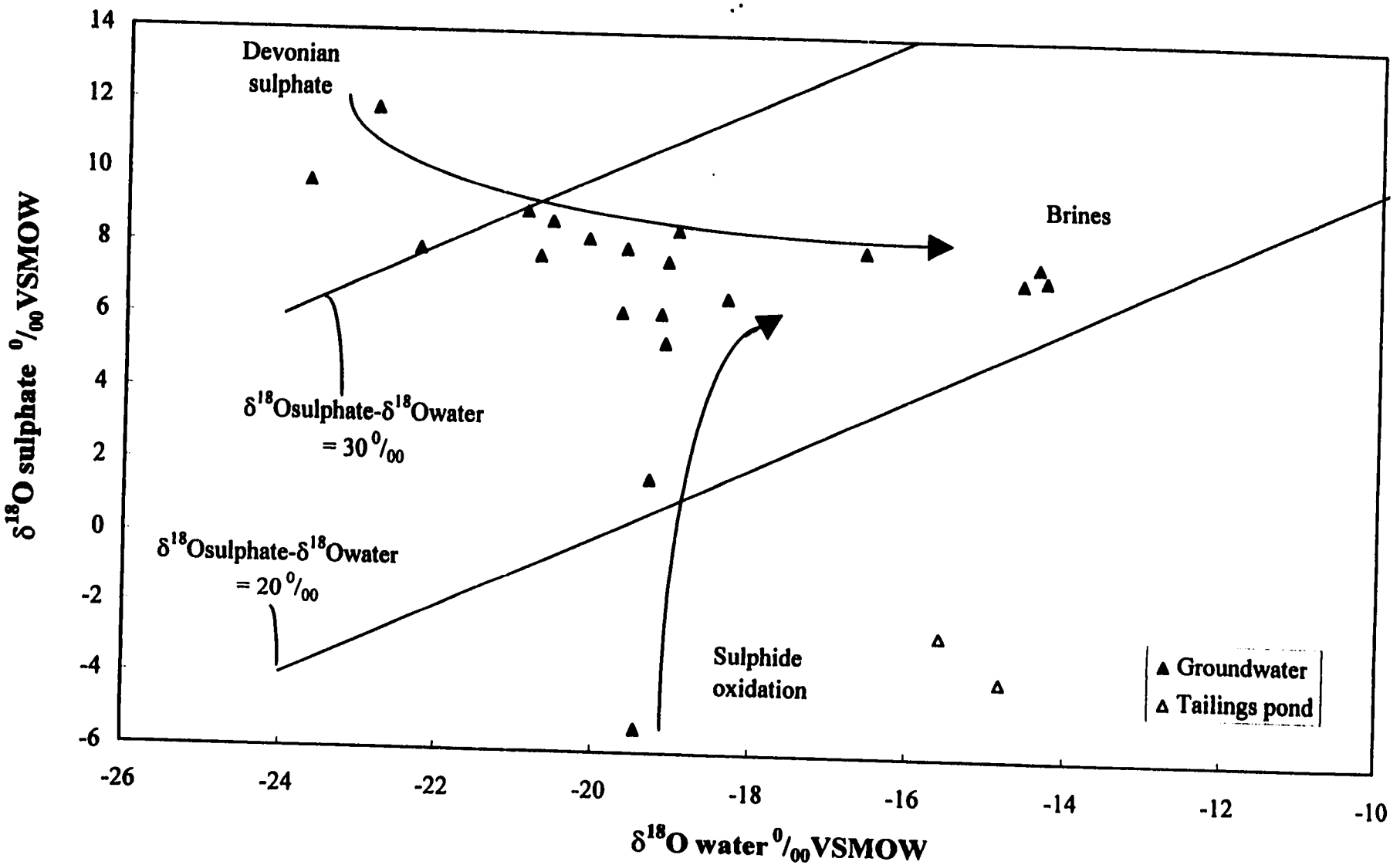

Fig. 3.11. Relationship between $\delta^{18}O$ in water and sulphate illustrating mixing (arrows) of sulphates from oxidation of sulphide, and Devonian evaporite. Guidelines indicating 20 $^{0}/_{00}$ and 30 $^{0}/_{00}$ difference in $\delta^{18}O$ between sulphate and water are shown.

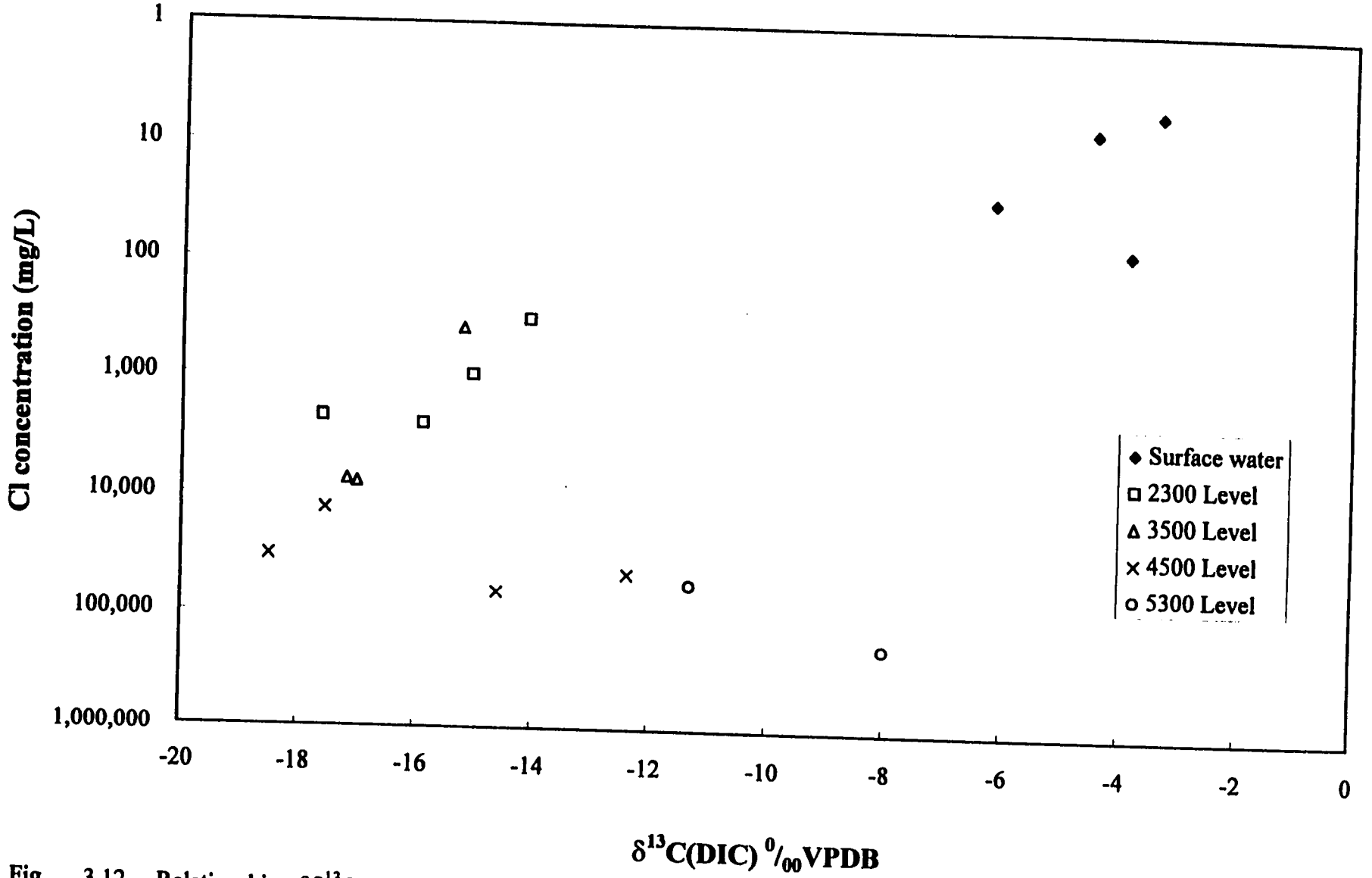

Fig. 3.12 Relationship of $\delta^{13}C$ and Cl concentration in groundwater.

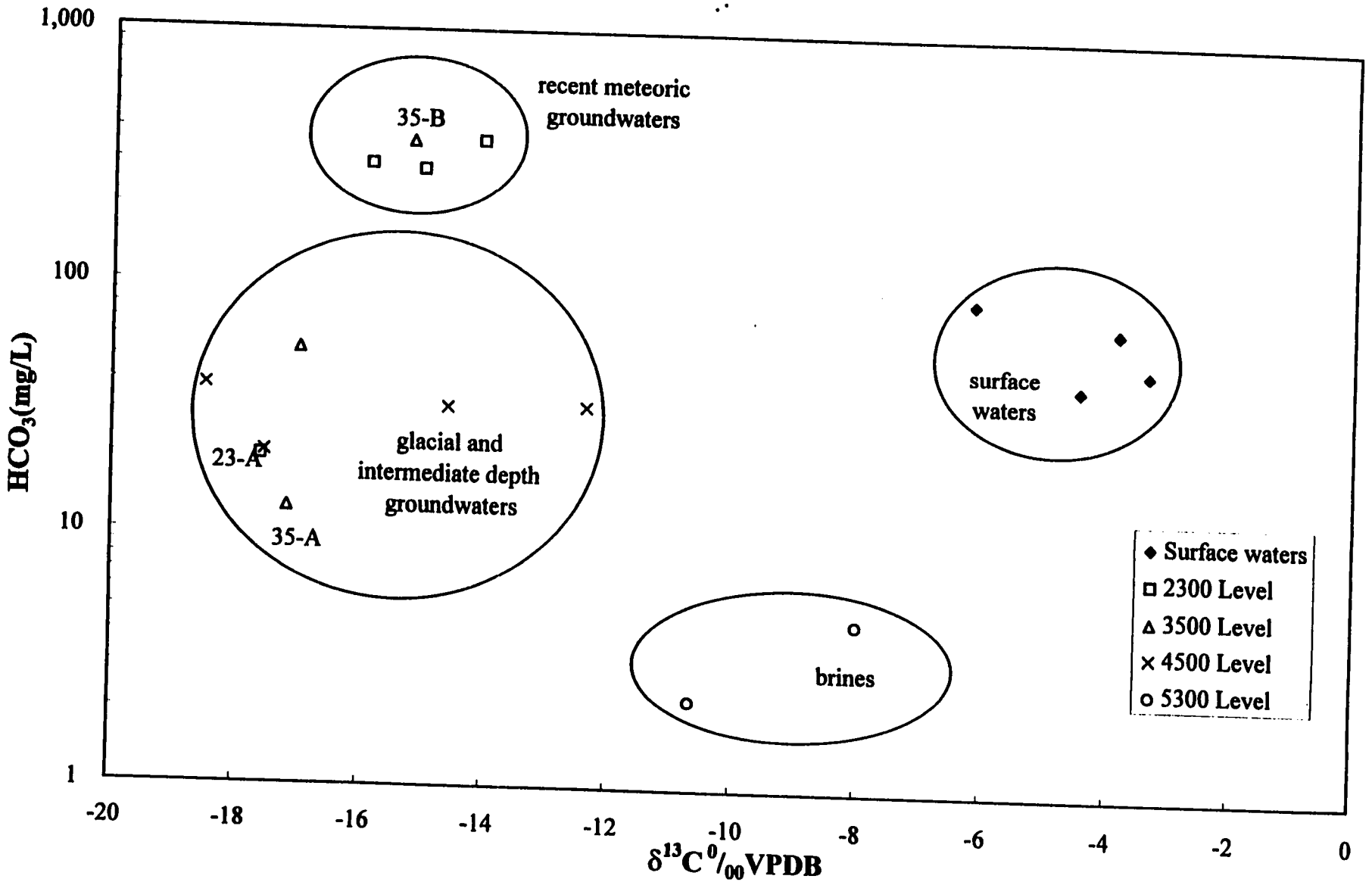

Fig. 3.13. Relationship of HCO_3 and $\delta^{13}C$, showing differentiation between waters depending on source.

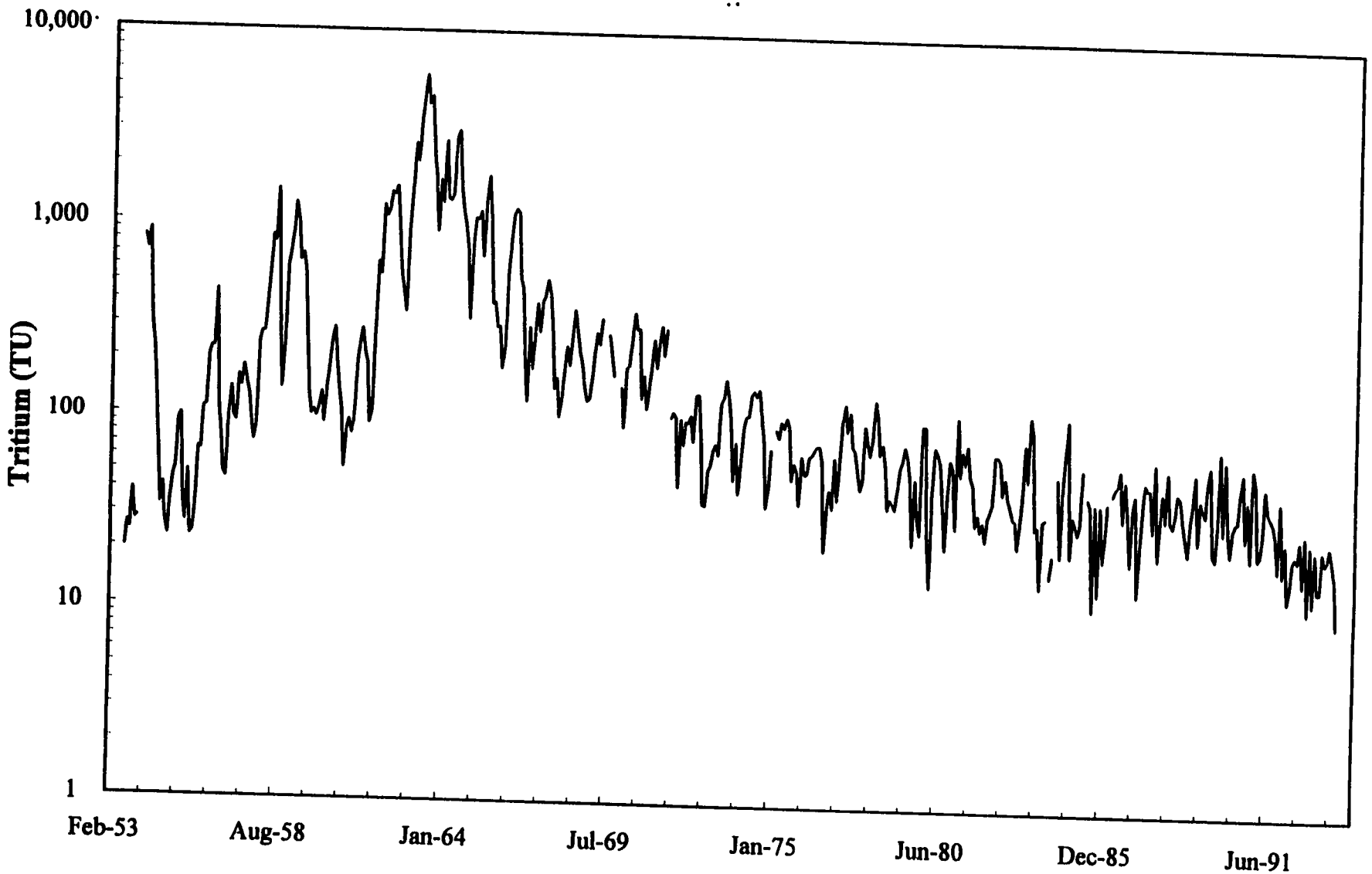

Fig. 3.14. Tritium data for Ottawa showing the change in relative levels in precipitation from 1953 to 1993.

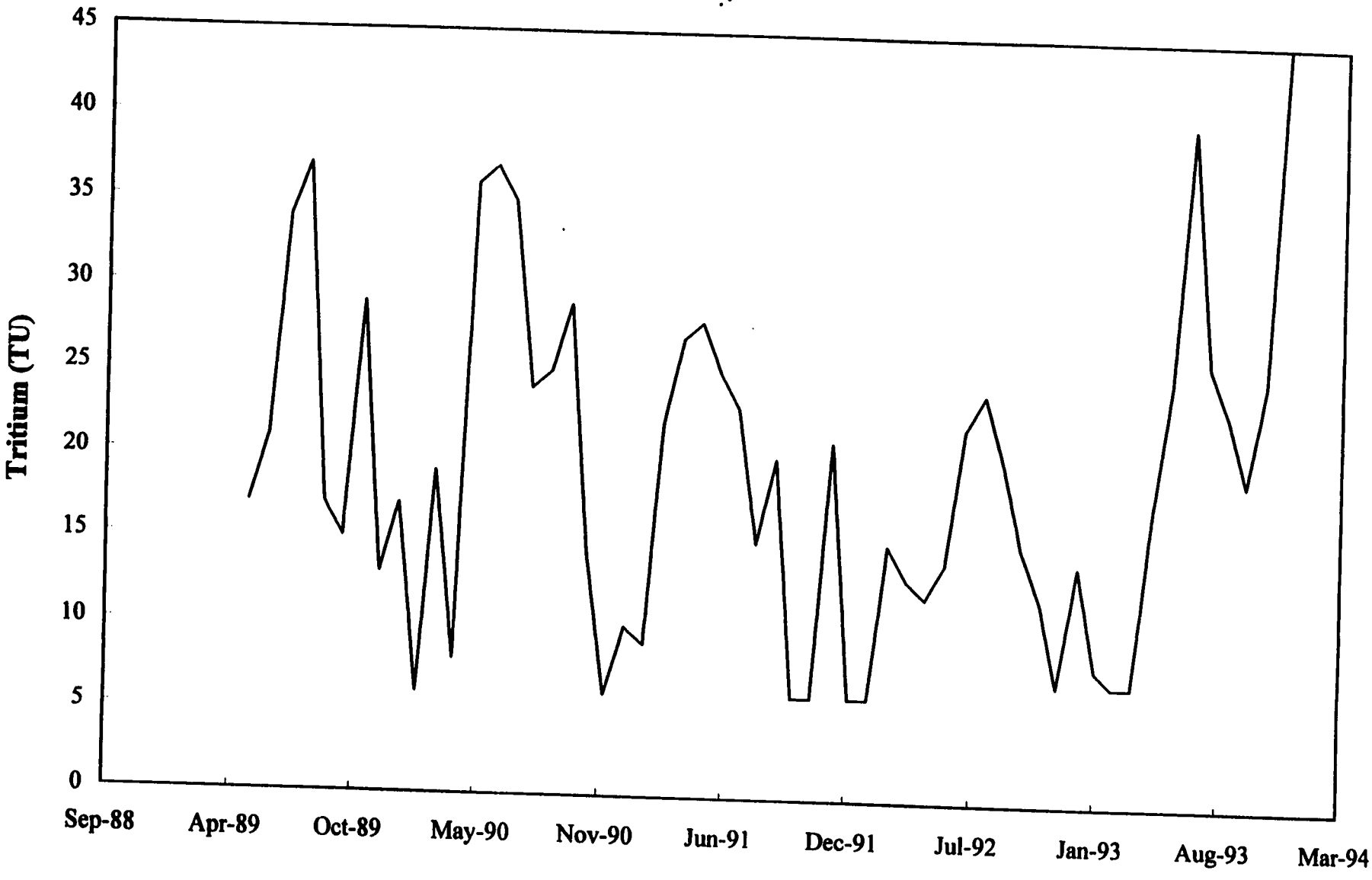

Fig. 3.15 Tritium in precipitation at Yellowknife (IAEA database).

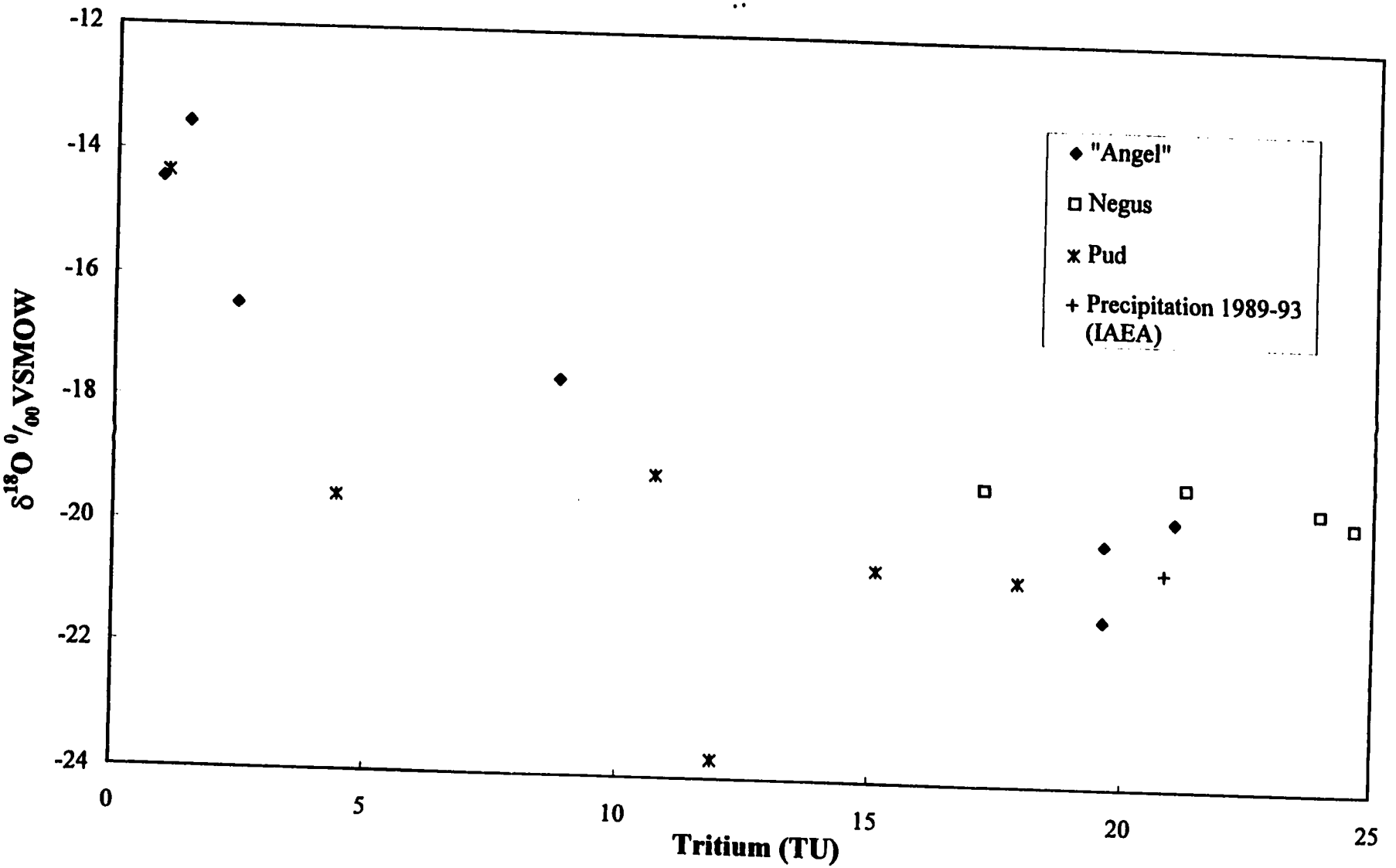

Fig. 3.16. Tritium content (most recent results for each location) related to faults producing flow.

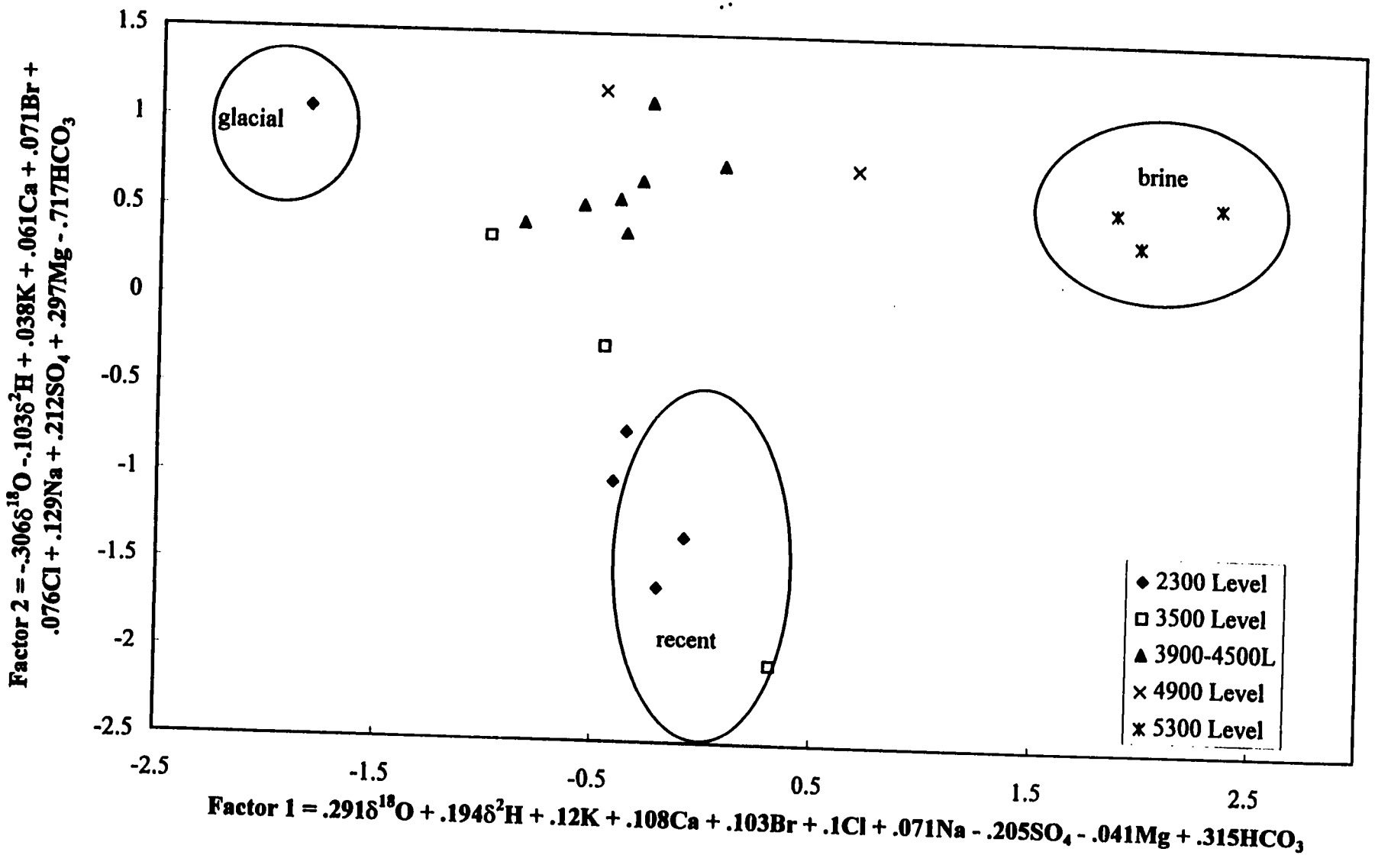

Fig. 4.1. Relative water character from Principal Component Analysis. Areas of maximum influence of the three water types are shown. Calculations are based on May 95 data.

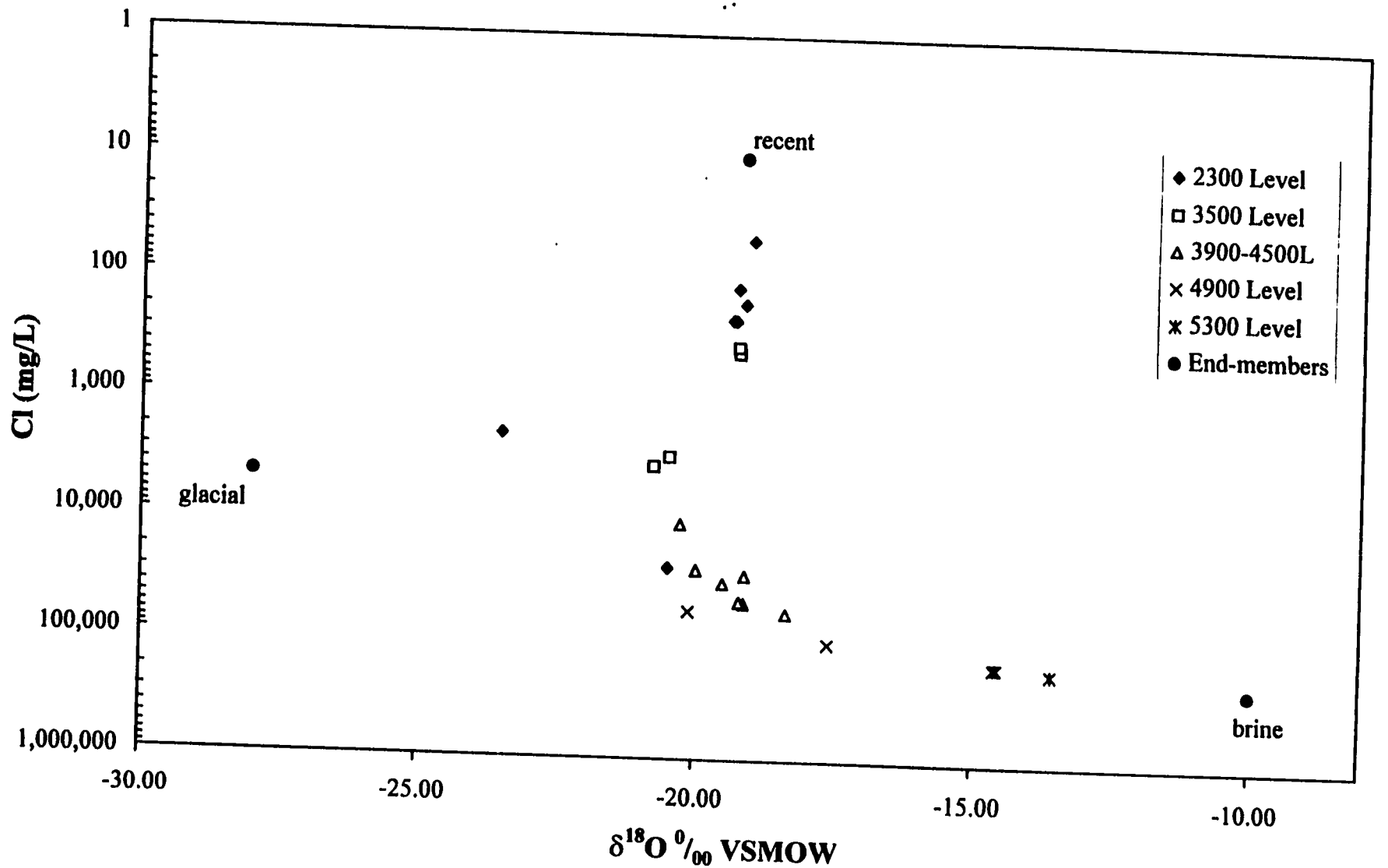

Fig. 4.2. Relationship between $\delta^{18}O$ and chloride concentration. Theoretical end-members used in the mixing model are plotted (May 95 data, with results for 23-D, and 35-D, not sampled at that time, added from June 96).

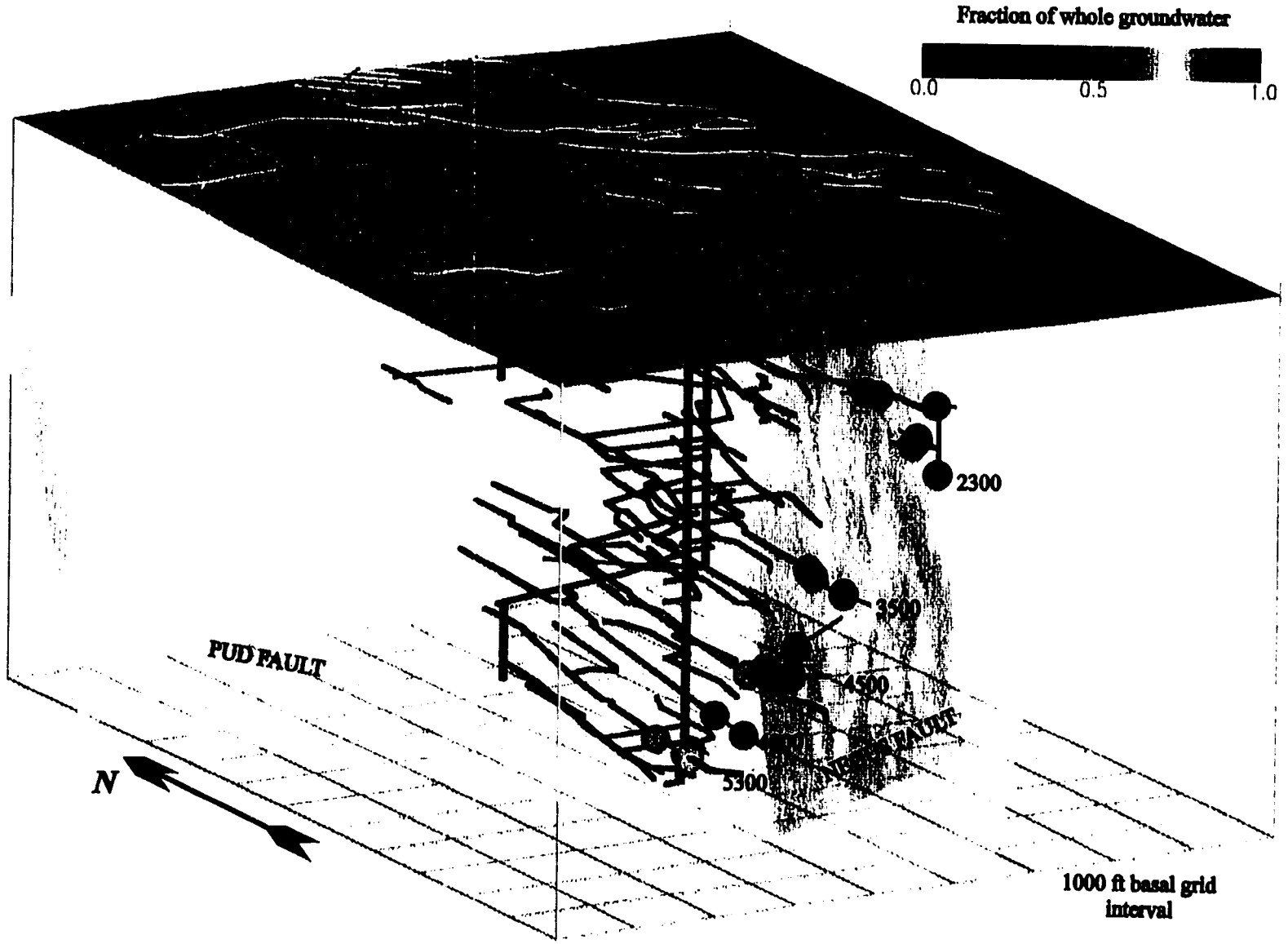

Fig. 4.3 Brine distribution in November 1995 (includes 45-F and 53-D data from June 1996), expressed as a fraction of total groundwater, showing the extent of dilution by meteoric water inflow.

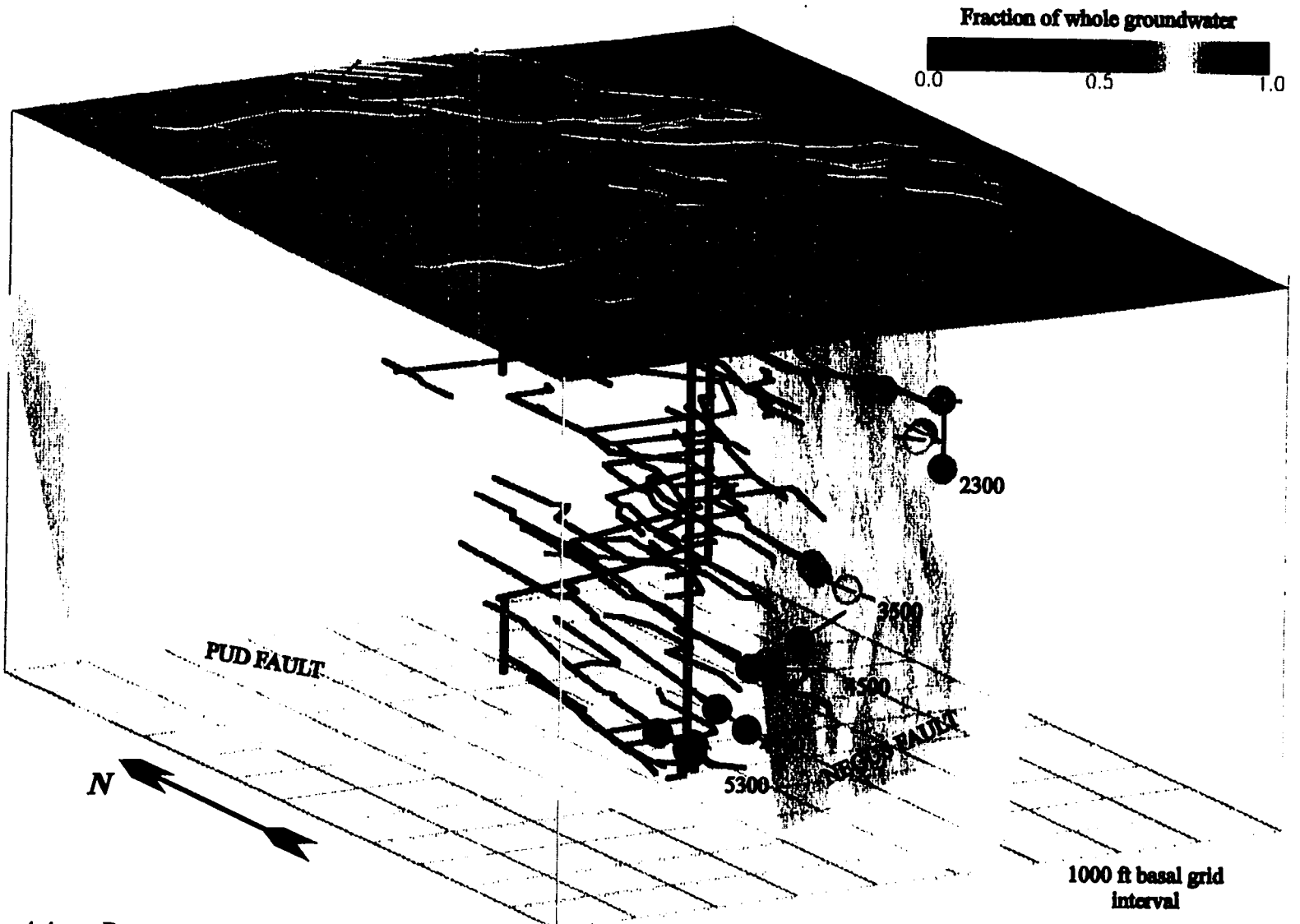

Fig. 4.4 Recent meteoric water distribution in November 1995 (includes 45-F and 53-D data from June 1996), expressed as a fraction of total groundwater, the spatial irregularity in content illustrating the effect of different faults. Angel-type faults (sub-vertical, E-W) have been omitted for clarity.

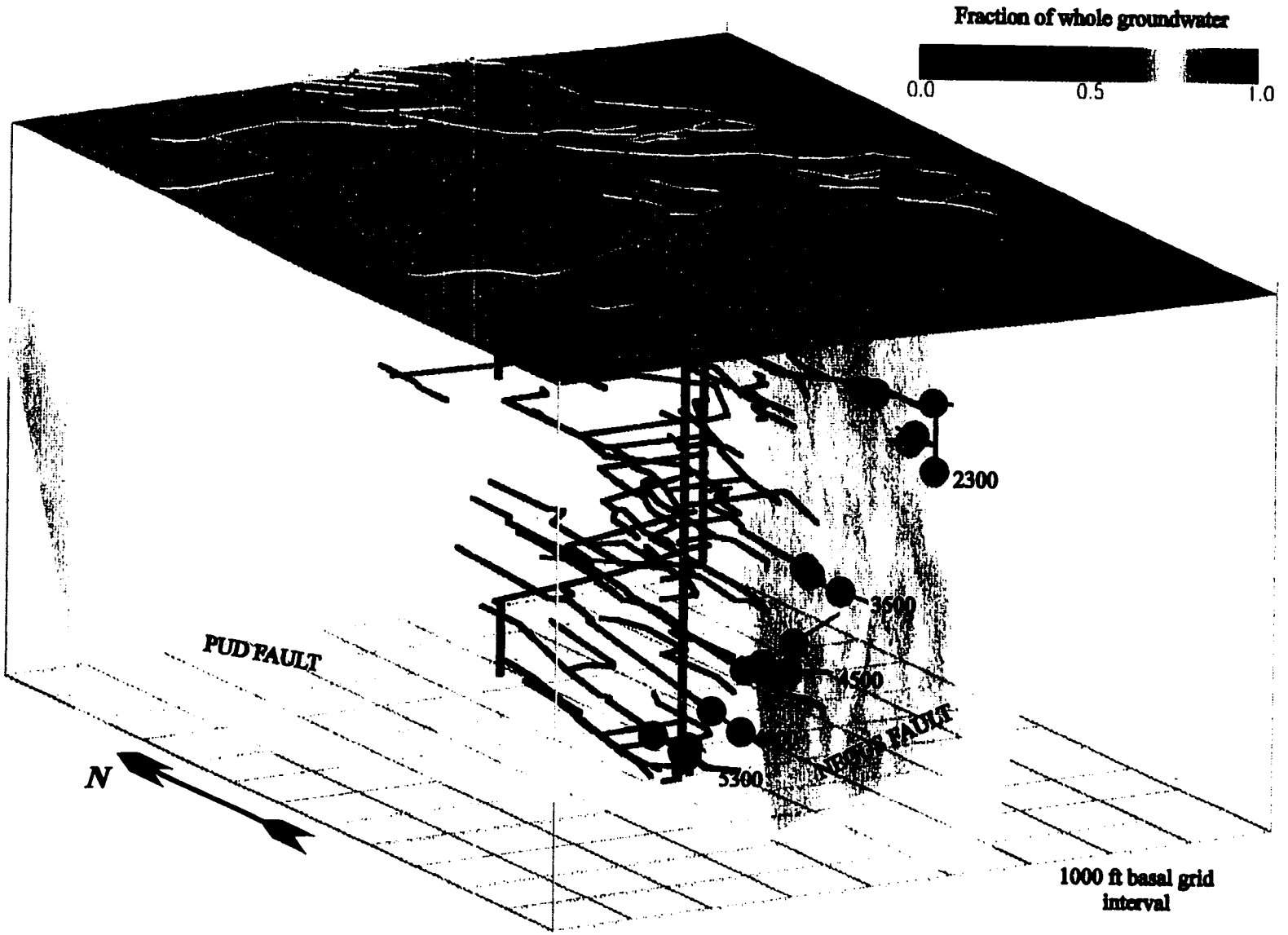

Fig. 4.5 Glacial water distribution in November 1995 (includes 45-F and 53-D data from June 1996), expressed as a fraction of total groundwater, showing highest proportions at the south end of levels 2300 and 4900.

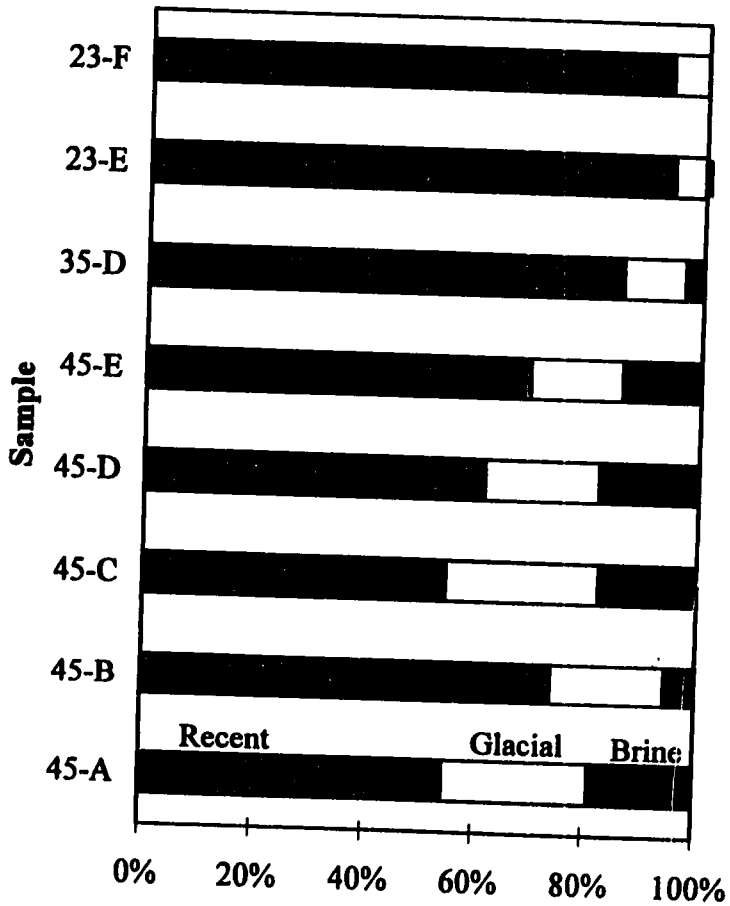

a. November 1995

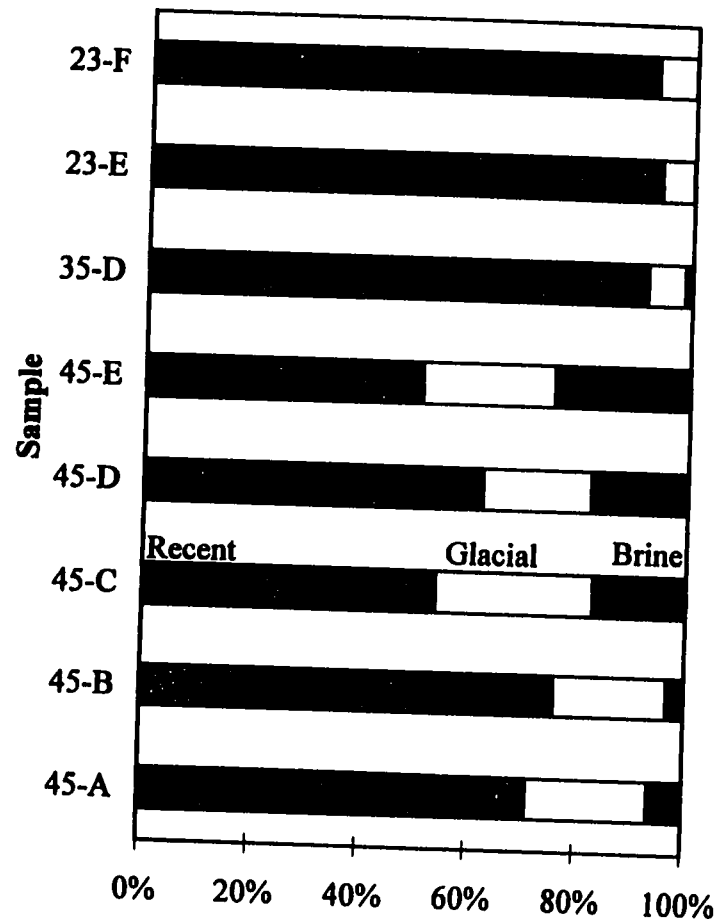

b. June 1996

Fig. 4.6. Progressive change in water composition at sample locations along the Negus fault.

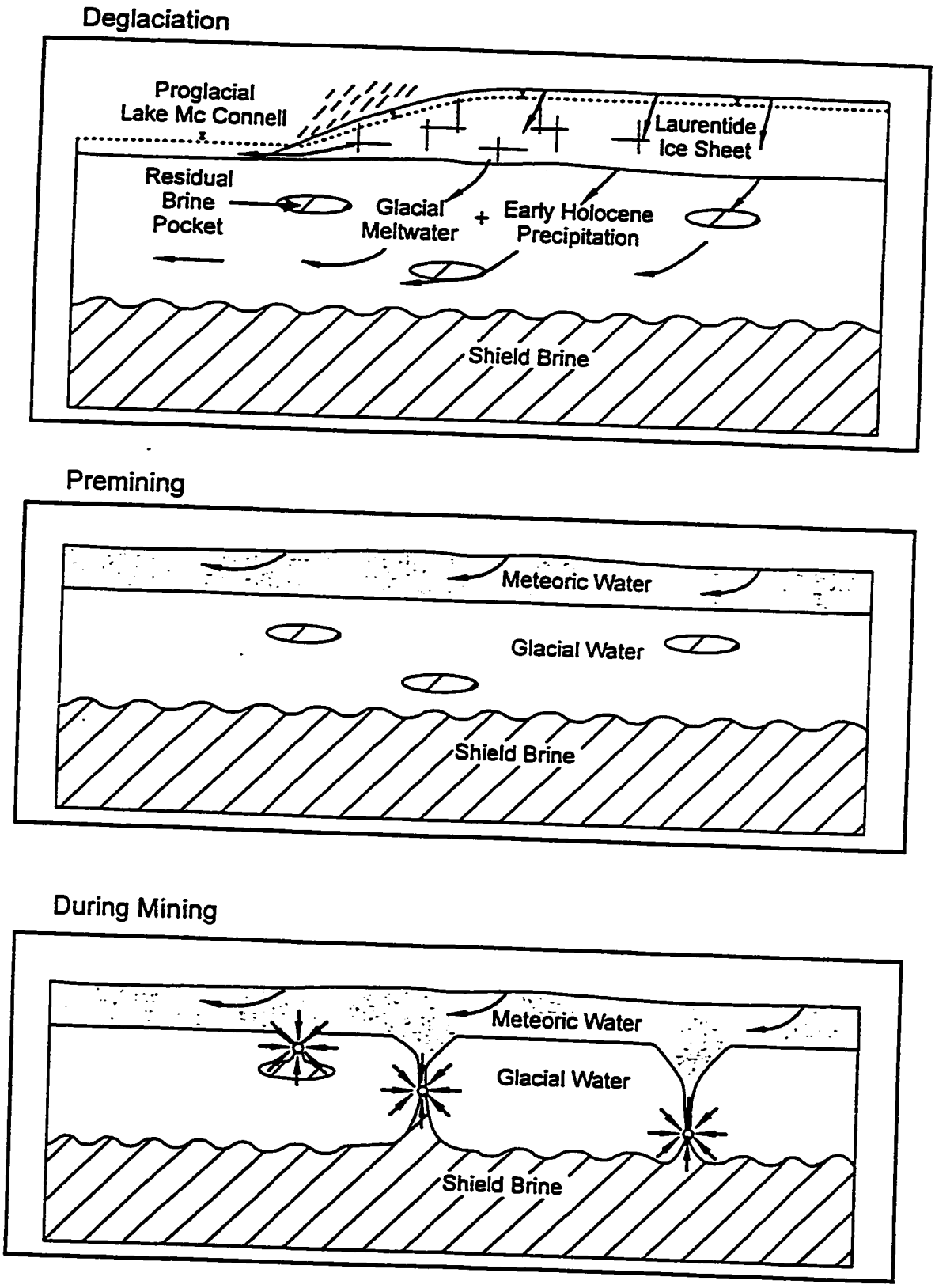

Fig. 4.7 Conceptual representation of infiltration and mixing of groundwater (from Intera, 1997).

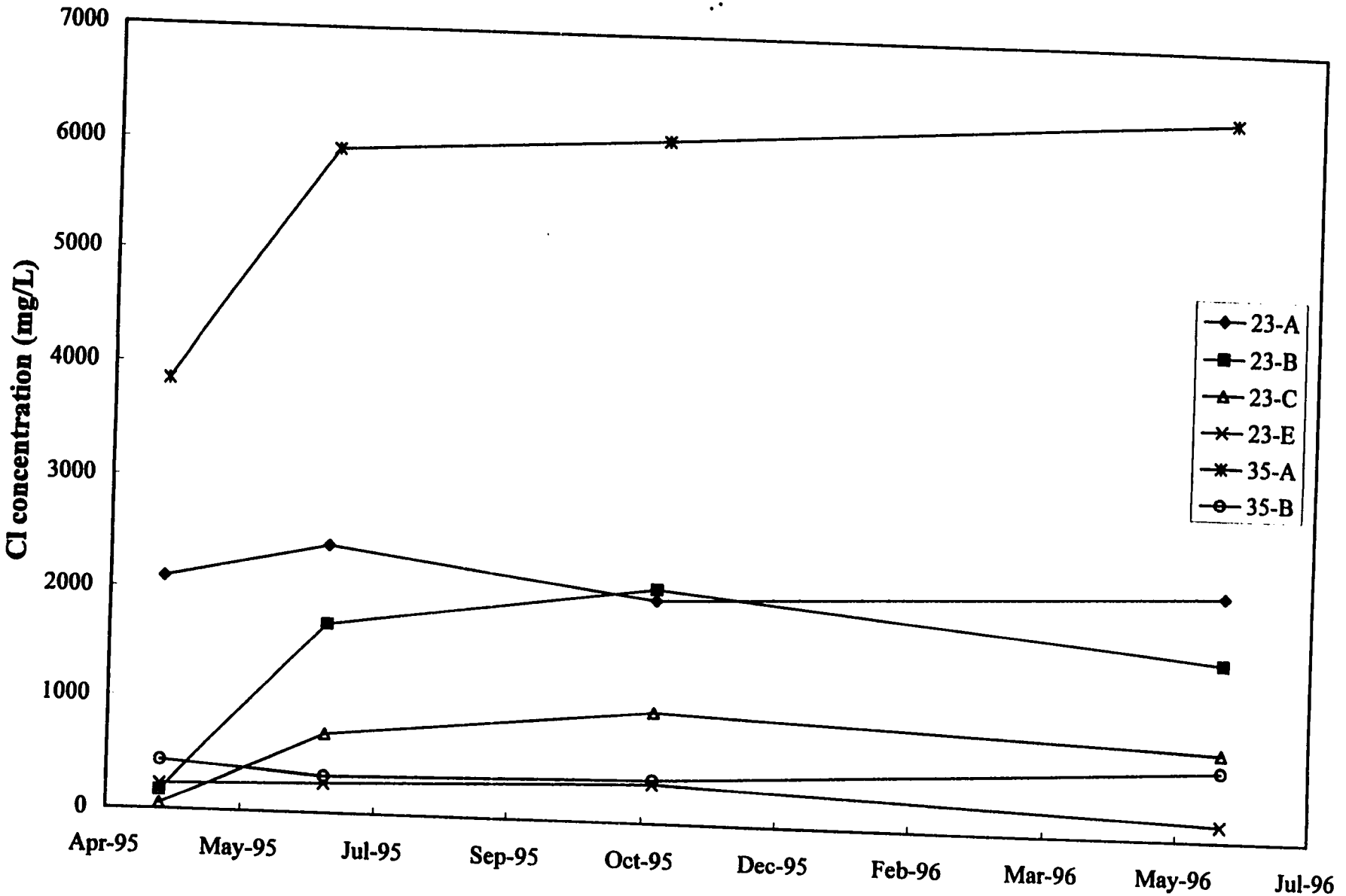

Fig. 4.8 Chloride change with time for least saline (shallowest) waters.

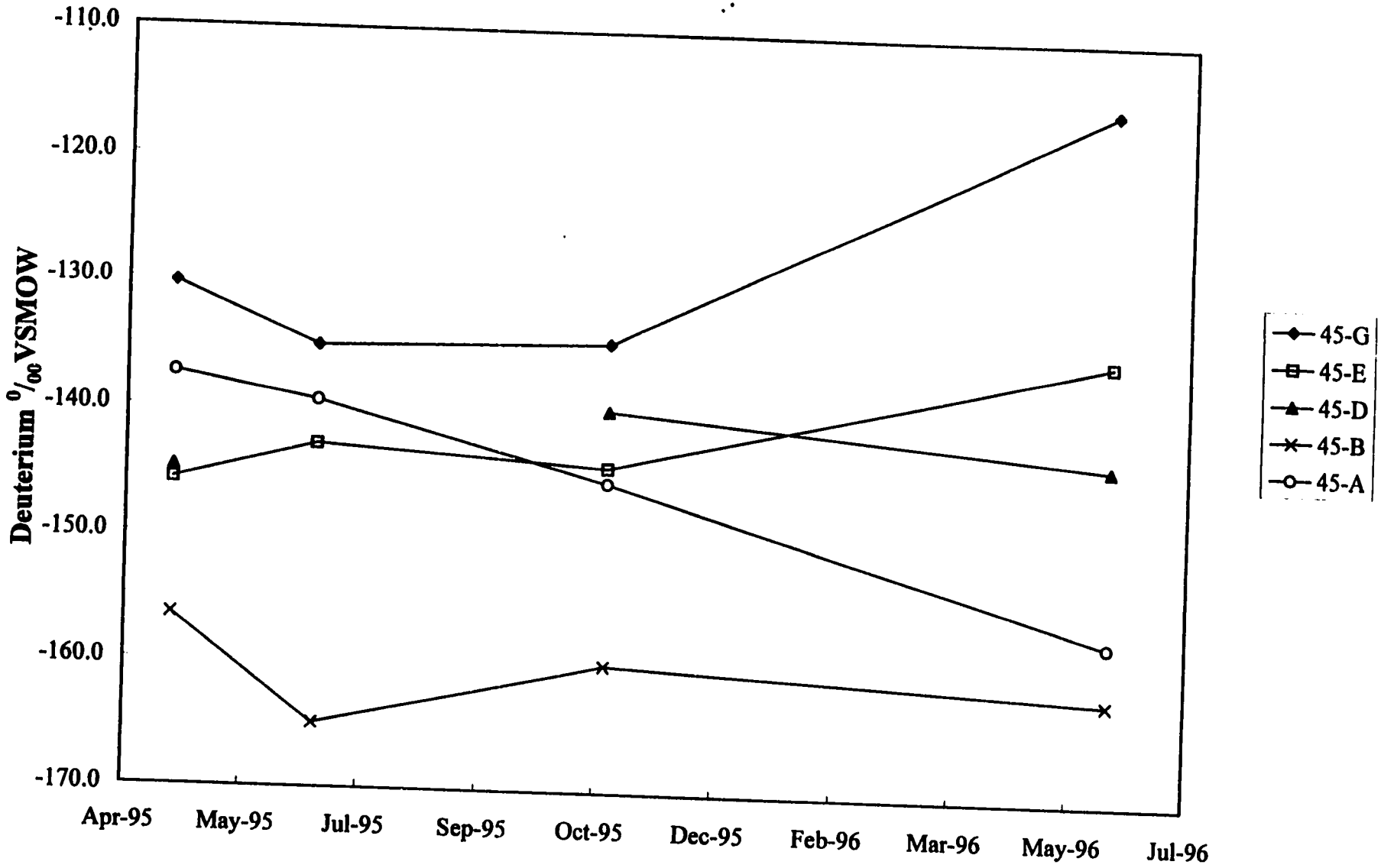

Fig. 4.9 Deuterium change with time - 4500 level. Boreholes were shut-in for eight months after sampling in November 1995.

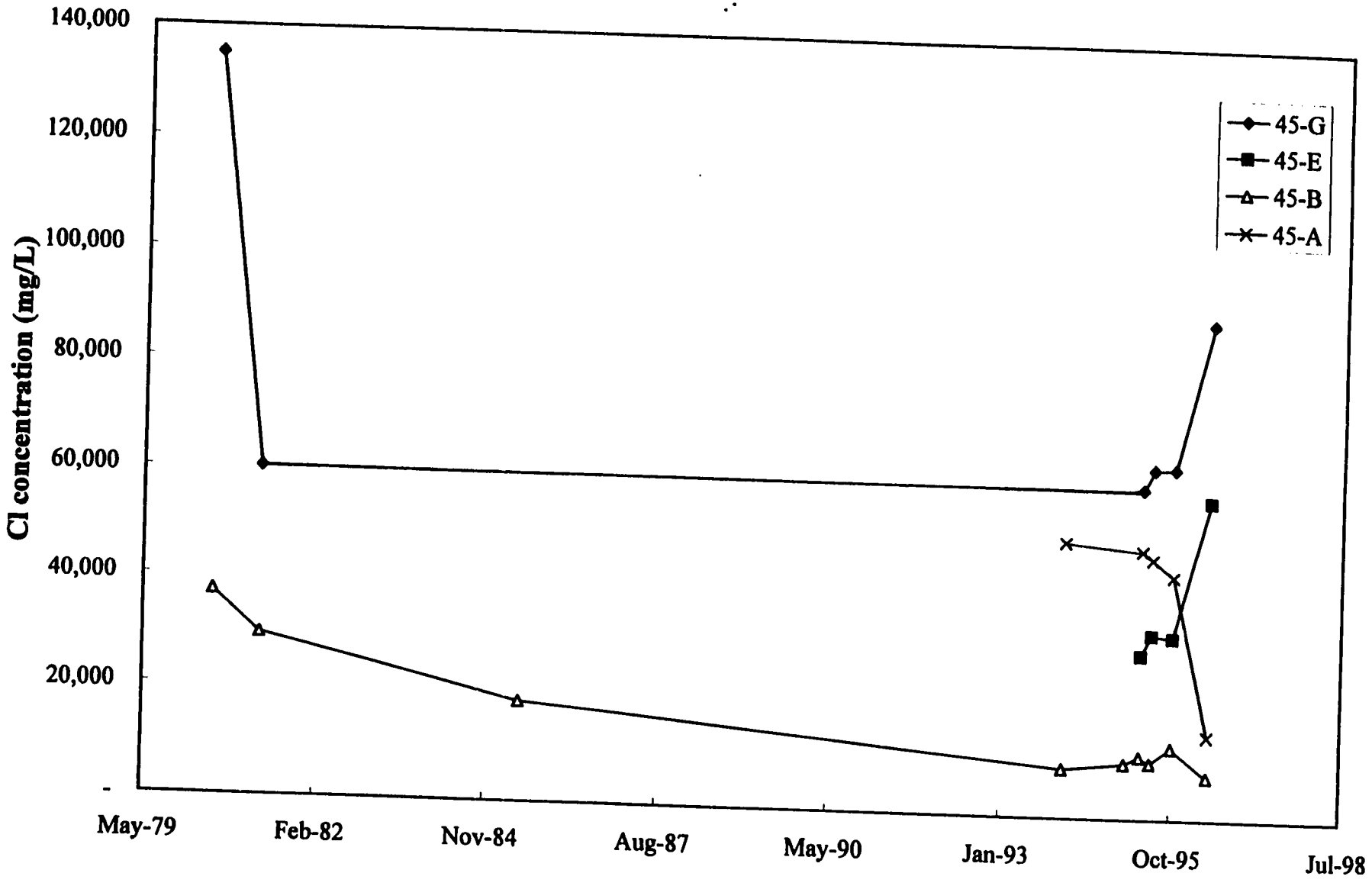

Fig. 4.10. Change in Cl concentration with time - 4500 level. Boreholes were shut-in for eight months after sampling in November 1995.

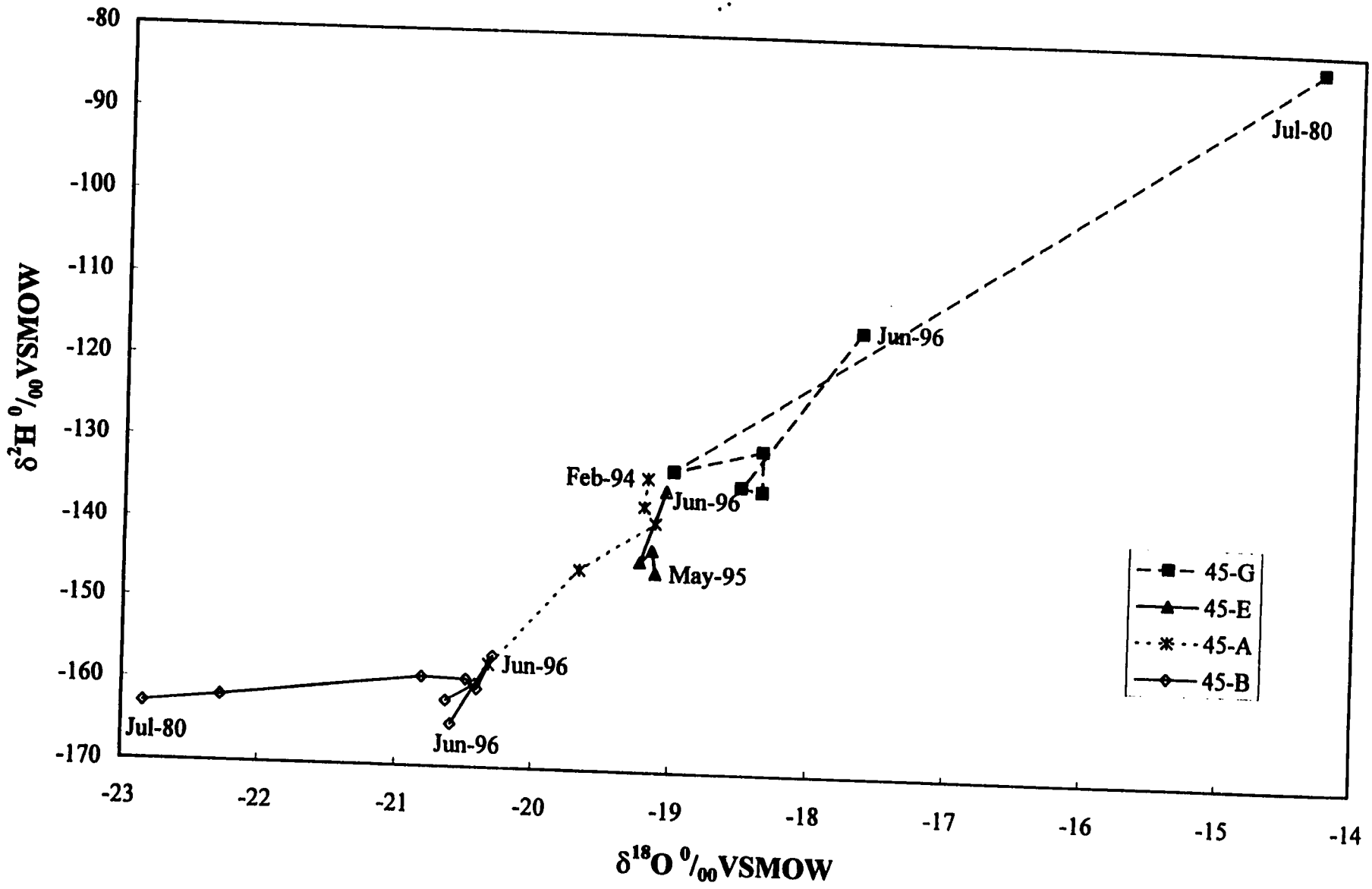

Fig. 4.11. Water isotope change with time - 4500 level sites.

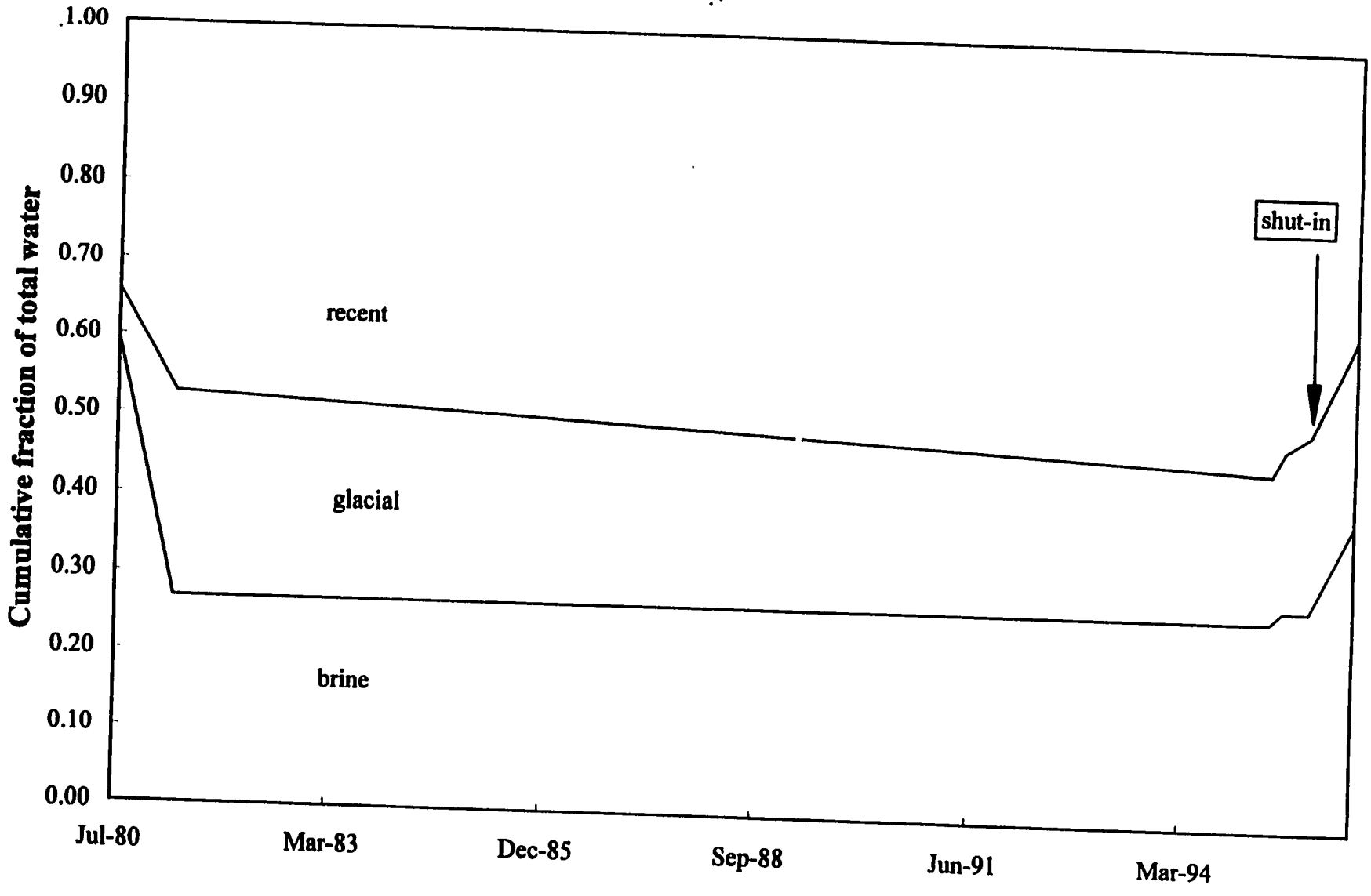

Fig. 4.12. Site 45-G - Change in water composition for the period 1980-1996. The borehole was drilled in December 1979.

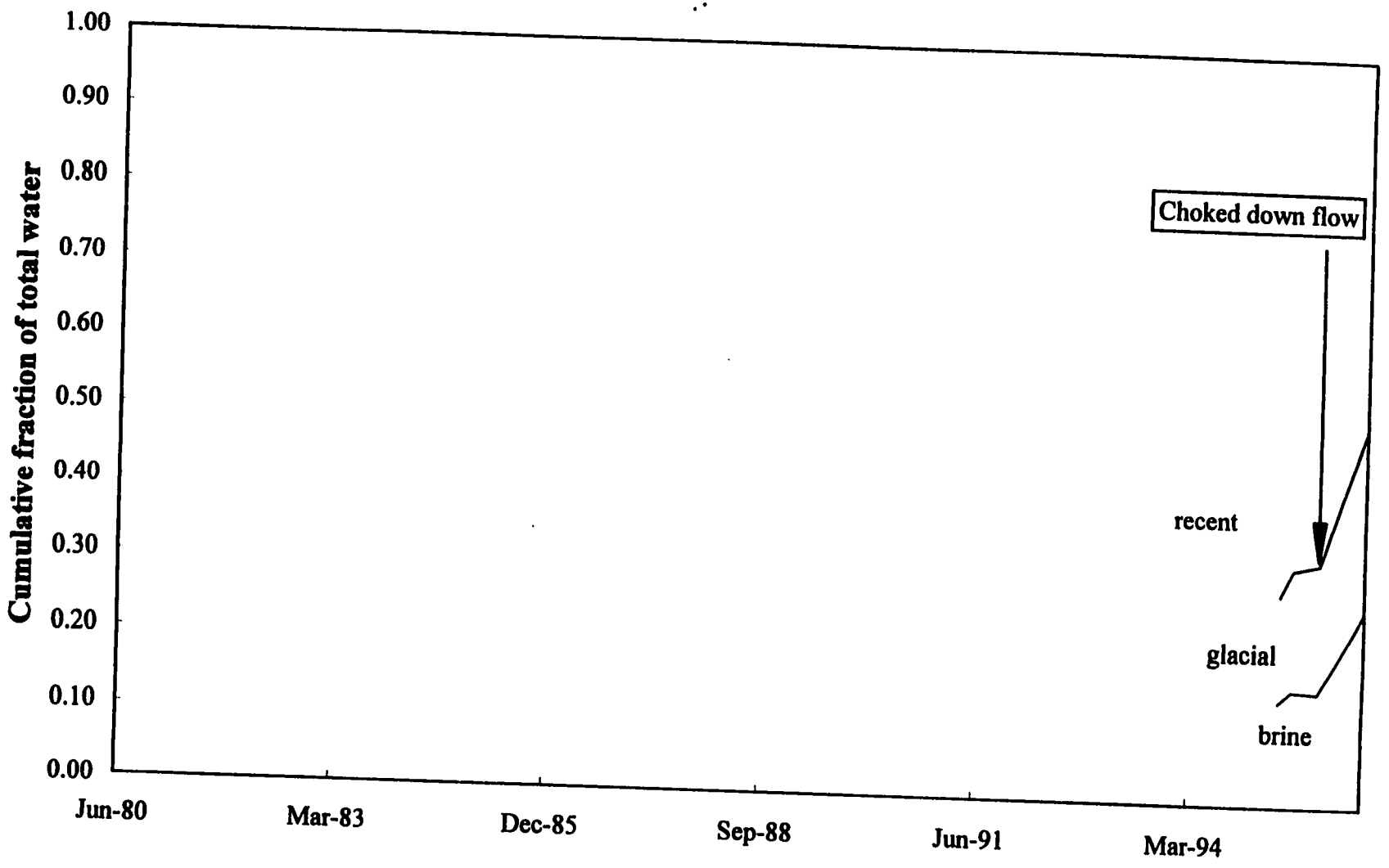

Fig. 4.13. Site 45.E - Change in water composition for the period 1995-1996.

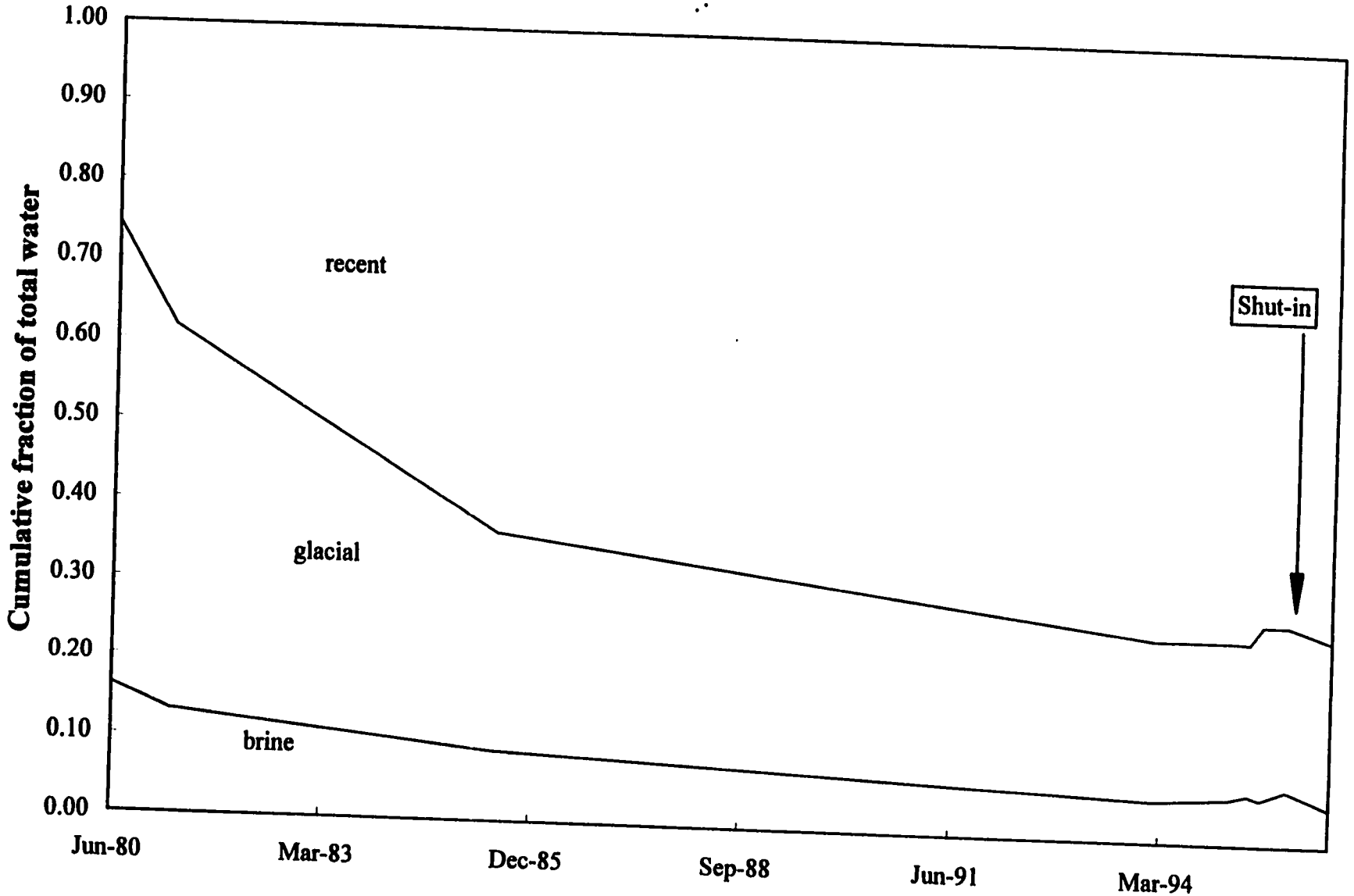

Fig. 4.14. Site 45-B - Change in water composition for the period 1980-1996. The borehole was drilled in March 1980.

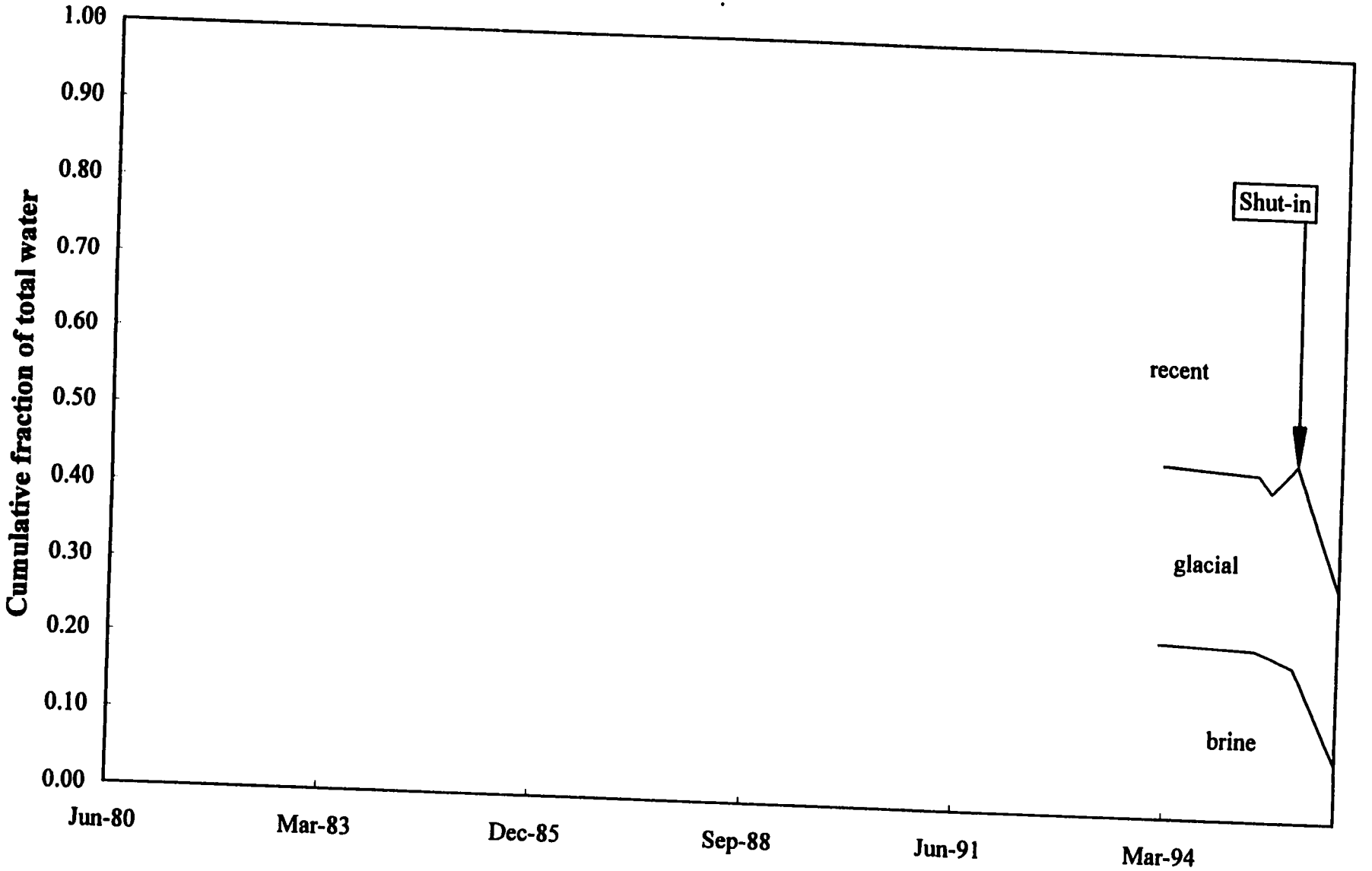

Fig. 4.15. Site 45-A - Change in water composition for the period 1994-1996.

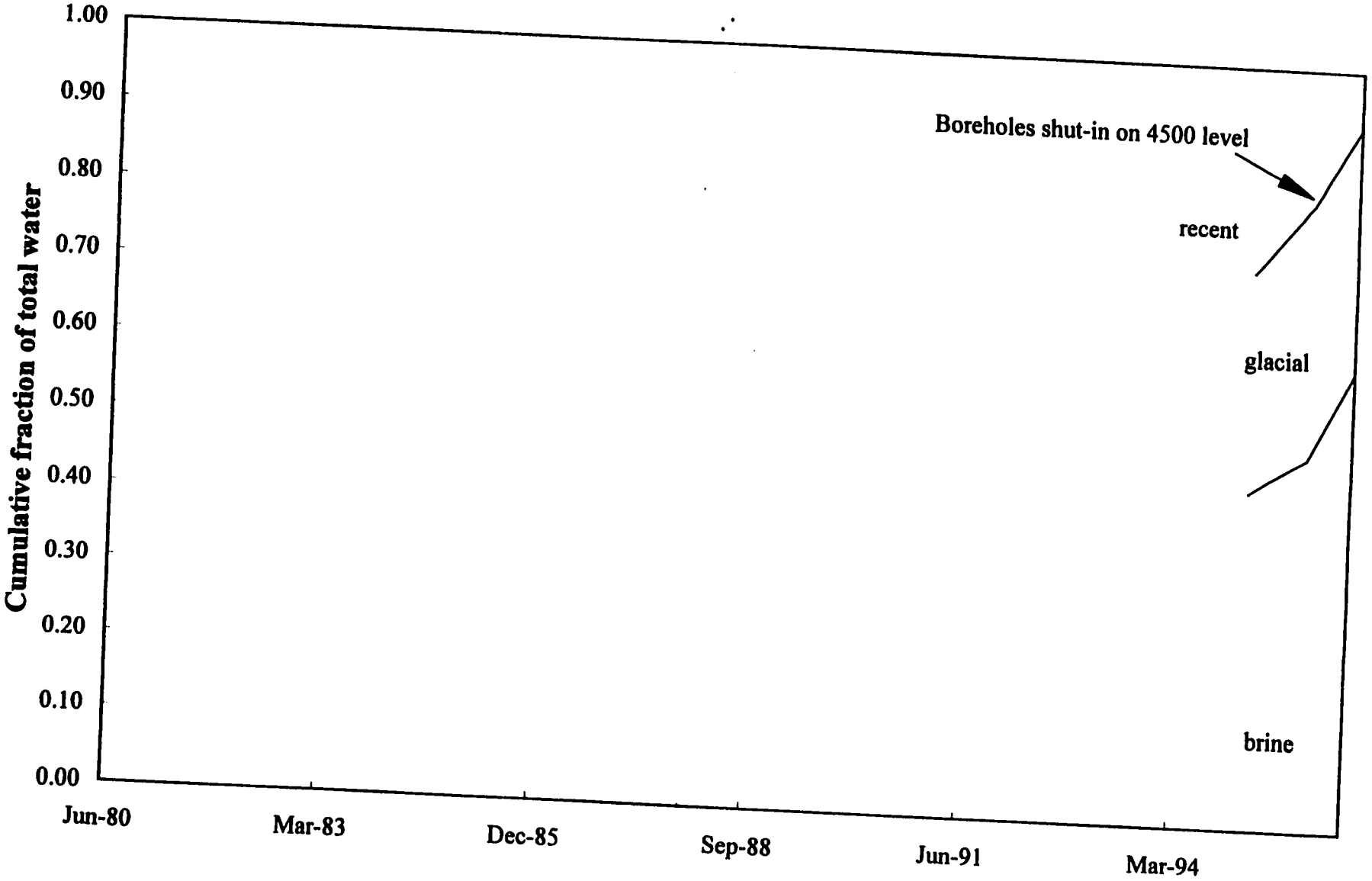

Fig. 4.16. Site 49-B - Change in water composition for the period 1995-1996.

IMAGE EVALUATION TEST TARGET (QA-3)

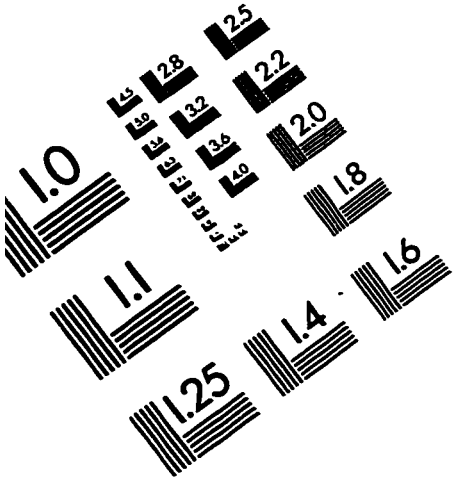

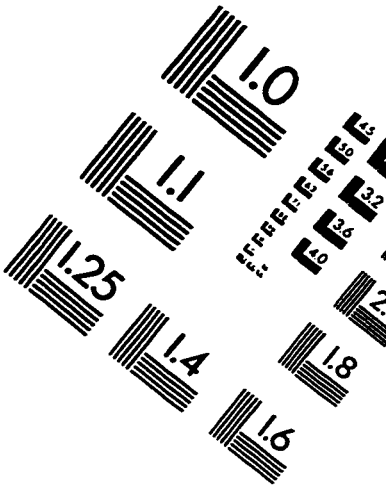

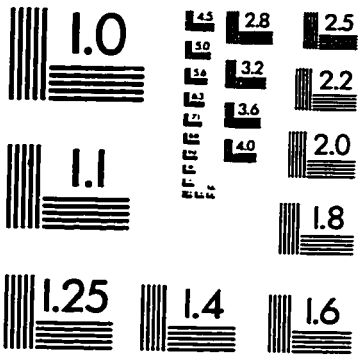

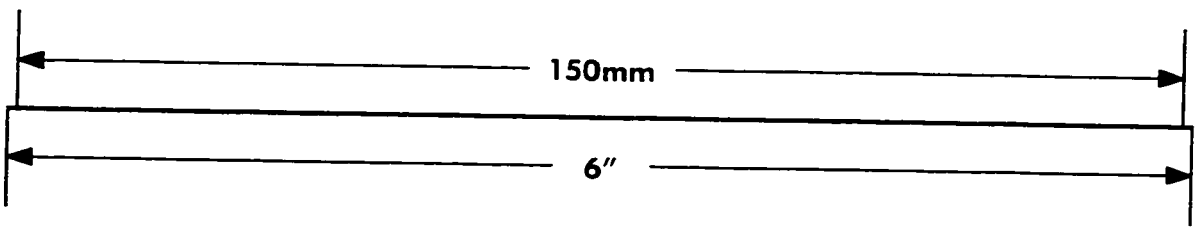

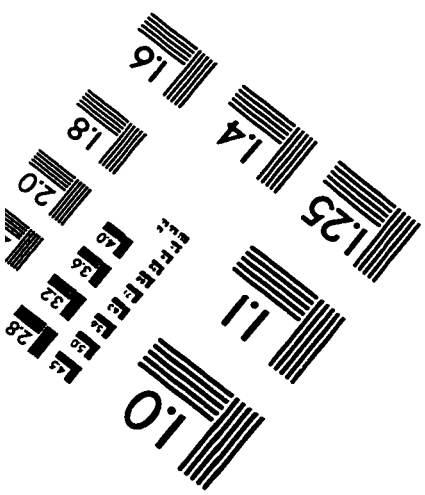

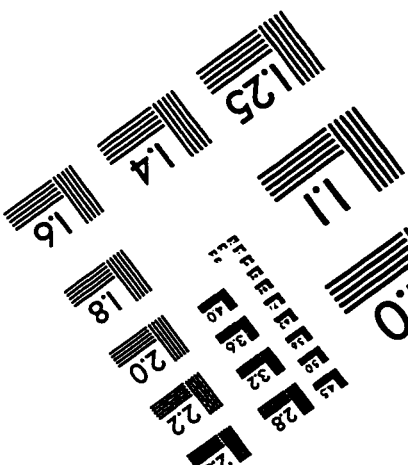

APPLIED IMAGE, Inc
1653 East Main Street
Rochester, NY 14609 USA
Phone: 716/482-0300
Fax: 716/288-5989